THE STRUCTURE AND MICROFABRIC OF A PART OF THE ARLTUNGA NAPPE COMPLEX, CENTRAL AUSTRALIA

A thesis submitted for the degree of

DOCTOR OF PHILOSOPHY

in

THE AUSTRALIAN NATIONAL UNIVERSITY

by

MOHAMMAD YAR KHAN

August 1972

PREFACE

This thesis comprises results of field and laboratory studies of a part of the Arltunga Nappe Complex, Central Australia. All field and laboratory work used in this thesis was done by myself and information compiled from other workers is acknowledged.

The work was carried out from July, 1969 to July, 1972 while I held an Australian National University Research Scholarship and I am grateful to Professors J.C. Jaeger and A.E. Ringwood for the facilities they made available to me in the Department of Geophysics and Geochemistry.

The logistic support provided by the Bureau of Mineral Resources, Geology and Geophysics, during fieldwork is gratefully acknowledged. Final drafting of Map 1 and Figure 2.3 was carried out at the B.M.R.

Professor B.E. Hobbs, formerly at the A.N.U., and Dr. D.J. Forman of the B.M.R. suggested Arltunga Nappe Complex as a suitable area. They together with R.D. Shaw of the B.M.R. showed a keen interest in the project throughout. I express my gratitude for their enthusiasm and assistance. Professor Hobbs has also supervized this research and spent considerable time in reading and criticizing the thesis. His advice and constructive criticizm are very much appreciated. I also thank Dr. A.R. Crawford for his supervision of this research during the final year and for reading the thesis.

Among the many who also showed interest in the project and or assisted me I wish to thank the following: R.M.Bank, Dr. J.N.Boland, J. Funk, G. Lister, Dr. M.S.Paterson, Dr. M.J.Rickard, Dr. A.J.Stewart and Dr. C.J.L.Wilson for useful discussions; Mr. M.E. Nancarrow for advice in the compilation of Map 1; Miss D.M. Pillinger and Mr. W. Shaffron for drafting Map 1 and Figure 2.3; Mr. A. Powell for

preparing excellent thin sections; and Mr. G. Milburn for advice in photographic work, and Mrs. Millgate for typing the thesis.

I am also grateful to my wife and son who helped in the drafting and colouring of some of the illustrations of this thesis.

Canberra, August, 1972.

Mohammad Yar Khan

M. Yar Khan

TABLE OF CONTENTS

ABSTRACT

The Arltunga Nappe Complex developed during Alice Springs Orogeny on the northeastern margin of the Amadeus Basin in Central Australia; the orogeny occurred either late in the Devonian or in the Carboniferous. The complex extends about 100 Km east-west and about 30 Km north-south. The Atnarpa Range area extending 19 Km roughly east-west and 1 to 6 Km north-south forms a small part of the complex. In this thesis the results of the study of structure and microfabric of this part of the complex are presented.

In the Atnarpa Range area as in other parts of the Arltunga Nappe Complex the basement rocks are part of the Precambrian Arunta Complex and the cover rocks comprising the Heavitree Quartzite and a part of the overlying Bitter Springs Formation represent the very basal part of the Amadeus Basin sequence. In these rocks the effects of a low grade metamorphism have been observed in the area and these effects are progressive in the cover rocks and retrogressive in the metamorphic rocks of the basement. The metamorphism increases in intensity with the proximity of thrust faults as well as generally from south to north.

Structurally the Atnarpa Range area is a pile of many folded thrust sheets and normal stratigraphy has been found to repeat in almost all these sheets. In the thrusting both, the basement and the cover rocks are involved. Structures of three generations have been recognised in the area but structures of the third generation are very rare in occurrence. Structures of the first generation are only developed in the northern parts of the area and of these a foliation defined generally by the planes of flattening of the quartz grains and a lineation defined by the direction of maximum elongation of the grains are most prominent.

The folds of this generation are tight to isoclinal and very close to similar in style but are rarely observed. Structures of the second generation are more widespread than those of the first and attain large size; the whole of Atnarpa Range is an anticline belonging to this generation. The second generation structures are mainly represented by concentric, disharmonic or conjugate folds and a crenulation or wrinkly lineation associated with their axes. The second generation folding at macroscopic scale is markedly non-cylindrical.

The progressive development of the microfabric, which has been studied in detail in the Heavitree Quartzite, is mostly related with the development of the first generation structures. The microfabric generally progressively develops from south to north in the area and in addition develops locally with the proximity to the thrusts. The study of the microfabric included the study of changes in the microstructure, in the type and amount of strain, in the quartz c-axis preferred orientation and in the orientations of quartz deformation lamellae. The changes in the microstructure of the quartzite start from virtually an undeformed state in which detrital, more or less spherical quartz grains rarely exhibit signs of deformation. An advanced stage of microstructural development is characterized by strong deformation of the grains resulting in about 50% shortening normal to the foliation and about 100% elongation parallel to the lineation and finally to their transformation into shapes resembling that of a ribbon. Another advanced stage of the development is associated with recrystallization and at this stage the new, small size, strain free, polygonal grains completely replace the old, deformed grains. The quartz c-axis preferred orientation is related

to the microstructural development and the patterns of preferred orientation change from random to weak, partial to complete, girdles to strong peripheral girdles to weak, acutely inclined, crossed girdles and finally either to a small circle girdle or to an elongated maximum in the plane of a partial to complete girdle. The preferred orientation is also related to strain so that its strength and degree of symmetry increases with the amount of strain. Recrystallization alters the pattern of preferred orientation and also destroys the homotactic relationship of the quartz sub-fabric and the mesoscopic sub-fabric. The effect of host control on the development of the preferred orientation during recrystallization has also been investigated. In the early stages of the microfabric development the deformation is of flattening type, in the advanced stages of the development it is of constrictional type.

On the basis of symmetric relationship of the two sub-fabrics, the quartz sub-fabric and the mesoscopic sub-fabric, and from the interpretation of some of the features of the quartz sub-fabric σ_1 is considered to have lain at or close to the pole of the foliation during the development of first generation structures.

The development of the microfabric is discussed with regard to the inferred physical conditions of deformation as well as in the light of the existing knowledge of experimental deformation of rocks, minerals and metals. An interpretation of the structural evolution of the area has also been presented.

CHAPTER 1

INTRODUCTION

1.1 General statement

For more than a century the existence of preferred orientation of minerals in naturally deformed rocks has been recognised. Sharpe (1849) and Sorby (1856) were among the early geologists who attempted to explain the parallel alignment of micas in slaty cleavage. However, presence of preferred orientation in the crystallographic elements of minerals was first realized by Sander, Schmidt and their associates (see Sander, 1911) and since the publication of the classic work of Sander in 1930, the preferred crystallographic orientation of minerals has been studied by many geologists. In fact in many of such studies the microscopic analysis of the preferred crystallographic orientation of minerals has been combined with the mesoscopic and macroscopic analyses of the preferred orientation of the planar and linear features of the rock fabric to attempt to unravel the physical conditions (viz., Stress, temperature, strain and strain-rate) of deformation.

Prominent among the minerals studied for their preferred orientation are quartz, mica and calcite and the literature shows, quartz has received most attention probably because of its simple optical properties and its widespread occurrence in rocks.

In most of the studies of the preferred orientation[1] of minerals the rocks used were of medium to high metamorphic grade. The minerals in the rocks, which have been the product of these types of metamorphic environments, usually undergo many cycles of physical and chemical changes associated with a number of deformational events. In each of these deformational events the minerals acquire some sort of preferred

---

1 Preferred orientation will subsequently be used for crystallographic preferred orientation unless otherwise stated.

orientation either due to syntectonic strains or due to syntectonic or post-tectonic recrystallization. The resultant pattern of preferred orientation thus may reflect many types of imposed strains or may only represent the last of these strains. In these circumstances it becomes exceedingly difficult to make use of the preferred orientation in the interpretation of the kinematic and dynamic aspects of the history of deformation. In order to understand the mechanisms of the development of preferred orientation and the changes in the physical conditions of deformation which induce such mechanisms it is essential to study the gradual development of preferred orientation from undeformed or weakly deformed rocks to strongly deformed rocks and from unmetamorphosed or low-grade metamorphic rocks to rocks of high metamorphic grade. This type of study will also provide an opportunity to relate the changes in the preferred orientation of minerals to changes in the microstructure of the rock. Another possibility of this study could be to correlate the magnitudes of strain with the changing patterns of preferred orientation. Recent studies of Sylvester and Christie (see Sylvester and Christie, 1968) of quartz preferred orientation in a contact metamorphic environment and of Wilson (1970) again of quartz preferred orientation in a prograde regional metamorphic sequence are examples of this type of approach.

Another important approach towards the understanding of physical conditions of deformation and means of developing preferred orientation relies on deforming rocks and minerals under the controlled conditions of experiments in laboratories. Although it is impossible to simulate the physical conditions of natural deformation in these experiments nevertheless much useful information has been obtained from experimental investigations and applied in predicting these conditions from the fabric of deformed rocks. The experimental work has gained considerable impetus during the last two decades particularly due to the efforts of Griggs

and co-workers (see Griggs and Handin, 1960).

The two approaches, described above, are complimentary in that the information obtained about the physical aspects of deformation through the application of one contributes towards the refinement of the techniques of the other.

1.2 Purpose and scope of this thesis

Keeping in view the framework of the first approach an area in the Arltunga Nappe Complex in Central Australia was selected for the study of the progressive development of quartz preferred orientation in a quartzite sequence under differing conditions of deformation and metamorphism. This sequence of quartzite forms the lower part of the cover rocks in the nappe complex and is of widespread occurrence throughout the complex. Metamorphism remains within the grade of greenschist facies and in the area of this study the rocks are virtually undeformed and unmetamorphosed in the south, become strongly deformed towards the north and start recrystallizing further north and north-east. As is always the case, detailed geological mapping and structural analysis on mesoscopic and macroscopic scales of fabric elements of the rocks are a prerequisite to an investigation of the preferred orientation of their minerals on a microscopic scale. The information about the former (viz., detailed mapping and mesoscopic and macroscopic analyses) was not available for the area to be investigated and so its acquisition and analysis also became an essential part of this research.

This thesis first describes in Chapter 2 the general geology of the Arltunga Nappe Complex on the basis of the previous investigations and then in Chapter 3 analyses the details of the stratigraphy and structure on mesoscopic and macroscopic scales of the area mapped in detail. Next in Chapter 4 a description of the changes in the micro-fabric of the quartzite is given and is followed by a discussion of the

development of the quartz c-axis preferred orientation in terms of the changing physical conditions of deformation and metamorphism in the area and in the context of the existing knowledge of naturally deformed rocks and minerals and experimentally deformed rocks, minerals, and metals. In Chapter 5 a summary and a synthesis of the results of this study is presented.

1.3 The problem of interpretation of preferred orientation

The interpretation of preferred orientation has remained the subject of a lively debate among geologists since the time its existence in minerals was realized. The results of theoretical and experimental studies, which form the basis for the interpretation of the preferred orientation in the subsequent parts of this thesis are briefly discussed in this section.

1.3.1 Symmetry Concept

This concept was first introduced into structural geology by Sander to interpret patterns of preferred orientations. According to this concept the symmetry of the preferred orientation of the fabric of a deformed rock reflects the symmetry of the movements involved in the deformation. Between the years 1930 and 1960, doubts about the validity of this concept in certain geological situations were expressed by geologists such as Martin (1935) and Kvale (1953). This controversy will be discussed in some detail in Chapter 5 as the area of present investigations is similar in structural setting to the areas where the application of the concept was questioned. The concept was revised and expanded by Paterson and Weiss (1961) who emphasized that, due to the lack of quantitative information on the past physical phenomenon in geology, the principle of the relationship of symmetry between aspects of a deformational event could be invoked to draw some conclusions about

the nature of the aspects, otherwise unknown. Applying the basic principles of "Symmetry Theory" governing the symmetries of cause and effect in physical phenomena they concluded that whatever the nature of the factors contributing to a deformation may be, the symmetry that is common to them can not be higher than the symmetry of the deformed fabric, and symmetry elements absent in this fabric must be absent in at least one of the contributing factors (viz., initial fabric, mean strain, and local perturbations).

The experimental research of Griggs, Handin, and others particularly on marble provided enough data on the relationship between patterns of preferred orientations of the deformed fabric, the deformation including the change of shape and rotation, the anisotropy of the initial fabric and the system of externally applied forces. This data confirms the genetic significance of the symmetry of the fabric of deformed rocks (Turner, 1957; Turner and Weiss, 1963).

1.3.2 Results of experimental investigations

Prominent among these investigations which have contributed towards the understanding of physical properties of minerals and their tendency of acquiring a state of preferred orientation are:

(1) For Calcite - Griggs (1938); Turner et al. (1954); Griggs et al. (1960) and Ferriera and Turner (1964).

(2) For Quartz - Carter et al. (1964); Christie et al. (1964); Raleigh (1965); Griggs and Placic (1965); Griggs (1967); Green (1967); Hobbs (1968); Green et al. (1971); and Tullis (1971).

(3) For Mica - Means and Paterson (1967); Tullis (1968 and 1971); and Ethridge (1971).

These investigations together with those, much more numerous, on metals have shown that the development of preferred orientation results from two different kinds of processes namely intracrystalline and recrystallization mechanisms.

1.3.2.1 Intracrystalline mechanisms The main mechanism of this process is slipping along crystallographic planes in crystallographic directions to produce a change of shape of the grain and a bodily rotation of its axes thus leading to the development of the preferred orientation. Measurements of strains in single crystals of certain metals, particularly face centered cubic, for instance aluminium (see Taylor, 1938), subjected to uniaxial stress, have established that plastic deformation occurs by slipping in one direction parallel to one crystal plane and that of all crystallographically similar planes the slipping occurs only on the one for which the shear stress in the direction of the slip is greatest. The slipping produces a rotation of the axes of the specimen relative to the axes of the crystal. This rotation ultimately brings a second possible slip plane into the most favourable position for slipping and then slipping begins on the second plane also. Taylor (1938) attempted to analyse the plastic strains in aluminium aggregates on the basis of the slip mechanism established for single crystals. The main difficulty in such an analysis lay in visualising the effect that the slipping inside each grain of an aggregate would have on the boundary relationship between grains. Taylor, therefore, assumed that the strain in each grain is identical with that of the aggregate as a whole - a condition possible only if shearing takes place on five independent slip systems in each grain simultaneously without volume change. From the principle of least work he deduced which systems would function in a grain of any given orientation and predicted theoretically changes in grain orientation

which agreed up to a point with those observed experimentally. Bishop and Hill (1951) also analysed the problem of plastic strain in a polycrystalline aggregate. They considered the distribution of stress among the possible slip planes and presented a clearer physical picture than Taylor's treatment. Their work also helped to remove one of the objections to Taylor's treatment of this problem (see Barett and Leverson, 1939), which arose through an arithmetical error in his original calculations. The other objection to Taylor's treatment, which also applied to that of Bishop and Hill, was concerned with the assumption of homogeneous strain in a deformed aggregate. Wonsiewicz and Chin (1970) have shown the validity of Taylor-Bishop-Hill analyses in the case of inhomogeneous deformation also. Recently Hobbs (personal communication, 1971), using the analysis of Bishop and Hill has derived the slip systems which operate in the individual grains of a quartzite in order to produce a homogeneous distortion of the rock.

Other complicated mechanisms in this process involve twinning, cross slip and climb of dislocations which most probably occur at elevated temperatures to produce preferred orientations where five independent slip systems are not available. The process of intracrystalline mechanisms is called cold-working in metallurgy where permanent deformation of metals is accomplished at room temperature through this process. In geological situations permanent deformation at low temperatures falls in this category.

1.3.2.2 Recrystallization Kamb (1959) investigated the influence of stress on recrystallization. According to him the theory of equilibrium under non-hydrostatic stress is capable of predicting stable patterns of preferred orientation. The theory assumes that some grains in a stressed aggregate grow at the expense of the

neighbouring grains. Brace (1960) applied this treatment to calculate stable orientations under axial compression for calcite and quartz. The validity of the theory is doubtful, (a) as the differences in chemical potential that constitute the driving force for recrystallization of elastic solids under non-hydrostatic stress are very small, (b) because of its inapplicability to plastically deformed crystals or rocks, and (c) it does not consider the factor of that type of recrystallization which depends upon the formation and subsequent growth of new grains through a dissipation of the stored energy of deformation. Experimental studies performed by geologists: Griggs et al. (1960 a, b); Carter et al. (1964); Raleigh, (1965); and Hobbs (1968) have confirmed the validity of this mechanism to give effect to recrystallization. When deformed crystalline materials, which include quartz, are annealed at temperatures higher than those required for recovery the remaining stored energy of deformation is released through the migration of high angle boundaries resulting in the growth of new unstrained grains at the expense of old, deformed, host grains. The growth of these strain free grains starts independently at many different locations, nuclei, in the deformed material. The new grains bear a strong relationship to the host grain. The role of this host control phenomenon has been observed in the experimental investigations by Griggs et al. (1960 a, b) with calcite and by Hobbs (1968) with quartz. Many investigators in the metallurgical field, such as Beck and Hu (1966), have also noted it. In syntectonic recrystallization experiments also, the resulting pattern of preferred orientation has been attributed to host control because of its similarity to that observed in annealing experiments (Hobbs, 1968). Syntectonic recrystallization takes place at high temperature and at a constant strain rate, conditions which are analogous to the process of hot working in metals.

Preferred orientation resulting from recrystallization may in some cases, therefore, be attributed to host control. It follows then that if the host grains had a strong preferred orientation, the new, recrystallized grains, are also very likely to develop a strong preferred orientation, not necessarily the same as that of the host grains but related to it.

CHAPTER 2

GENERAL GEOLOGY OF THE ARLTUNGA NAPPE COMPLEX

2.1 General statement

The area of the present study, on which this thesis is based, is a part of the Arltunga Nappe Complex. The knowledge of the geology of the complex is an essential prelude to the analysis of the results of this study to be dealt with in subsequent chapters of the thesis. In this chapter, therefore, the geology of the complex is briefly described and the description is based on the reports of the previous workers concerning the geology of the complex.

2.2 Location and access

The Arltunga Nappe Complex lies in the Eastern MacDonnell Ranges on the northeastern margin of the Amadeus Basin within lat. 23° 16' and 23° 42' and long. 134° 8' and 135° 12' (Fig. 2.1). The Amadeus Basin is one of many intracratonic depressions in the Precambrian shield of central Australia. It has an area of about 150,000 square kilometres and lies across the Northern Territory extending into Western Australia (Fig. 2.1). It contains about 10,000 metres of miogeosynclinal shelf sediments mostly of Late Precambrian to Middle Paleozoic age and some of Permian and Tertiary ages (Wells *et al.*, 1970).

The nappe complex extends 100 kilometres eastward along the strike from about 40 kilometres east-northeast of the town of Alice Springs. The extent of the complex across the strike is about 30 kilometres. The area of the complex is accessible by many graded roads and vehicle tracks from the main Adelaide-Alice Springs-Darwin Road.

2.3 Geological investigations in the nappe complex

Since 1890, the northeastern margin of the Amadeus Basin, on

Fig. 2.1. Locality map.

which the nappe complex lies, has been visited by a number of geologists mostly in connection with mineral investigations. These geologists also made general geological observations and a detailed account of their observations is given by Forman and Milligan (1967). Notable among these and more pertinent to the area of the nappe complex and the present study are the following: H.Y.L. Brown (1902, 1903) made a detailed survey of the goldfields near Arltunga and recognised that plutonic rocks were overlain by sediments of possible Cambrian age. Chewings (1894, 1914, 1928, 1935) proposed Cambrian and Ordovician ages for the sedimentary rocks of the Amadeus Basin and suggested that the basal members such as the Arltunga/White Range quartzites were infolded and partly assimilated in the basement. Mawson and Madigan (1930) introduced the term 'Arunta Complex' for the crystalline basement rocks of the MacDonnell Ranges and Madigan (1932a) proposed a sub-division of the rocks in the MacDonnell Ranges into Archean (Arunta Complex), Upper Proterozoic (Pertaknurra and Pertatataka Series), Cambrian (Pertaoorrta Series) and Ordovician (Larapintine Series). Ellis (1937) noted the concordance of strike of the Heavitree Gap quartzite, near Alice Springs, with the foliation in the Arunta Complex and concluded that the Heavitree Gap quartzite and the Winnecke and Arltunga quartzites (in the area of the nappe complex) were part of the Arunta Complex. Voisey (1939) and Hossfeld (1936; 1937 a, b, c,; 1940; 1954) recognised structural and lithological differences between the Heavitree Gap quartzite and the White Range/Arltunga quartzite and included the latter in the Arunta Complex. Joklik (1955) was the first to prepare a comprehensive regional geological map of the area of the nappe complex. He subdivided the Arunta Complex into several units and named the quartzite which lies at the base of the Amadeus Basin sequence at Heavitree Gap as Heavitree Quartzite but emphasized the difference between it and the White Range Quartzite. He assigned the White Range

Quartzite to the Lower Proterozoic and considered that it lay uncomformably between the Arunta Complex and the Heavitree Quartzite. He also named the thick formation of carbonate rocks overlying the Heavitree Quartzite at Bitter Springs Gorge (lat. 23° 33', long. 134° 27') the 'Bitter Springs Limestone', this name was later revised to 'Bitter Springs Formation' by Ranford, Cook and Wells (1965). A regional gravity traverse in the Amadeus Basin was made by Marshall and Narain (1954) and in 1961 and 1962 the Geophysical Branch of the Bureau of Mineral Resources completed a regional gravity survey of the basin (Langron, 1962; Lonsdale and Flavelle, 1963). Forman and Milligan in 1964 mapped the geology of the nappe complex at a scale of 1:250,000 and described in detail the stratigraphy and the structure as well as interpreted the overall structure as a nappe complex. They also showed that the White Range Quartzite and the Heavitree Gap Quartzite were stratigraphically the same. Petrographic, structural and age determination studies were carried out by Stewart in the western half of the complex during 1968-1969 period (Stewart, 1971). Detailed mapping at a scale of 1:25,000 of some parts of the area of the nappe complex was started by the Bureau of Mineral Resources and Australian National University in 1969. Forman (1971) published another account of the nappe complex incorporating in it the results of his part of the detailed mapping.

2.4 Stratigraphy

The Amadeus Basin contains about 10,000 metres of sediments mostly of Late Precambrian to Paleozoic age and some of Permian and Tertiary ages (Wells *et al.* 1970). The sediments rest unconformably on the Precambrian basement of crystalline rocks. On the northeastern margin of the Amadeus Basin the crystalline basement rocks known as the 'Arunta Complex' are overlain unconformably by the Upper Proterozoic Heavitree

Quartzite. The quartzite is the basal formation of the Amadeus Basin succession and is overlain by a generally conformable sequence of Upper Proterozoic, Cambrian and Ordovician sediments; a few unconformities are present in the younger sediments which overlie the sediments, mentioned above, unconformably (Forman et al., 1967). In the area of the nappe complex the basement and a part of the Upper Proterozoic consisting of the Heavitree Quartzite and Bitter Springs Formation are present.

2.4.1 Arunta Complex

The Arunta Complex consists of metamorphic rocks intruded by granitic, mafic and ultramafic rocks. The metamorphic rocks include schists, schistose gneiss, porphyroblastic augen gneiss, metaquartzite, marble, calc-silicate rock and amphibolite (Forman et al., 1967). In parts of the nappe complex these rocks are represented by their retrograded equivalents.

Six samples of gneiss from the front of the nappe complex were dated by Rb/Sr measurements and the results indicated the age of the formation of the gneiss somewhere between 1500 million years to 1900 million years (Forman, 1971, reports of dating carried out by Miss Bennet).

2.4.2 Heavitree Quartzite

The Heavitree Quartzite is predominantly a silicified quartz sandstone with minor amounts of conglomerate, conglomeratic sandstone or arkose which generally occur in its basal part. The middle part is generally a massive to thick bedded coarse to medium grained quartzite with occasional thin bands of siltstone. Sedimentary structures are generally found in this part where the quartzite is relatively undeformed. The upper part is a platy quartzite with beds thinning

upwards in the sequence. The thickness of the Heavitree Quartzite is variable in the area of the nappe complex but an average estimate of its maximum thickness is about 300 metres.

The quartzite has been tentatively assigned an Upper Proterozoic or Adelaidean age (Forman et al., 1967; Forman, 1971). The term Proterozoic is used for rocks between the fossiliferous Cambrian sediments and the unconformity at the base of the Amadeus Basin sequence. The provisional isotopic ages of a few samples of the sedimentary rocks suggest that the rocks below the base of the Cambrian are not more than about 1400 million years old (Wells et al., 1970).

2.4.3 Bitter Springs Formation

This formation conformably overlies the Heavitree Quartzite and in its basal part consists of shale and siltstone interbedded with thin quartzite and dolomite. Carbonate rocks (predominantly dolomite) with thin interbeds of shale overlie the basal beds. The only complete section of this formation at Ellery Creek outside and west of the area of the nappe complex (Prichard and Quinlan, 1962) is 800 metres thick. A part of this formation is present in the nappe complex and although it has been subdivided into two members elsewhere, it is not possible to recognise those in the nappe complex because of complicated folding and thrusting. The formation is also regarded as of Adelaidean age.

2.5 Orogenies and Metamorphism

Two orogenies with associated episodes of metamorphism have been recognised in the area of the nappe complex. The older, the Arunta Orogeny, is defined as the orogeny which folded and metamorphosed the Arunta Complex before the Heavitree Quartzite was deposited (Forman

et al., 1967). During this orogeny the Arunta Complex was isoclinally folded about north-south axial planes and was tightly refolded about east-west axial planes and the grade of metamorphism reached upto amphibolite facies. The orogeny occurred about 1700 million years ago (Forman, 1971).

For the younger orogeny Forman (1965) introduced the term 'Alice Springs Orogeny'. The development of the Arltunga Nappe Complex occurred in this orogeny by the folding and thrusting of the Arunta Complex, the Heavitree Quartzite, and the Bitter Springs Formation. The sediments above the Bitter Springs Formation and some of it were detached from the nappes and moved southward over a major plane of tectonic transport within the Bitter Springs Formation. The metamorphism that accompanied the orogeny is slight in the front of the nappe complex but is of greenschist facies grade deeper in the nappes. This metamorphism was also responsible for the retrogression of the rocks of the Arunta Complex. The age of the orogeny has been deduced both by dating the unconformity in the Amadeus Basin and by isotopic dating of the metamorphic minerals formed during the orogeny. The former is based on paleontological and stratigraphical grounds and suggests a probable Carboniferous age for the orogeny, the latter is based on dating the muscovite from four samples of metamorphosed Heavitree Quartzite and one whole rock sample from the Bitter Springs Formation; these were found to be of Early to Middle Carboniferous (358-322 m.y.) age (Stewart, 1971).

2.6 Structure

The nappe complex according to earlier interpretation (Forman et al., 1967) contained two fold nappes; the underlying Winnecke Nappe and the overlying White Range Nappe. In the most recent interpretation (Forman, 1971) the lower nappe has been referred to

as the Ruby Gap Nappe (Fig. 2.2) and it has been suggested that it formed by overthrusting from the north. It has also been suggested that the upper nappe or the White Range Nappe formed by a combination of recumbent folding and overthrusting as it contains extensive areas of overturned rocks and that it was transported at least 24 km across the strike.

The structural features of the nappe complex are shown in Figures 2.2 and Map 3. Map 3 is a structural relief diagram drawn on the basis of the structural interpretation of the complex by Forman. The diagram shows the surface of contact, unconformable or thrust, of the Arunta Complex with either the Heavitree Quartzite or the Bitter Springs Formation recurring at various levels, called structural levels, each of which has been shown on the diagram by a different colour.

The nappes have a core of metamorphic rocks of the Arunta Complex and an envelope of the Heavitree Quartzite and the Bitter Springs Formation. Forman (1971) has shown that there is a sharp discontinuity in style and pattern of deformation along the thrust fault surface that defines one of the lower thrust nappes. The autochthonous rocks beneath the thrust are folded about east-west axes and the southern limb of each fold is overturned; the allochthonous rocks above the thrust are isoclinally folded about north-south axes and display prominent northerly lineation due to the elongation of the quartz grains. Structurally higher in the inverted Heavitree Quartzite at the base of the upper most nappe elongated conglomerate pebbles also trend north-south.

The nappes front to the south where deformation of basement and cover rocks is slight. They root to the north in a belt of crystalline rocks of the Arunta Complex originally in the amphibolite facies grade of metamorphism but retrograded to the greenschist facies. North of the retrograded zone a belt of rocks in the granulite facies and amphibolite facies is exposed. The Bouguer gravity anomalies also increase strongly

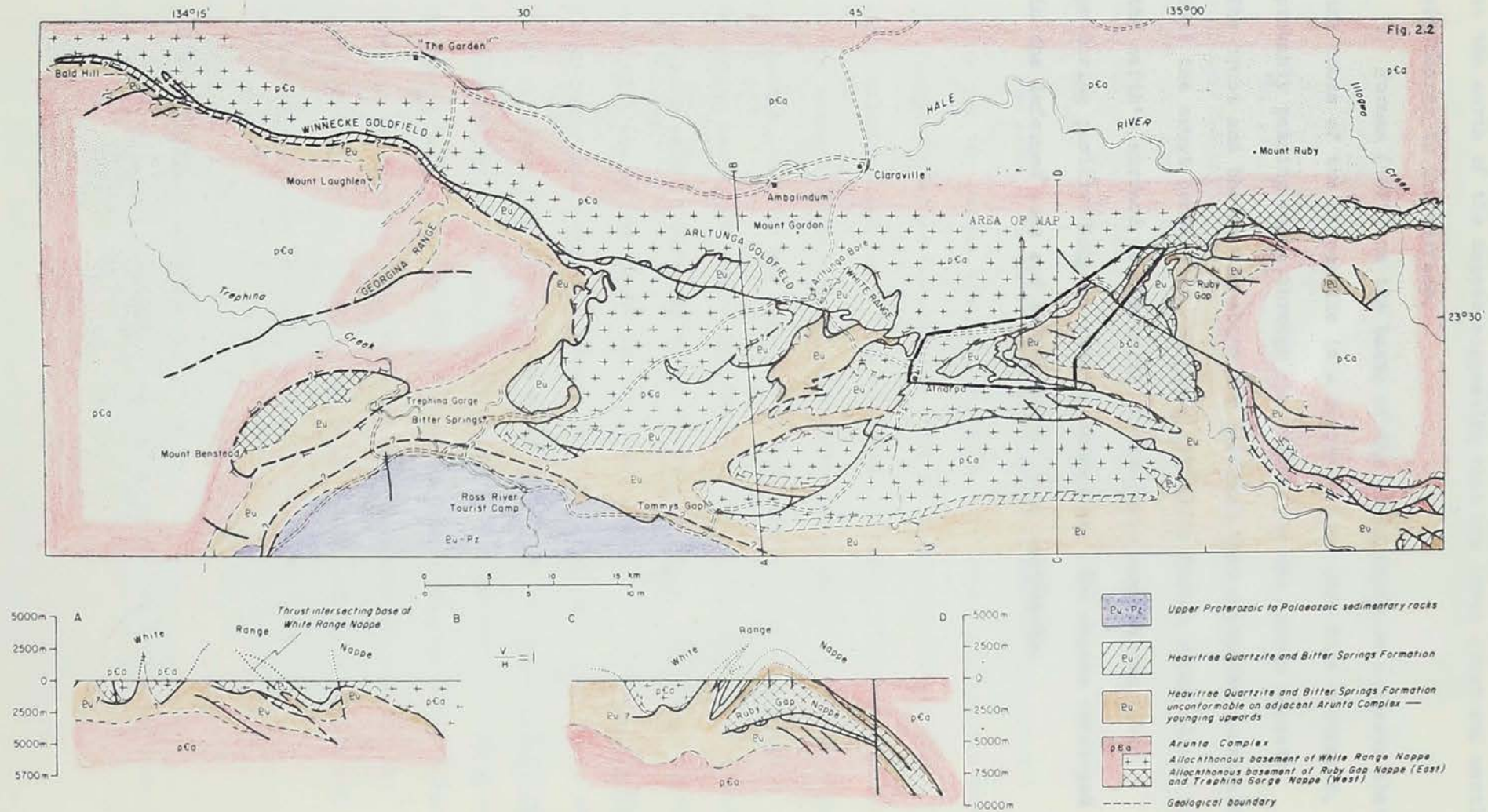

Fig. 2.2. GENERALISED GEOLOGICAL MAP OF THE ARLTUNGA NAPPE COMPLEX
(FROM B.M.R. Record 1971/66, modified after Forman 1971)

to the north of the nappes suggesting that the lower crust and mantle are nearer to the surface.

Forman (1971) on the basis of the above evidence suggests that the roots of the nappes lie in a deformed zone that dips northward, probably passing right through the crust into the mantle beneath. The crust and the mantle above the deformed zone travelled southward over the crust beneath it, bringing granulite facies rocks closer to the earth's surface to the north of the nappe complex and also producing positive Bouguer gravity anomalies. The nappes developed in the deformed zone and subsequently moved southwards.

CHAPTER 3

STRATIGRAPHY AND STRUCTURE OF THE ATNARPA RANGE AREA

3.1 Introduction

3.1.1 Location and extent

The Atnarpa Range area (Map 1) lies in the eastern part of the Arltunga Nappe Complex (see Fig. 2.2) and extends about 19km eastwards from about half a kilometre west of Atnarpa homestead covering hill ranges that rise about a couple of hundred metres above the local plains.

The name, Atnarpa Range, has been introduced by the present author for the ranges trending eastwards from about a kilometre east of Atnarpa homestead because they did not have any official geographical names and names have also been proposed for certain parts of the Atnarpa Range area to facilitate reference to various localities within the area for the purposes of this study. The hill range extending eastwards about 5km. from about a kilometre east of Atnarpa homestead will be referred to as the Western Hill, the valley adjoining this hill eastwards, about 3km long and 1.5km wide, as the Small Valley, the arcuate range with a northern limb and a southern limb extending about eastward from east of the Small Valley as the Eastern Hill Range, and the valley in between the two limbs of the Eastern Hill Range as the Large Valley. A vehicle track which lies alongside the northern front of the Atnarpa Range for most of its length and crosses the northern limb of the Eastern Hill Range about 17km east of Atnarpa Homestead will also be used for reference to the area.

3.1.2 Methods of mapping

The detailed geological mapping on which the following description

of the stratigraphy and the structure of the Atnarpa Range area is based was carried out during the winter months of the years, 1969, 1970, and 1971, and in all about six months were spent in the field. The geology was plotted at a scale of about 1:23,000 on aerial photographs enlarged to a scale double of the original. The geology was then transferred to a controlled base and during the transferring the distortion of the scale on the aerial photographs was eliminated radially by eye. The geological map (Map 1), one of the illustrations in this thesis, is at a scale of 1:15,000 and has been enlarged to this scale from its original compilation. Additional orientation data for structures was obtained subject to the availability of good exposures besides that recorded during the course of detailed mapping.

3.2 Stratigraphy

Like other parts of the Arltunga Nappe Complex, in the Atnarpa Range area also the basement rocks are part of the Precambrian Arunta Complex and the cover rocks representing the lower most part of the Amadeus Basin sequence are of Upper Proterozoic age. The junction between the basement and the cover rocks in the area is either marked by an unconformity or a thrust fault or is apparently conformable where the rocks have undergone strong deformation.

3.2.1 Basement rocks

In the area of the Arltunga Nappe Complex as well as in the Atnarpa Range area these rocks are part of the Precambrian Arunta Complex and comprise a variety of igneous and metamorphic rock types. These rocks are extensively present on both sides of the Atnarpa Range and in the Small and Large Valleys. At other places in the range they crop out in areas of small dimensions situated within the

cover rocks. Criteria of establishing a stratigraphy are lacking in these rocks, moreover such an attempt would have required coverage of a large area of exposure of these rocks which was beyond the scope of the present study. Felsic to mafic igneous and meta-igneous rocks are present around the Western Hill and in the Small and Large Valleys. On the northern limb of Eastern Hill Range metamorphic rocks of dominantly quartzo-feldspathic composition are present and are therefore light colored. These have been separated on Map 1 from the other metamorphic rocks lying to the north of these rocks. The mineral assemblage of the basement rocks in the Atnarpa Range area usually consist of quartz, feldspar (predominantly microcline and albite), muscovite, chlorite and epidote. Biotite generally occurs in rocks lying to the north of the quartzo-feldspathic rocks on the northern limb of the Eastern Hill Range and amphibole in the mafic rocks.

3.2.2 Cover rocks

The distribution of the cover rocks is shown on Map 1. The stratigraphy of the cover rocks which comprise the Heavitree Quartzite and the overlying Bitter Springs Formation has been found to be of great importance in the understanding of the structure. Details of stratigraphy are shown in Fig. 3.1, which is a composite representation of it, prepared from observations and measurements at a number of localities, particularly in the western half of the Atnarpa Range area. The following description of the lithology of the cover rocks looses its validity to some extent on the northern limb of the Eastern Hill Range as the metamorphism modifies the lithology and obliterates the sedimentary structures.

Fig. 3.1 Columnar Section of Cover Rocks in Western Arnarpa Range

3.2.2.1 Heavitree Quartzite This is the formation with which the present study is mostly concerned. It is extensively present in the Atnarpa Range area and crops out in the form of a prominent ridge or range, usually with a gentle dip slope and a steep escarpment. Its unconformable contact with the underlying basement rocks is marked at a number of localities by the presence of a conglomeratic horizon. On the basis of lithology the Heavitree Quartzite has been subdivided into a basal, a middle and an upper member and has been mapped accordingly (Map 1). In parts of the northern limb of the Eastern Hill Range the quartzite is extensively flattened and, there, it has not been possible to separate the individual members.

The basal member consists of conglomerate, loosely cemented, generally coarse grained arkose and pebbly sandstone, these are interbedded. Thin bands of siltstone are associated occasionally with it. The conglomerate attains a maximum thickness of 3 metres and its pebbles are angular to sub-rounded and about 3cm. across in size. At places where the conglomerate is strongly deformed the pebbles are flattened and elongated. In the northern part of the Western Hill the conglomerate contains fragments of vein quartz as much as 12cm. long. The arkosic part of the basal member is light to medium gray and varies in thickness. The thickness of the member as a whole varies from about 3 metres to about 8 metres. The member is not well developed at some localities such as in the vicinity of Specimen Localities 281, 155 and 262 on the south and east facing escarpments of the Eastern Hill Range. This may be due to the irregularities on the basement surface on which the cover rocks were being deposited.

The middle member is very light gray when fresh but weathers to pale orange and grayish orange. It is gritty and very coarse grained at

the base. Upwards in the section it grades from coarse to medium grained and also from massive to thick bedded. It is extensively cross bedded in its lower part, and attains a maximum thickness of about 100 metres.

The upper member is platy and grades from thick bedded to thin bedded upwards in the section. It is darker toned than the middle member, is medium gray when fresh but weathers to purplish and bluish gray shades of color. Ripple marks are occasionally present. It attains a maximum thickness of about 140 metres. The topmost part of this member is marked by the presence of about 3 metres to 8 metres thick, white, soft shales. X-ray diffraction studies have shown that the shales predominantly consist of quartz and very subordinate amounts of illite and kaolinite.

3.2.2.2 Bitter Springs Formation The formation conformably overlies the Heavitree Quartzite and although the change in lithology from the one formation to the other is not abrupt, it is marked by the absence of the slabby character of the bedding, appearance of a brownish tinge, most probably due to increase in the iron content, on the weathered surfaces of the massive and thick bedded rocks and the presence of dolomite. At the contact of the formation with the Heavitree Quartzite a dark brown lateritic layer about 1 to 2 metres thick is occasionally present. The formation consists of quartzite interbedded with olive gray shales, siltstone, and thin irregular layers of dolomite. Only the lower most part of this formation with a maximum thickness of about 90 metres is exposed in the Atnarpa Range area because the formation is truncated by thrust faults and overlain either by the Arunta Complex or the Heavitree Quartzite. The formation occupies a much less part

of the mapped area (Map 1) in comparison to the Heavitree Quartzite.

3.3 Metamorphism

In the Atnarpa Range area metamorphism is closely associated with zones of dislocations defined by thrust faults but it also increases gradually from south to north. This implies that the metamorphism is of two types, the dynamic (Harker, 1939) or the dislocation (Turner and Verhoogen, 1960) type and the regional type, although the effects of the former are more pronounced than the latter. As a result of this metamorphism which is of low grade, the sediments of the cover rocks were subjected to a progressive metamorphism and the basement rocks were either altered or subjected to a retrogressive metamorphism.

3.3.1 Basement rocks

On a mesoscopic scale a foliation and a lineation develops in the igneous rocks and this becomes strongly marked in dislocation zones. Augen structure becomes more pronounced in the foliation with the proximity to the thrusts but finally disappears as the relics of grains, which form 'eyes', are shattered and ground down. On the northern limb of the Eastern Hill Range where the rocks are foliated and lineated, the coarse foliation is changed to very closely spaced planes and the lineation becomes strongly streaky in the vicinity of the thrusts suggesting strong flattening of the rocks.

On a microscopic scale the foliation in a high degree of its development is marked by the parallel arrangement of elongate and strained grains of quartz and micaceous minerals, which wrap around the resistant felspar grains (Plate 3.13b). The rocks with this type of foliation occur on the north side of Western Hill and the Small Valley.

Further north on the northern limb of the Eastern Hill Range quartz recrystallizes into small polygonal grains and these grains along with the micas wrap around the cracked and sericitized felspar grains (Plates 3.14b, c and 3.15b). Within 2 metres of the thrust contact felspars are rarely observed and the rock is quartz-mica ± chlorite schist (Plate 3.15a). The changes start in brecciation and granulation of the grains or in their plastic deformation leading to flattening and elongation and finally depending on the conditions of metamorphism to their complete recrystallization or neomineralization. Felspars are sericitized and saussuritized leading to the formation of white mica and epidote respectively and at many localities this alteration is complete in many of the grains. The sericite formed as a result of the alteration of felspars becomes coarser towards the north and distinct muscovite grains are the final product. Where biotite occurs in the rocks it alters to chlorite. In the mafic rocks amphibole alters to chlorite but nowhere extensive alteration of amphiboles is observed. The cleavage in micas or felspars is either occasionally curved or deformed into conjugate kinks. The effects of retrogression in the basement rocks are found throughout the mapped area but their intensity diminishes away from the thrusts and in the south as compared to the north. In the north, on the northern limb of the Eastern Hill Range and in the vicinity of Specimen localities 270 and 271 (Map 1) quartz veins have developed along the foliation planes of the basement rocks (Plate 3.6b) indicating mobility of rocks as a result of the increase in the metamorphism in this area.

3.3.2 Cover rocks

In the cover rocks the mesoscopic effects in the southern part of the Atnarpa Range area are marked by the brecciation of the quartzite

and the obliteration of the sedimentary structures like bedding. In the more deformed rocks within a zone of two to three metres along thrust faults a flinty crush rock or microbreccia of dark gray color develops. It is very fine grained and has no layering. Microscopic study of this rocks has shown that it is traversed by thin veins of glassy rock also referred to in the literature as Psuedotachylyte (see Plate 4.4a) although there is confusion about the actual meaning of this term with regard to its genetic significance (see Christie, 1960). In similar circumstances of occurrence this type of rock, i.e. the flinty crush rock, on the northern limb of Eastern Hill Range is well laminated and lineated and there is a complete gradation from this rock to the quartzites lying below and away from the thrust (see Plate 4.10). The rock is very similar in appearance to a mylonite but microscopic observations have shown complete recrystallization of the quartz grains and the presence of a granoblastic texture, so that blastomylonite is a better term for this rock (see Christie, 1960). This indicates that the physical conditions of metamorphism must have varied from south to north in the area. The other evidence for such a variation is that the foliation and lineation in the quartzite, which is due to the flattening and elongation of the grains, is restricted to narrow zones of dislocation on the north side of the Western Hill (see Map 1) but is widespread and penetrative further north on the northern limb of the Eastern Hill Range. The shales in the Bitter Springs Formation also acquire a distinct phyllitic sheen on their cleavage surfaces northwards in the Atnarpa Range area. In the northern most part of the area the sheen becomes much stronger due to the growth of muscovite and chlorite from their clayey counterparts. The detrital quartz in the shales also recrystallizes into strain free polygonal

grains (see Plate 3.14a). The shales in this area become phyllites. The microstructural development in the quartzite will be described in more detail in the subsequent chapter on the microfabric study of the quartzite.

3.4 Structure

The structure of the Atnarpa Range area is dominated by the development of the thrusts and therefore this section starts with their description.

3.4.1 Thrusts

The distribution of the thrusts in bold lines has been shown on Map 1. Map 1 also shows that the boundary of the cover rocks on both flanks of the Atnarpa Range is always marked by a thrust. Several thrusts of about the same orientation give rise to an imbricate structure resulting in a pile of thrust sheets within the range as well as in the small area east of Atnarpa homestead. The thrust sheets or slices consist of either both the basement and the cover rocks or one of them. Fig. 3.2 shows seven such sheets which were mapped and in Map 2 the sheets are shown in structure sections, six of the sections drawn across the range and the seventh along it. The demarcation of the sheets on the northern limb of the Eastern Hill Range above sheet no.3 is somewhat arbitrary owing to the effects of metamorphism which obliterates the sedimentary features of the rocks. The structure of the Atnarpa Range area is further complicated as the thrusts are folded and their strike parallels at many places that of bedding or foliation.

The thrust contacts in the southern and central parts of the Atnarpa Range area are marked by extensive brecciation of the Heavitree Quartzite

FIGURE 3.2

An enlarged copy of this figure is placed with the maps.

Fig. 3.2.

MAP SHOWING THE THRUST SHEETS, ATNARPA RANGE AREA

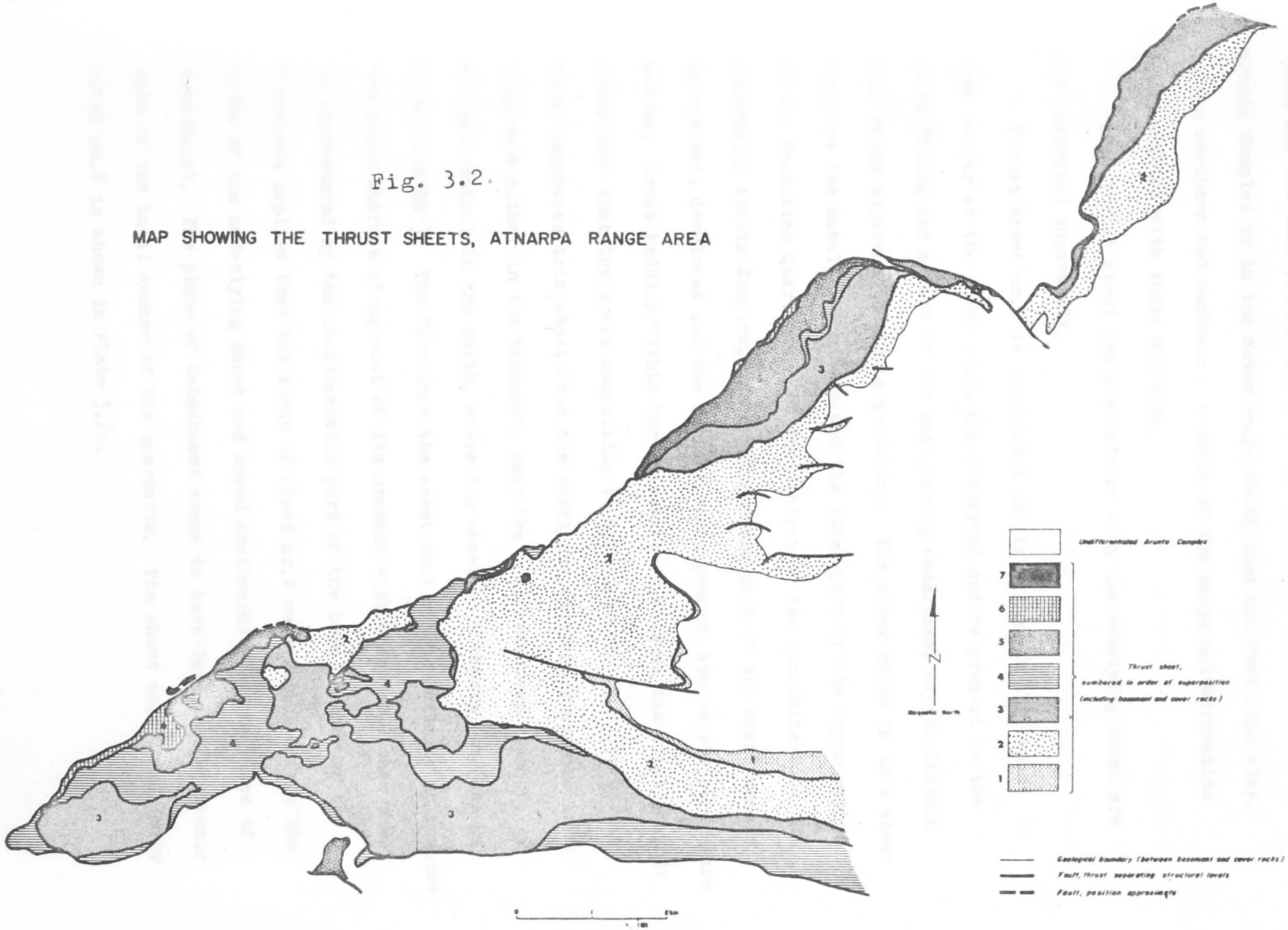

giving rise to a dark gray flinty crush rock with psuedotachylitic veins and the near pulverization of the soft rocks either in the Arunta Complex or in the cover rocks which look and feel like clay. In the northern and northeastern parts of the range mylonitization is associated with these contacts.

Each thrust sheet and its contact with the overlying sheet are now described separately.

Thrust sheet no.1 is restricted in its extent in the mapped area so far as the cover rocks are concerned and is present on the north facing and a part of the east facing escarpment of the Eastern Hill Range adjacent to the Large Valley. The cover rocks in this sheet comprise the basal, the middle and the lower part of the upper member of the Heavitree Quartzite. At the contact of the quartzite with the underlying Arunta Complex, the conglomeratic part of the basal member is not well developed and the pebbles where present are only a centimetre across. Cross bedding within the quartzite as well as its stratigraphic order show that the rocks comprising it are right way up. The thrust which separates this sheet from the overlying sheet No.2 appears to originate either in the basement, near the basement-cover contact, or at that contact in the north, where the sheet no.1 tapers out (see Map 2, section EE'). The fact that the sheet no.1 starts building up towards the south whereas along most of its contact with sheet no.2 that sheet is represented by the conglomeratic part of the basal member of the Heavitree implies that the rocks of sheet no.2 were detached from the rocks of the underlying sheet and moved southwards over the plane of detachment. The plane of detachment seems to have lain in the arkosic part of the basal member of the quartzite. The sheet no.1 overlain by sheet no.2 is shown in Plate 3.2c.

Thrust sheet no.2 is of a large extent and is present along the E.H.R.,[2] along the eastern and northern borders of the Small Valley, and in a small area in the northeastern protrusion of the Western Hill (see Fig. 3.2). The sheet comprises both the basement and cover rocks but in Fig. 3.2 only the cover rocks have been delineated in it as the limit of this sheet in the basement rocks is indeterminable. The unconformity between the basement and cover rocks within this sheet is shown in Plate 3.9c, and the arkosic and conglomeratic beds of the basal member of the Heavitree Quartzite are generally present above it. In the central part of the E.H.R. and including the eastern part of the Small Valley a complete section of the Heavitree Quartzite with a part of the Lower Bitter Springs Formation overlying it is present in this sheet. (It has been stated in the earlier parts of this chapter that nowhere in the Atnarpa Range area a full section of the Bitter Springs Formation is developed). Cross bedding in the middle member and ripple marks in the upper member of the quartzite as well as the normal sequence of units in the cover rocks prove that the stratigraphic order in them is undisturbed in the E.H.R. In the other two areas of exposure of this sheet the Bitter Springs Formation and the upper member of the quartzite are partly present. It has not been possible to establish the nature of stratigraphic order in these areas due either to poor exposure or lack of sedimentary structures. The only point worth mentioning in this connection is the presence of the White Shale horizon overlying the Bitter Springs Formation beds along the thrust contact of this sheet with the sheet no.3 in the area along the northern border of the Small Valley. On the footwall of the thrust, which defines the contact of

---

2. Eastern Hill Range

this sheet with the overlying sheet no.3 or no.4, lie either the White Soft Shales, being the topmost part of the quartzite sequence, or another horizon of similar nature in the Bitter Springs Formation. These horizons due to their incompetent and plastic nature facilitated movement on the surface of the thrust. The hanging wall of the thrust is either represented by the middle member of the quartzite in sheet no.3 or by the Arunta Complex in sheet no.4. The thrust is folded about the E.H.R. and plunges westward beneath the Small Valley. It reappears due to reversal of the plunge on the northern side of the Small Valley and partly on the northeastern slope of the Western Hill as well as around a small tectonic window of thrust sheet no.2 in the northeastern protrusion of Western Hill. Plate 3.3a shows this sheet overlain by sheet no.3 and or sheet no.4 in the Small Valley and in the northeastern part of the Western Hill. Plate 3.4a and plate 3.5a show this sheet overlain by sheet no.3 in the southern and northern limbs of E.H.R. respectively. Map 2, cross sections CC' to GG' show the structural relationship of this sheet with the sheets nos. 3 and 4.

Thrust sheet no.3 is also of a large extent. It crops out in the Small Valley in narrow bands along the thrust separating it from the sheet no.2. It is also present on both the limbs of the E.H.R., along the eastern border of the Western Hill, in the east-west hill range south of the Small Valley, and in the northeastern part of the Western Hill. The sheet comprises mostly the Heavitree Quartzite of which a nearly complete section develops south of the Small Valley. Cross bedding in the middle member of the quartzite (Plate 3.3c), ripple marks in the upper member of the quartzite (Plate 3.1c) and the normal stratigraphic order of the units (Plate 3.1b) show that the cover rocks in this sheet are also right way up. On the northern limb of the E.H.R. metamorphism obliterates sedimentary features of the rocks and only the

gross stratigraphic order within the sheet supports the aforesaid point. In the Small Valley and in the adjacent Western Hill and on the northern limb of E.H.R. the footwall of the thrust separating this sheet from the overlying sheet no.4 is in the middle member of the quartzite and the hanging wall in the Arunta Complex (Plates 3.3a and 3.5b). On the southern limb of the E.H.R. the foot wall remains in the same horizon but the hanging wall is the conglomerate of the basal member of the quartzite. South of the Small Valley the thrust migrates upwards in a step-like fashion in the Heavitree Quartzite sequence so that the topmost part of the quartzite lies at its foot wall (see Map 2 sections CC' and DD'). In the Western Hill exposure of this sheet the thrust also migrates upwards with the result that the White Soft Shales lie at the footwall and the middle member of the Quartzite at the hanging wall (Plate 3.1b). This could also be due to the effect of topography in this area as the Western Hill is at a higher elevation than the Small Valley (see Map 2 Section GG'). The thrust branches off and rejoins other thrusts as shown in Fig. 3.2 and is also folded about two axes, roughly speaking for the present east-west and north-south. Its folding is shown in sections CC', DD' and GG' of Map 2. It reappears due to reversal of plunge and erosion around small tectonic windows in the Small Valley and a large tectonic window in the Western Hill. These windows are mostly shaped as elongated domes. It is also present on both sides of sheet no.3 on the eastern border of Western Hill on account of the folding. Map 2 shows the structural relationship of this sheet with the other sheets.

Thrust sheet no.4 comprises the middle member of the quartzite in the Western Hill, the Arunta Complex and the basal and the middle member of the quartzite in the Small Valley and on the northern limb of E.H.R., and a nearly complete section of the quartzite on the southern

limb of E.H.R. Cross bedding and ripple marks (Plate 3.4c), where preserved, as well as the normal stratigraphic order of various rock units in this sheet bear testimony to the fact that the cover rocks in this sheet are right way up in the Small Valley and on the southern limb of the E.H.R. The basement-cover contact in this sheet while preserved at some localities in the Small Valley like at Specimen Locality 117 (Map 1) is disturbed at other localities in the valley such as the one adjacent to Specimen Locality 259 (Map 1), and also on the eastern slope of the Western Hill at Specimen Locality 255 (Map 1). Some movement of the normal fault type is suspected at the contact because of two reasons, the first being the absence of the conglomeratic part of the quartzite and the second being the very brecciated nature of the quartzite lying above the contact. The stratigraphic order in the quartzite representing this sheet in the Western Hill is not clear because, (a) sedimentary structures in it have been destroyed by the brecciation, it has undergone, (b) the lone occurrence of one of its members in the hill, and (c) the disturbed nature of its contact with the Arunta Complex where exposed. The occurrence of basal conglomerate under it at Specimen Locality 295 (Map 1) in the northeastern part of the Western Hill is the only evidence for its being right way up stratigraphically but does not carry much weight in the absence of more supporting evidence. Along the thrust which separates this sheet from the overlying sheets in the Western Hill the middle member of the quartzite in this sheet is in contact with the Arunta Complex or the basal member of the quartzite in the overlying sheets. On the southern limb of E.H.R. the upper member of the quartzite or the lower most part of the Bitter Springs Formation in this sheet is in contact with the Arunta Complex of the overlying sheet along the thrust. The thrust is folded in the Western

PLATE 3.1

(a) Western end of the Atnarpa Range; Western Hill anticline plunging westwards towards Atnarpa homestead; thrust contact between cover rocks and basement rocks lying in the valley shown by red line; thrust contact between thrust sheet no.3 and no.4 also shown.

(b) Thrust contact between thrust sheets no.3 and no.4 in the Western Hill in line with hammer head; White Soft Shales at the foot wall, middle member of the Heavitree Quartzite at the hanging wall.

(c) Asymmetric ripple marks in the upper member of the Heavitree Quartzite in thrust sheet no.3 in the Western Hill.


3
4

PLATE 3.2

(a) Thrust contact, shown by red line, between thrust sheets nos. 4 and 5 on the north side of the Western Hill.

(b) Looking west, thrust contact shown by red line between thrust sheets nos. 4 and 5 in the area east of (a) above and at Specimen Locality 294. Dark gray flinty crush rock with a darker tone than the underlying white quartzite forms the upper most part of the sheet no.4, Arunta Complex in the valley, and the basal member of the Heavitree Quartzite including conglomerate forms the low ridge to the right.

(c) Large Valley in the fore ground, Eastern Hill Range in the background and thrust contact, shown by red line, between thrust sheets nos. 1 and 2. Scarp to the left is along a fault.


5
4
5
4


4


3
2
1

PLATE 3.3

(a) Looking northwest through the Small Valley, thrust contacts marked by a red line and thrust sheets numbered in order of superposition.

(b) Thrust contact, marked by red line, between thrust sheets nos. 3 and 4 in the Small Valley; the Heavitree Quartzite at the foot wall and the Arunta Complex at the hanging wall.

(c) Cross bedding in the Heavitree Quartzite in thrust sheet no.3 in the Small Valley.

PLATE 3.4

(a) Looking east, thrust contact indicated by a red line between thrust sheets nos. 2 and 3 on the southern limb of the Eastern Hill Range; White Soft Shales at the foot wall, middle member of the Heavitree Quartzite at the hanging wall.

(b) Looking west, thrust contact indicated by a red line between thrust sheets nos. 3 and 4 on the southern limb of the Eastern Hill Range; middle member of the Heavitree Quartzite at the foot wall, conglomerate at the hanging wall.

(c) Oscillation ripple marks in the quartzite in thrust sheet no.4 on the southern limb of the Eastern Hill Range.


2
3


3

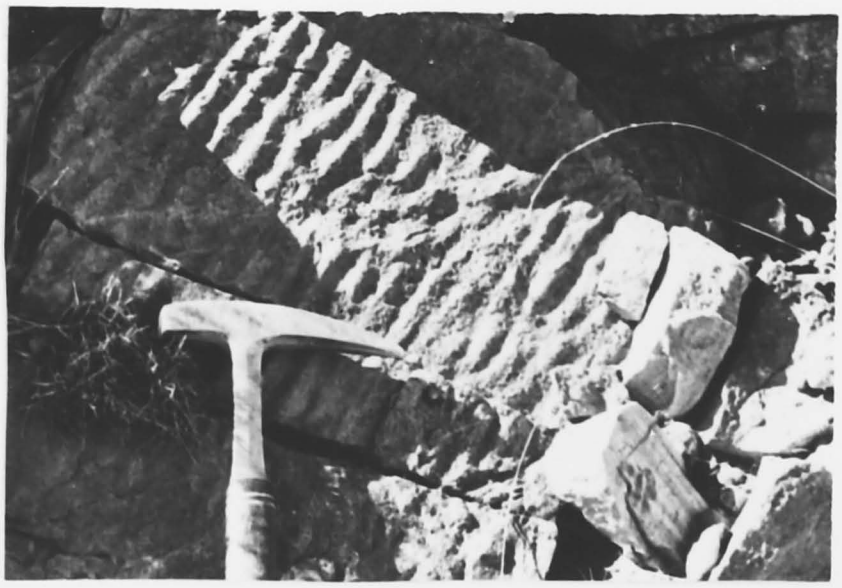

PLATE 3.5

(a) Looking northeast, thrust contact indicated by a red line between thrust sheets nos. 2 and 3 on the northern limb of the Eastern Hill Range; upper part of the Heavitree Quartzite and the Bitter Springs Formation overlain by the middle member of the Heavitree Quartzite.

(b) Looking northeast, middle member of the quartzite in thrust sheet no.3 overlain by the Arunta Complex in thrust sheet no.4, upper member of the quartzite in thrust sheet no.5? overlying the Arunta Complex in the sheet no.4; on the northern limb of the Eastern Hill Range.

(c) Looking southwest, the quartzite in thrust sheet no.2 overlain by the Arunta Complex and the quartzite of thrust sheet no.3 on the northern limb of the Eastern Hill Range in the vicinity of the Specimen Locality 270.


3
2


5
4
3


1
2
3

Hill.

Thrust sheets nos. 5, 6, and 7 crop out in narrow belts on the northern front of the Western Hill and thrust sheet no.5 also in an isolated outcrop in the valley south of the Atnarpa Range. The sheets nos. 5 and 6 have also been shown on the northern limb of E.H.R. in Fig.3.2, but as explained earlier their demarcation is rather questionable. In the Western Hill and in the isolated outcrop these sheets consist of the Arunta Complex and the basal and the middle member of the quartzite. Cross bedding at two localities, one of them being Specimen Locality 189 (Map 1) and the normal stratigraphic order of the rock units in these sheets suggest that the rocks in each of these sheets young upwards. On the northern limb of E.H.R. the presence of the Bitter Springs Formation beds on top of the upper member of the quartzite in sheet no.5 is the only evidence for its being right way up. The fault separating thrust sheet no.5 from thrust sheet no.4 in this area is a low angle normal fault or lag along which the sheet no.5 slid down with respect to the sheet no.4 (see Map 2, cross section FF'). There can be another possibility that the fault of the kind described above displaced rocks within one sheet, in that case sheets nos. 4 and 5 would be one sheet and it would not be necessary to show the fourth thrust from the left in the section FF' of Map 2. The first possibility is preferred because thrust sheet no.5 consists of three small thrust slices which because of their size and slight relative movement have been grouped into one sheet.

3.4.2 Planar structures, Lineations and Folds

3.4.2.1 Introduction The factors that contribute towards the development of these structures as well as influence their study are, (a) increase in metamorphism from south to north in the Atnarpa Range

area and also in zones of dislocation, (b) thrust faulting, which divides the Atnarpa Range area into several thrust sheets thereby necessitating the study of the structures in different compartments, and as a result of this faulting the rocks are more deformed in the zone of thrusting than outside, and (c) the presence of competent and incompetent rocks in the area which are differentially strained during deformation, for example the thin bedded strata in the upper part of the Heavitree Quartzite is less resistant to folding because of the numerous slip planes available in it than the thick or massive beds in the middle part of the quartzite (Weiss and McIntyre, 1957, have described differential deformation of rocks at Loch Leven).

For the understanding and deciphering the deformational history of an area it is important that age relationships between the structures be established. The criteria of overprinting and style have been used by English speaking geologists during the last three decades for this purpose. Weiss and McIntyre (1957) and Turner and Weiss (1963) have emphasized that structures of similar style and similar patterns of preferred orientation should be regarded to be of the same generation. Means (1963 and 1966) and Williams (1968) have shown that this assumption is not universally applicable. Hobbs (1965) points out that the style may or may not be unique from one generation of structures to another but coupled with the pattern of preferred orientation it may provide a useful feature for the use in delineation of deformation phases. He goes on further to say that with these criteria it is possible to separate structures into a number of groups each characterized by a certain style and certain pattern of preferred orientation but the erection of a sequence of deformation phases may prove difficult or even impossible in complex areas where unique styles coupled with unique patterns of preferred orientation are not developed.

An attempt has been made to separate the structures in the Atnarpa Range area into groups on the basis of style and their mutual relationships although the factor of orientation has also been considered. Then, where structures of one group have been found to overprint those of the other group, the former have been considered to be younger than the latter and of a different generation. It has been observed in the area that as the physical conditions of deformation change from one part of the area to the other the folds change their style but there is no indication that the phase of deformation has changed. The study of the mutual relationships of the structures has been hampered due to the paucity of axial plane structures and one group of folds. The grouping and mutual relationships of the structures have been summarised in table 3.1.

3.4.2.2 Bedding S This is the dominant planar structure in cover rocks in the western, southern and central parts of the Atnarpa Range area. Sedimentary structures such as cross bedding and ripple marks remain preserved at a number of localities and the lithologic layers of peculiarly sedimentary type are generally continuous and are stratigraphically in sequence representing bedding. In the areas mentioned above sedimentary structures are usually obliterated by brecciation at or near the faults.

3.4.2.3 Foliation S1 The term foliation is used here as defined by Turner and Weiss (1963, p.97). This is the first generation planar structure in the cover rocks. In the metamorphic rocks of the basement it is considered to have been generated in the same deformation phase as in the cover rocks but it can not be categorised a first generation structure because the history of deformation of those rocks is much

TABLE 3.1 : Summarised account of structures in the Atnarpa Range area

Generation, unknown in basement rocks (n)	COVER ROCKS			BASEMENT ROCKS		
	Group of Structures	Style	Mutual Relationship	Group of Structures	Style	Mutual Relationship
	Bedding	Lithologic layering of sedimentary origin	Folded by F_1 and F_2 folds	Pre-existing foliation	Metamorphic layering mostly unknown	Folded by F_1 folds
First generation in cover rocks equal to (n+1) generation in basement rocks	Foliation S_1	Preferred dimensional orientation of minerals, parallel arrangement of minerals, and mylonitic layering.	Transposes bedding. Folded by F_2 folds	Foliation S_1	Same as in cover rocks	Transposes pre-existing foliation, folded by F_2 folds, in igneous rocks develops as a first generation structure.
	Lineations L_1	Mineral and pebble elongation, streaks, fold mullions, slickensides	In the plane of S_1, parallel to F_1 axes Folded by F_2 folds	Lineations, L_1	Streaks, fold mullions	In the plane of S_1, parallel to F_1 axes Folded by F_2 folds.
	Folds F_1	Very tight to isoclinal	Fold bedding, F_1 axes parallel to L_1	Folds, F_1	Tight and similar	Fold pre-existing foliation, F_1 axes parallel to L_1.
Second generation in cover rocks equal to (n+2) generation in basement rocks	Lineation L_2	Crenulations or wrinkles, bedding mullions, very local dimensional orientation of minerals	Parallel to F_2 axes, Folded by F_3 folds	Lineations, L_2	Foliation mullions, crenulations	Parallel to F_2 axes, probably folded by F_3 folds.
	Folds, F_2	Nearly concentric to conjugate	Fold bedding and S_1; Fold L_1; F_2 axes parallel to L_2	Folds, F_2	Nearly concentric to conjugate	Fold S_1, fold L_1, F_2 axes parallel to L_2
Third generation in cover rocks equal to (n+3) generation in basement rocks	Folds, F_3	Open to gentle and nearly concentric	Fold bedding and S_1, fold L_2.	Folds, F_3?	Probably same style as in cover rocks	Probably fold S_1 and L_2

older than the cover rocks and is not yet fully understood. It is restricted to narrow zones along thrust faults in the western and central parts of the Atnarpa Range area but as compared to other sheets is less localized in thrust sheets overlying sheet no.4. On the north side of the Western Hill along the thrust contact between the sheet no.4 and either the sheet no.5 or the sheet no.6 the foliation is developed in the hanging wall of the thrust which mostly consists of either the Arunta Complex or the basal member of the quartzite. It has not developed in the foot wall of the thrust which represents the middle member of the quartzite. Instead the quartzite in the foot wall is brecciated and a flinty crush rock about 1 metre to 1.5 metres thick is formed along the thrust (see Plate 3.2b in which this rock at Specimen Locality 294 (Map 1) is shown). This implies that in this area the foliation tends to develop in the hanging wall of the thrust or it preferentially develops in certain lithologies. The feature has also been noted in the Small Valley and locally on the southern limb of the Eastern Hill Range. On the northern limb of the Eastern Hill Range the foliation is widespread and penetrative at all scales except in the southwestern part of thrust sheet no.2 where it is localized. It is only present in the northern part of the Large Valley in the basement rocks along their contact with the cover rocks.

In the western and central parts of the Atnarpa Range area the foliation in the cover rocks and especially in the quartzite develops as the quartz grains are first deformed into a shape resembling that of an oblate spheroid with one of the axes shorter than the other two equal or nearly equal axes and then finally transformed with increasing deformation into a much flattened triaxial ellipsoid. The foliation at this stage is defined by the parallel alignment of the planes of

flattening of the grains as well as their axes of maximum elongation (see Plates 4.5b and c) and this plane of flattening generally remains parallel to the bedding. These observations are supported by microscopic study and by the measurements made on the grains for determining strain. In the northeastern part of the Atnarpa Range area microscopic study shows that the flattened grains defining the foliation start recrystallizing and the process of recrystallization reaches its maximum intensity at or within a couple of metres of the thrusts (see Plate 4.10). The quartz mylonite which develops at the thrust contacts has a well defined foliation marked by layers less than a cm in thickness and varying in color but not in composition. On a microscopic scale this foliation is defined by the parallel arrangement of the aggregates of recrystallized quartz grains. In the phyllites representing the Bitter Springs Formation in this area a fine layering with layers less than a mm. thick represents the foliation. On a microscopic scale this foliation is defined by the preferred orientation of micas and aggregates of recrystallized quartz grains. The foliation in this area also remains generally parallel to the gross orientation of the lithologic units. No positive evidence has been observed in the Atnarpa Range area for the foliation to be an axial plane structure. The only folds which may have some genetic relationship with the foliation are shown in Plate 3.7a and b. These folds can only be observed in a small area north and northeast of Specimen Locality no.176 on the northern limb of the Eastern Hill Range. The existence of any axial plane structure is not clear from the fold profiles but a quartz elongation lineation is parallel to the fold axes.

The foliation is represented in the igneous rocks of the basement by a metamorphic layering developed as a result of their deformation

(see Plates 3.13a and b) and in the metamorphic rocks of the basement by the layering formed by transposition of the pre-existing foliation in those rocks. In the former case the layering exhibits augen shaped structures which with increasing deformation are also drawn out in the form of lenses parallel to the layering. Dimensional orientation of highly strained elongate quartz grains or of the aggregates of recrystallized grains with those of micaceous minerals defines the foliation. In the metamorphic rocks a weak axial plane fabric is already present (Plate 3.8b) and this seems to develop with the proximity to the thrust and finally transforms into a mylonitic layering transposing the earlier foliation. The relationship of the foliation S1 to the pre-existing foliation is not clear and differs in different parts of the area in that at some localities it seems to be a slaty cleavage whereas in others a strain slip cleavage (Plate 3.13c). The foliation is further illustrated in Plates 3.14 and 3.15

3.4.2.4 Lineation L1 It is represented by the following features:

(a) Direction of maximum elongation of quartz grains or pebbles. The grains and the pebbles generally resemble a triaxial ellipsoid in shape and are necked with tapered ends. The cobbles and boulders in the basal conglomerate of the quartzite in the White Range, a hill range about 5km. northeast of the Atnarpa Range, are also of similar shape (Forman, 1971, Plate 8). Hills (1963, p.92) states that when tested in tension, ductile metals approaching the rupture-point firstly contract to form a 'neck' and then rupture by a combination of shear-fractures and fibrous fractures, the latter being normal to the axis of the tension. The pebbles in the conglomeratic part of the quartzite in the Atnarpa Range are also ruptured normal to the axis of the elongation.

(b) Streaks and trains of parallel elongate aggregates of quartz and micaceous minerals. The quartz aggregates either consist of elongate grains and comparatively small, inequant, polygonal grains or entirely of the latter.

(c) Hinges of tight folds or fold mullions.

(d) Slickensides along surfaces of the thrust faults. This lineation has been shown on Map 1 by a line having three arrowheads and coming off from the line of fault. Where this line comes off from the strike line of the bedding it indicates slickensides generated during flexural slip folding. The slickenside lineation associated with thrust faulting may be analogus to the streaky lineation except that in rocks where it is developed it is restricted to a rather thin plate of rock.

The first two types of the lineation are locally developed like the foliation S1 on the north side of the western and central parts of the Atnarpa Range area. On the northern limb of the Eastern Hill Range the second type of the lineation is extensively present and at or in proximity to the thrust faults becomes strongly streaky so that the more deformed the rock is the more streaky the lineation becomes. In this area the third type shows up in sheet no.5 and becomes more and more extensive in the northeast. Although present in both the basement and cover rocks it is more obvious in the former. This lineation is parallel to the streaky lineation and the fold axes of F1 folds. Another important feature of this lineation is that it is predominantly contained in the north to northwest dipping foliation planes on the north side of the Atnarpa Range and is generally north trending although there are variations of about 45° from this trend towards east and west.

3.4.2.5 Lineation L2 It is dominantly characterised by crenulations (Plate 3.9a), wrinkles and bedding mullions all parallel to the fold axes of asymmetric and conjugate folds. It is well developed in the hinge areas of major folds with which it is sympathetic. In the Western Hill in thrust sheet no.3 at Specimen Locality 202 (Map 1) and in its vicinity where this lineation is well developed in the hinge area of a major fold quartz elongation is associated with it. Microscopic study of thin sections cut parallel to and normal to the lineation shows that the quartz grains are definitely elongate parallel to it but there is no significant elongation of the grains in the sections cut normal to it so that the deformed grains are more like a rod in shape than a tri-axial ellipsoid. Another type of lineation which is locally developed in the quartzite and is shown as an undifferentiated lineation at Specimen Localities 118, 120, and 174 (Map 1) along a thrust fault may also be mentioned here. It faintly appears on the surface of the bedding and looks like elongation of quartz grains but when the grains are examined microscopically in the same way as described above these are found to be flattened into a shape resembling that of an oblate spheroid. The lineation may be due to slight deformation of the grains in the plane of an incipient cleavage.

3.4.2.6 Folds F1 One type of these, which occurs in the quartzites, is characterized in style by very tight (tightness is a measure of inter limb angle as defined by Fleuty, 1964) to isoclinal folds. According to Ramsay's classification (Ramsay, 1967, p.365) these could be placed in class 1C but closer in form to similar than parallel folds. The folds are steeply inclined to nearly recumbent with a plunge not

not exceeding 20°. These are shown in Plates 3.7a and b. An axial plane structure does not seem to be present but the streaky lineation L1 parallels their axes. It can be seen in Plate 3.7a that in the thick layer near the upper right hand corner their form is not obvious and this may be the reason that they are rarely seen. The only area where their profiles are well developed so as to be distinctly observable lies about 600 to 700 metres northeast of the yard on the northern limb of the Eastern Hill Range (Map 1). Discordance in the foliation simulating cross bedding shown in Plate 3.6c indicates the presence of these folds in the quartzite at the locality represented by the Plate.

The F1 folds of the other type, which have only been seen in the basement rocks, are tight and similar in style. The axial plane of the folds dips about 35° and the axial plunge is within 10°, so according to Fleuty's (1964) classification of fold orientations these are inclined folds. Their profiles are shown in Plate 3.8b and fig.3.4a. A weak axial plane structure is developed but a strong streaky lineation, L1, parallels their axes. Again their profiles have been clearly seen in one small area which lies along the right bank of the main creek that cuts across the northern limb of the Eastern Hill Range about 4km east of the yard, mentioned above (Map 1).

3.4.2.7 Folds F2 As compared to F1 folds, the F2 folds are not restricted in occurrence and are well developed in most of the sub-areas shown in Fig. 3.3. Plates 3.8a; 3.9a and b; 3.10a, b and c; 3.11a, b and c and Figs. 3.4b, c and d show the styles of their profiles. These styles are generally of two types. The first type is characterized by close nearly concentric to disharmonic folds. The concentricity is not perfect because the orthogonal thickness between folded surfaces varies

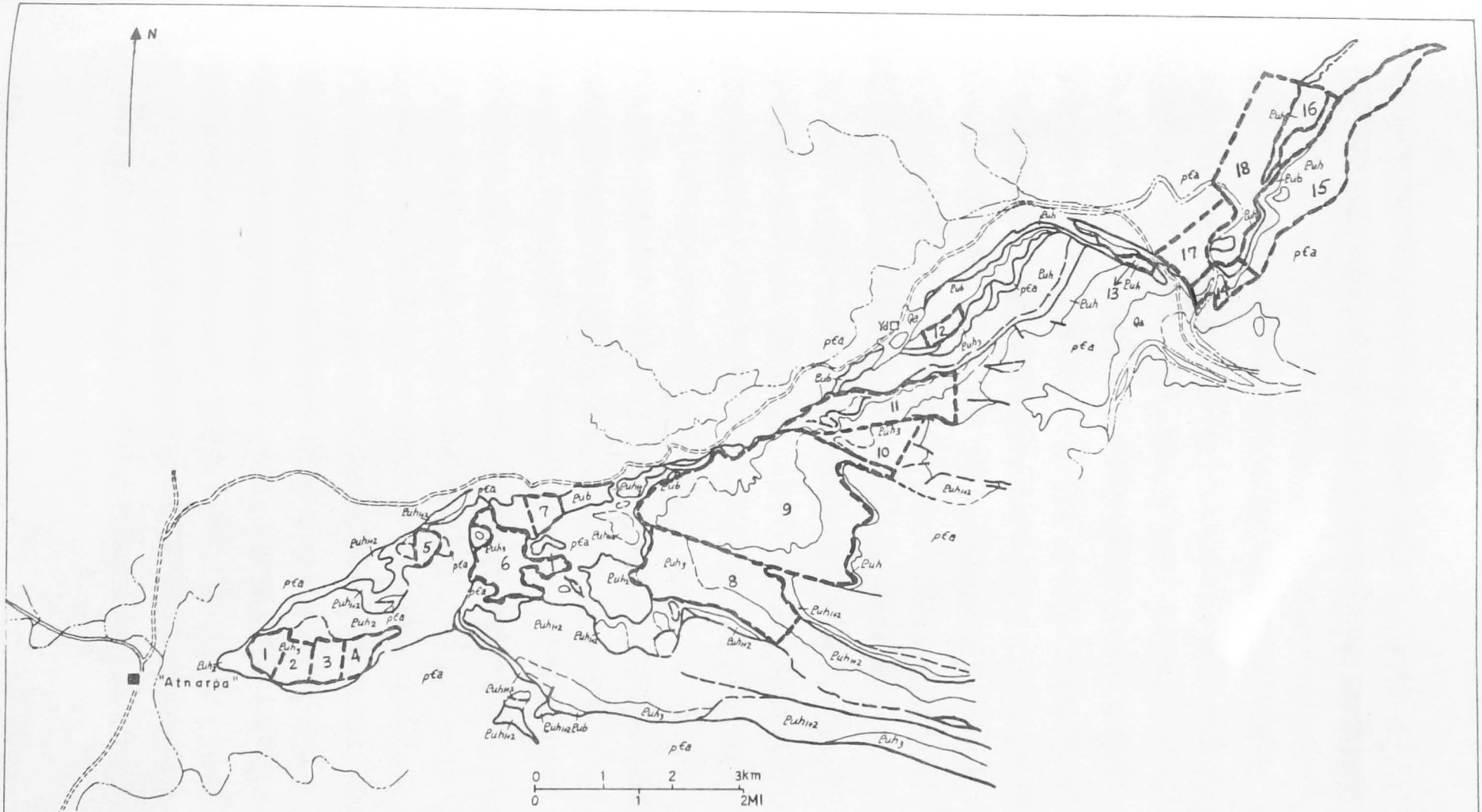

Fig. 3.3. Location of sub-areas.

FIGURE 3.4

(a) Profile of an F1 fold.

(b), (c), and (d): Profiles of F2 folds

(e), (f), and (g): Outcrop pattern on a horizontal surface of plane cylindrical, noncylindrical plane, and nonplane noncylindrical folds respectively. Solid line separates unit A from unit B, and dashed line is the trace of axial surface. The last outcrop pattern (g) is similar to the pattern on the north side of the Western Hill.

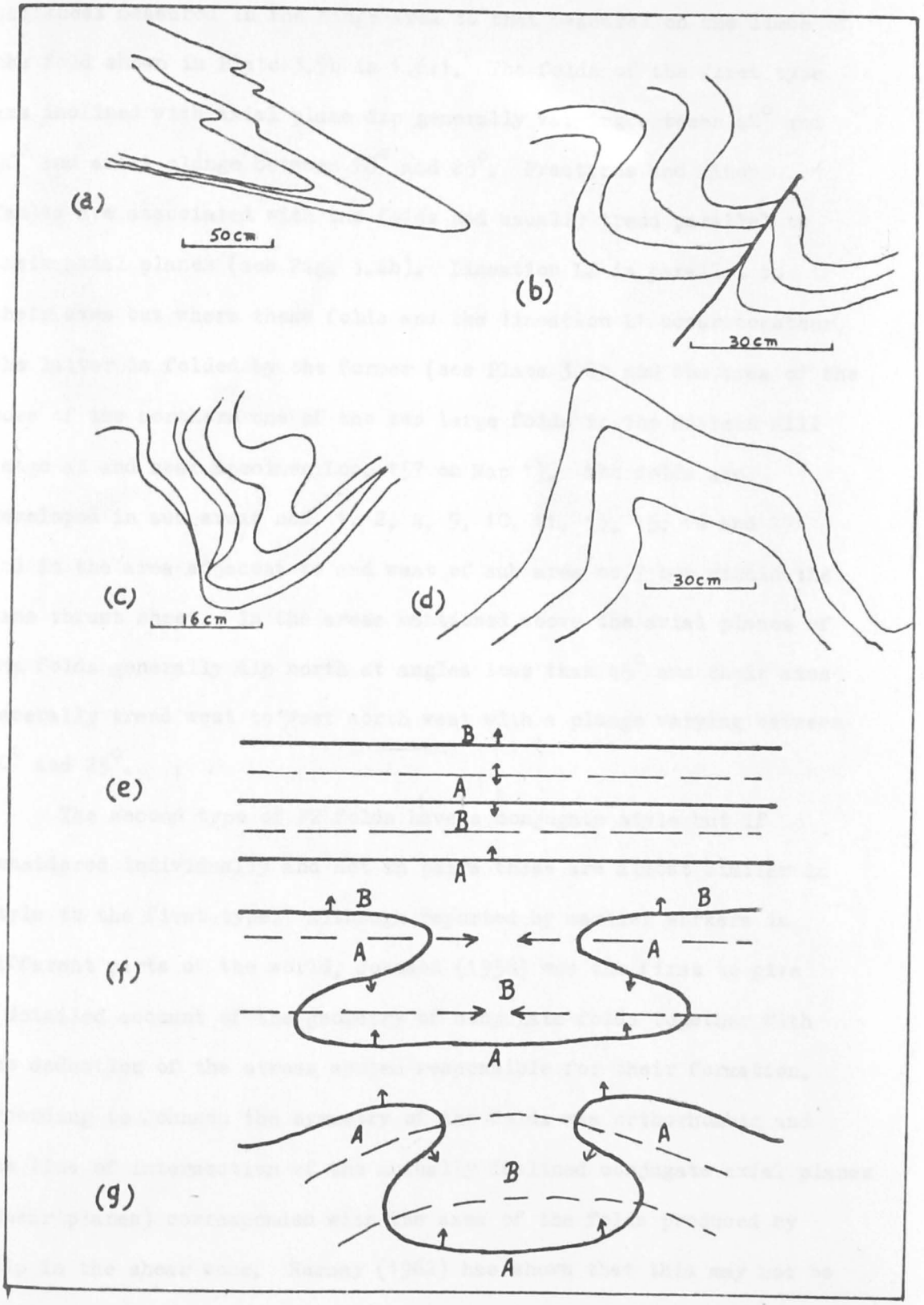
(a)
50cm
(b)
30cm
(c)
16cm
(d)
30cm
(e)
B
A
B
A
(f)
B
B
A
A
B
A
(g)
A
A
B
A

in different parts of the fold. For example the ratio of this type of thickness measured in the hinge area to that measured on the limbs of the fold shown in Plate 3.9b is 1.6:1. The folds of the first type are inclined with axial plane dip generally varying between 40° and 50° and axial plunge between 18° and 25°. Fractures and minor faults are associated with the folds and usually trend parallel to their axial planes (see Fig. 3.4b). Lineation L2 is parallel to their axes but where these folds and the lineation L1 occur together, the latter is folded by the former (see Plate 3.8c and the area of the core of the northern one of the two large folds in the Eastern Hill Range at and near Specimen Loc. 157 on Map 1). The folds are developed in sub areas nos. 1, 2, 4, 9, 10, 11, 13, 15, 16 and 17 and in the area adjacent to and west of sub area no.7 but within the same thrust sheet. In the areas mentioned above the axial planes of the folds generally dip north at angles less than 45° and their axes generally trend west to west north west with a plunge varying between 10° and 25°.

The second type of F2 folds have a conjugate style but if considered individually and not in pairs these are almost similar in style to the first type. Although reported by earlier workers in different parts of the world, Johnson (1956) was the first to give a detailed account of the geometry of conjugate folds together with the deduction of the stress system responsible for their formation. According to Johnson the symmetry of the folds was orthorhombic and the line of intersection of the mutually inclined conjugate axial planes (shear planes) corresponded with the axes of the folds produced by slip in the shear zone. Ramsay (1962) has shown that this may not be the case always because the line of inter-section of the shear planes

may not lie in the surface being folded and therefore there is no coincidence either between the two sets of fold axes related to the two sets of shear planes or between the line of intersection of the shear planes and the fold axes. The resulting symmetry of such a structure could either be monoclinic or triclinic. The orientations of the axial planes and axes of four conjugate folds, two from sub-area no.1, one from sub-area no.8 and one from sub-area 12 are plotted on the lower hemisphere of an equal area net and are shown in Fig.3.5. The plots show the orientation of the stress axes determined from the orientation of the axial planes and also show the non-coincidence of the fold axes with the line of intersection of the planes. The L2 lineations are parallel to the axes of the conjugate folds but they fold the L1 lineations and this relationship is excellently evident in sub-area no.12, Fig. 3.3 and is also shown in Plate 3.7c. In this area the axial trend of these folds varies from NE-SW to NNE-SSW. In sub-areas nos. 1 and 4, Fig. 3.3, in the Western Hill where these folds and the folds of the first type are both present, the axial trend and plunge vary from northeast and a gentle plunge in sub-area no.4 to WNW and a plunge of about 30° in sub-area no.1.

On a macroscopic scale the F2 folds are represented by an anticline in the Western Hill, a second anticline south of the Small Valley and a large anticline forming the Eastern Hill Range. The steep and overturned limbs of the folds that form part of the Large Anticline are associated with faults which consistently strike E-W, and dip at high angles towards the north. In fact the three anticlines are part of a very large anticlinal structure.

3.4.2.8 Folds F3 In some areas these can be seen but very locally, in others they are hard to see on the ground but are indicated by map

FIGURE 3.5

Orientation diagrams of axial planes and fold axes of conjugate folds, also showing the orientation of stress axes. Diagrams (a), (b) and (d) represent conjugate folds shown in Plates 3.10a, b, and 3.12a respectively and diagram (c), a conjugate fold in sub-area 8.

o = fold axis; Pint. = intermediate stress axis.

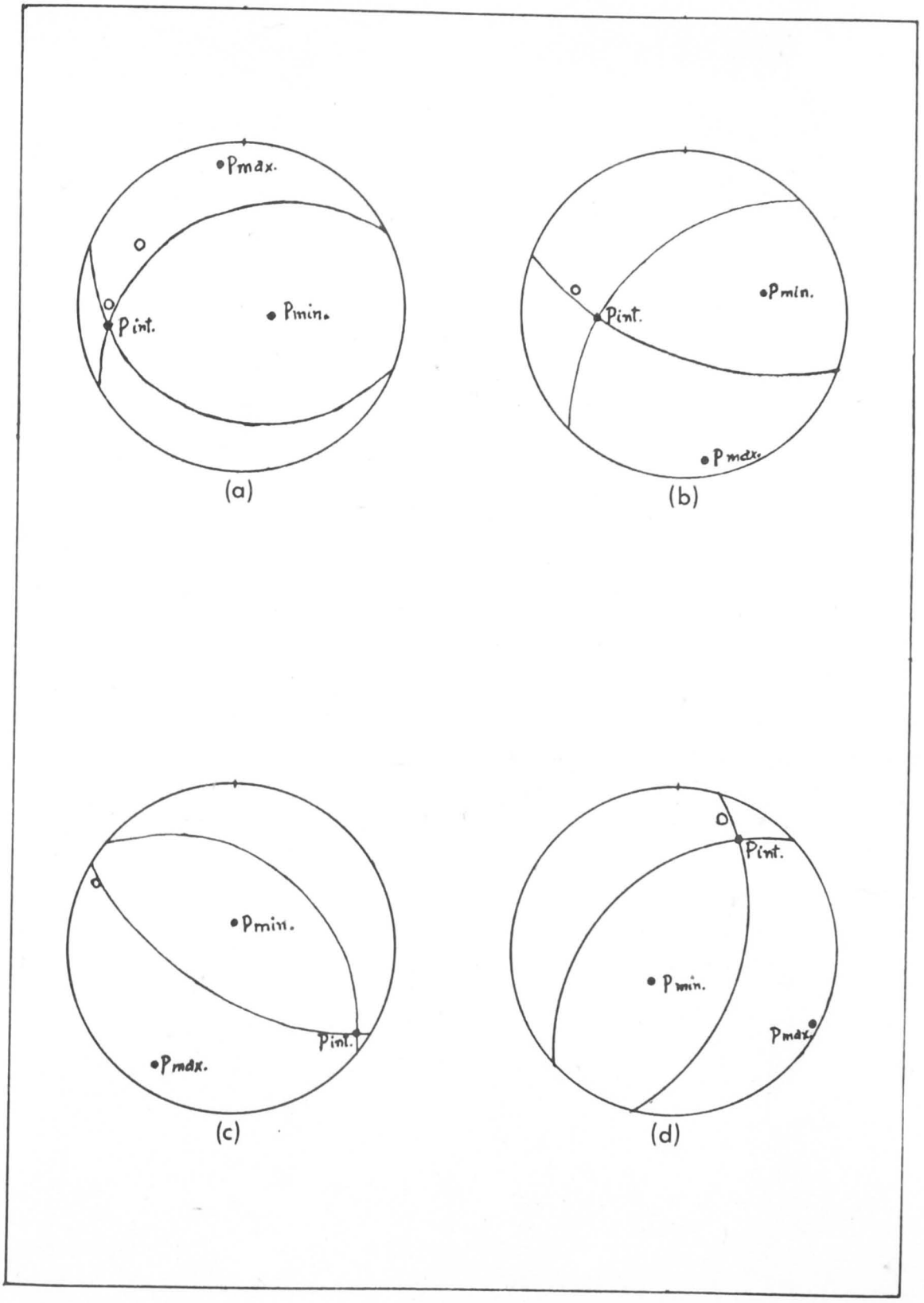
Pmax.
Pint.
Pmin.
(a)
Pmin.
Pint.
Pmax.
(b)
Pmin.
Pint.
Pmax.
(c)
Pint.
Pmin.
Pmax.
(d)

PLATE 3.6

(a) A nearly complete section of the Heavitree quartzite at Specimen Locality 215 on the left bank of the main creek and on the northern limb of the Eastern Hill Range.

(b) Quartz veins along the foliation planes in the Arunta Complex on the northern limb of the Eastern Hill Range at Specimen Locality 271.

(c) Discordant layering within the quartzite in the foreground on the northern limb of the Eastern Hill Range and northeast of the crossing of the Atnarpa Range and the vehicle track; Arunta Complex in the background.

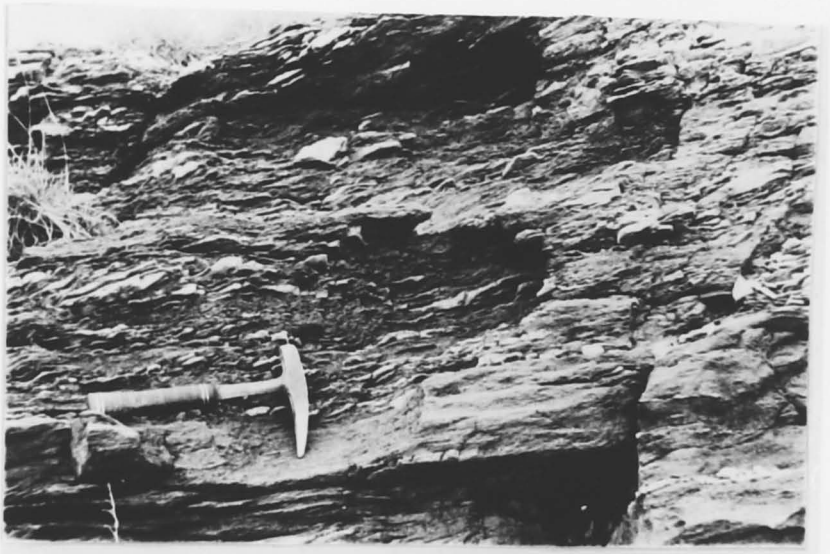

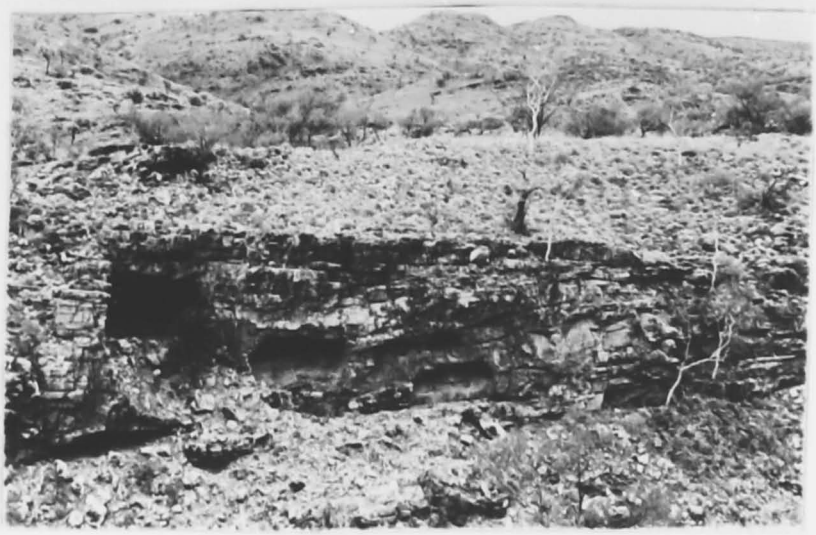

PLATE 3.7

(a) Isoclinal F1 folds in the Heavitree Quartzite about 400 metres southeast of the yard; looking northwest.

(b) Same folds as in (a) above and in the same area but with a gently dipping axial plane, streaky lineation, L1, parallel to the fold axis.

(c) Lineation, L1, folded by F2 conjugate folds about 800 metres east of the yard.

PLATE 3.8

(a) Tight, F2 folds in the quartzite about 200 metres south of Specimen Locality 243 in the vicinity of Atnarpa Range and the vehicle track crossing.

(b) F1 similar folds in the Arunta Complex at Specimen Locality 300 and on the right bank of the main creek that cuts across the northern limb of the Eastern Hill Range.

(c) F2 folds in the quartzite folding L1 lineation about 500 metres southwest of Specimen Locality 279 on the northern limb of the Eastern Hill Range and northeast of the Atnarpa Range and the vehicle track crossing.

PLATE 3.9

(a) F2 crenulations in the quartzite in the Eastern Hill Range anticline.

(b) Nearly concentric and asymmetric F2 fold in the quartzite in thrust sheet no.2 near Specimen Locality 160 in the central part of the Eastern Hill Range; looking west.

(c) Unconformity at hammer head between the Arunta Complex below and the Heavitree Quartzite in thrust sheet no.2 above, at Specimen Locality 237 and on the Eastern Hill Range

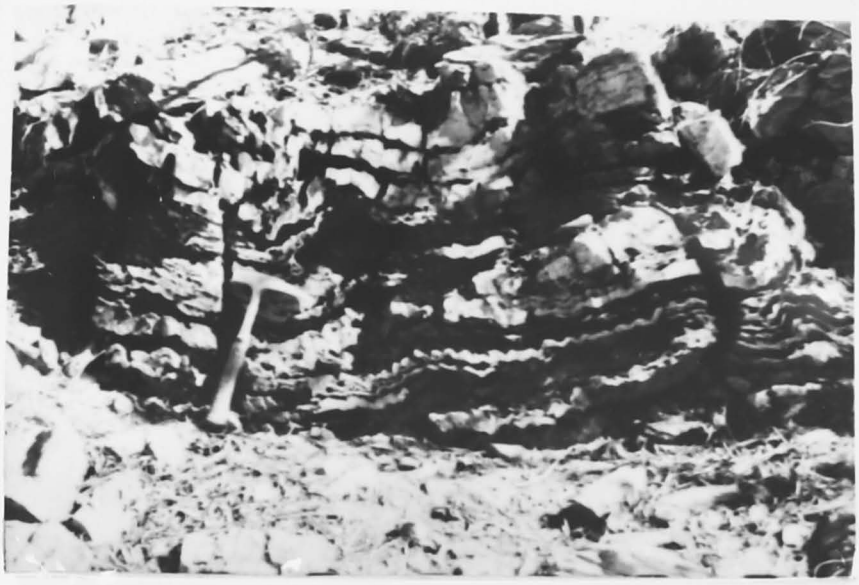

PLATE 3.10

(a) F2 nearly concentric to conjugate folds in the quartzite in the western part of the thrust sheet no.3 in the Western Hill; looking west-northwest.

(b) F2 conjugate fold in the quartzite sheet no.3 in the Western Hill; looking west.

(c) F2 nearly concentric to conjugate fold, in the quartzite in the eastern part of thrust sheet no.3 in the Western Hill; looking north-northeast.

PLATE 3.11

(a) F2 fold in the core of the Western Hill anticline at Specimen Locality 202 and in the quartzite, showing development of cross fractures related to the axial plane and another fracture at a low angle to the bedding above the hammer handle.

(b) Asymmetric F2 fold in the quartzite in thrust sheet no.4 at Specimen Locality 294 on the north side of the Western Hill; looking west.

(c) Profile of an F2 fold in the Bitter Springs Formation in thrust sheet no.2 on the north side of the Small Valley; looking east.

PLATE 3.12

(a) F2 conjugate folds in the quartzite in the thrust sheet no.5? near Specimen Locality 214 on the northern limb of the Eastern Hill Range; looking northeast.

(b) Development of kinks in the same area as (a) above.

(c) Open F3 fold folding axis of F2 conjugate folds in the quartzite near Specimen Locality 221 on the northern limb of the Eastern Hill Range; F3 axis plunges north.

PLATE 3.13

Arunta Complex, (a) at Specimen Locality 142, (b) at Specimen Locality 106 and (c) close to Specimen Locality 194. In (a) foliation is not evident, in (b) it is characterised by quartz and mica layers which wrap around the resistant felspar grain. Development of cracks in the felspar grain is noticeable. (c) shows development of strain slip cleavage. (Scale 0.1mm in (a), 0.4mm in (b) and 1.0mm in (c); crossed nicols)

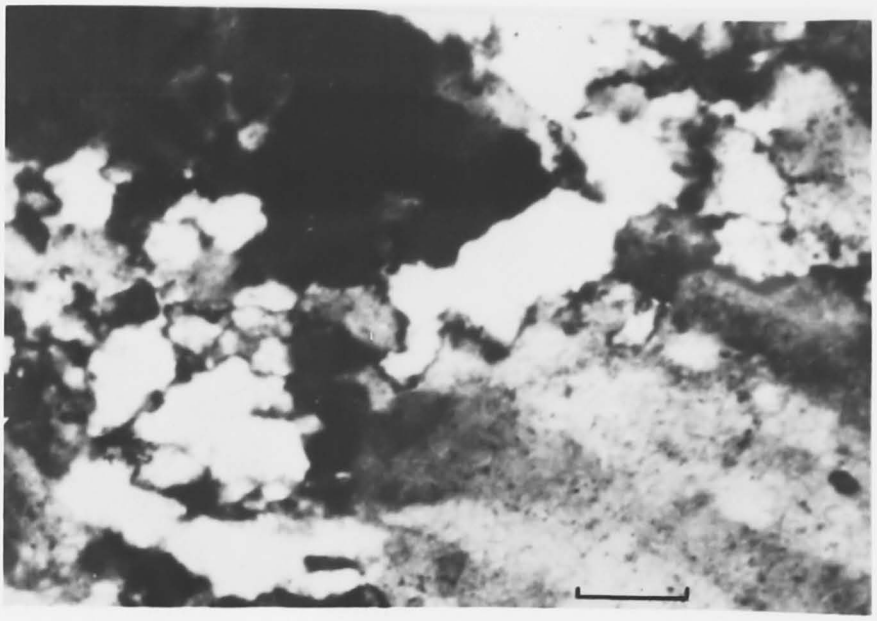

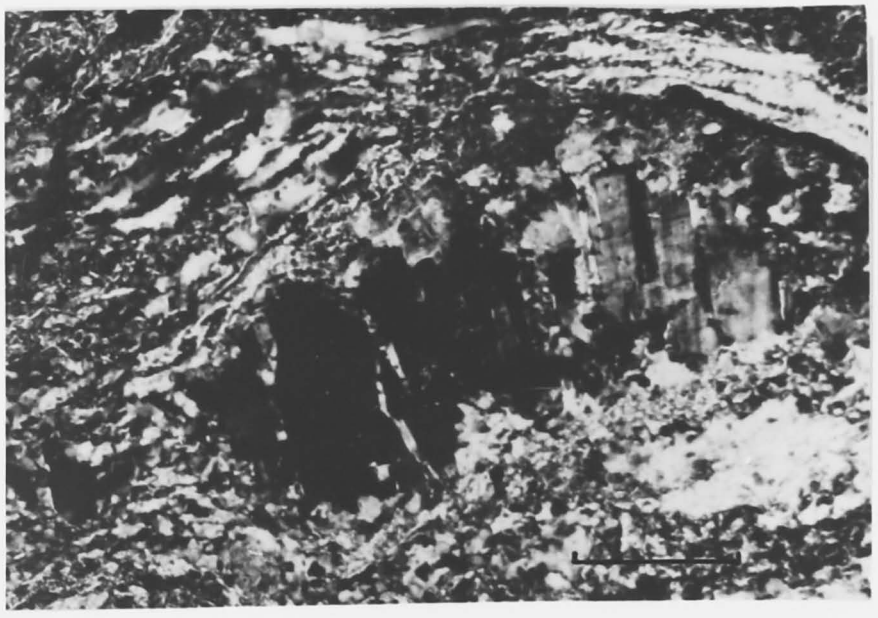

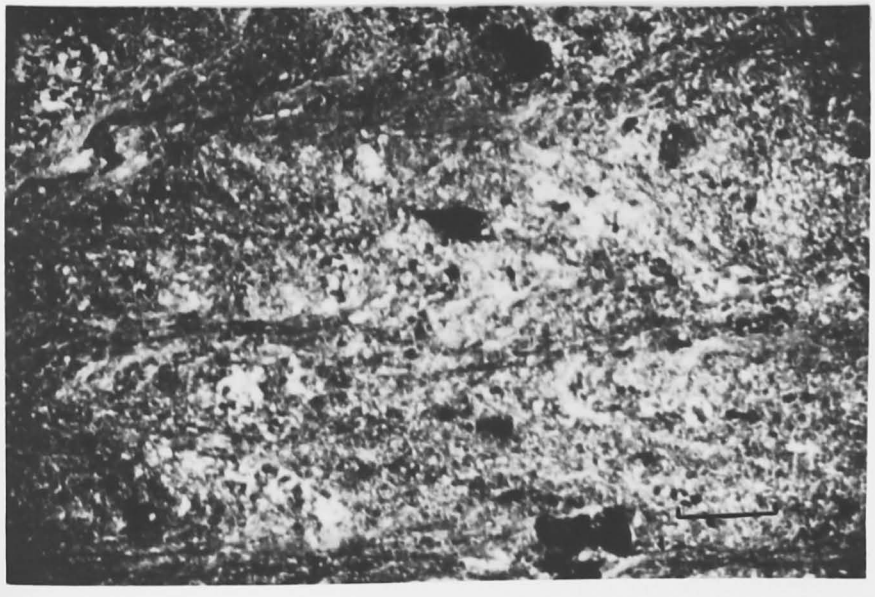

PLATE 3.14

Bitter Springs Formation in (a) at Specimen Locality 249, Arunta Complex in (b) and (c) at Specimen Localities 244 and 224 respectively. Sections normal to the lineation. Characteristics of the foliation are shown at the localities as well as alteration and cracking of felspar grains in (b) and (c). (Scale 0.1mm in (a), 1.0mm in (b), and 0.4mm in (c); crossed nicols)

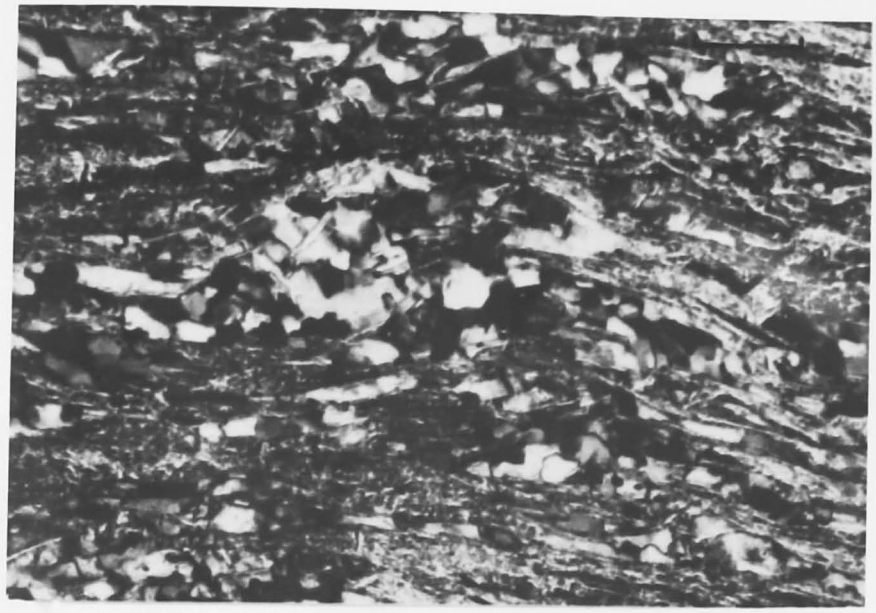

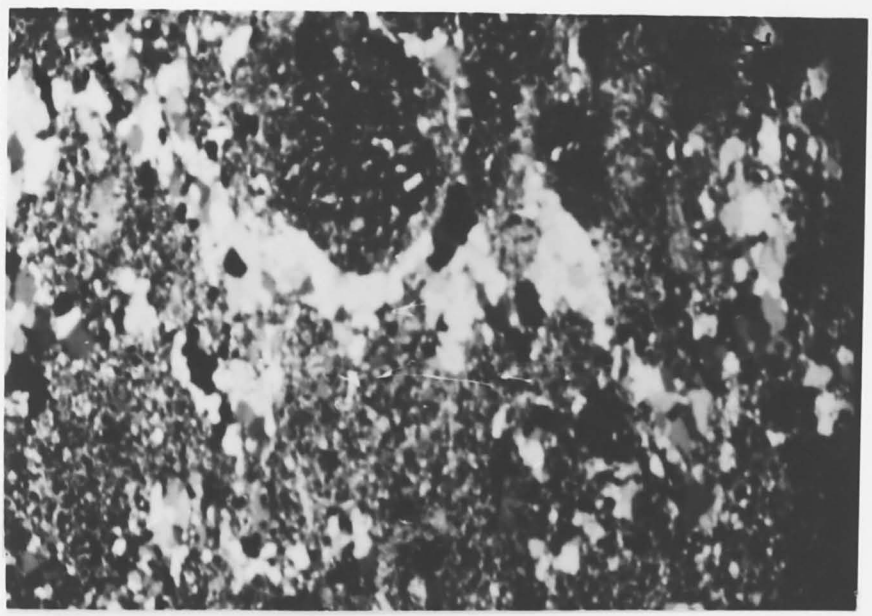

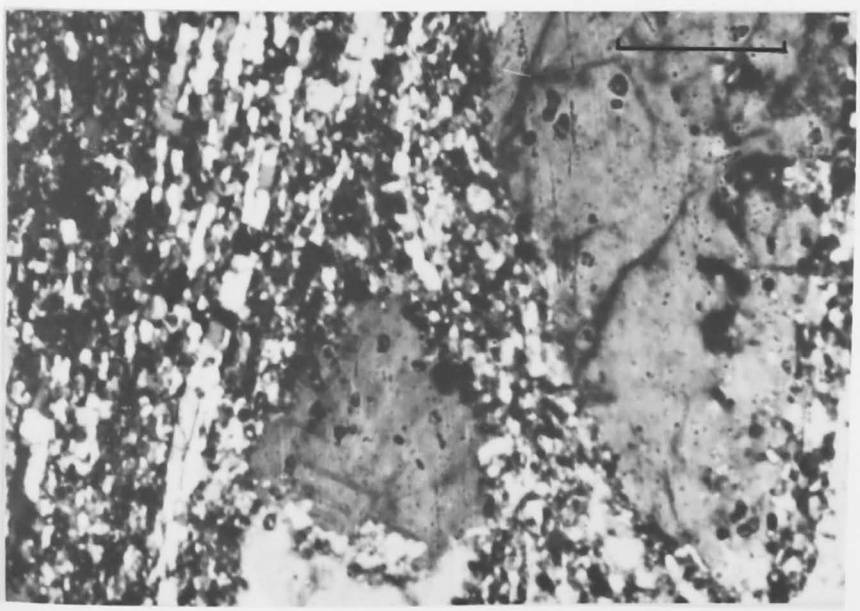

PLATE 3.15

Arunta Complex, (a) close to Specimen Locality 248, (b) close to Specimen Locality 300 and (c) at Specimen Locality 304. The development of the foliation from north to south or towards the thrust is shown. (Scale 1.0mm in (a) and (c) and 0.4mm in (b); crossed nicols)

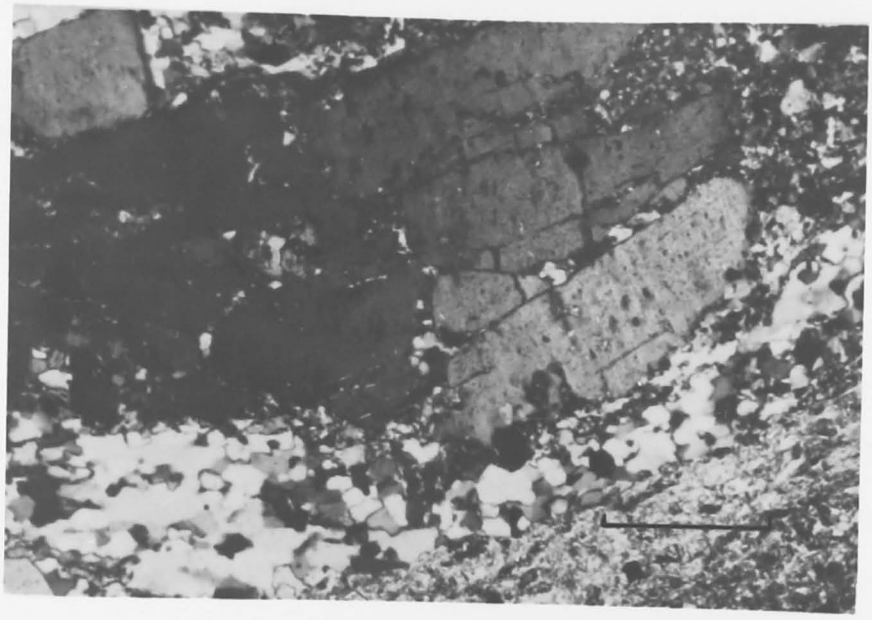

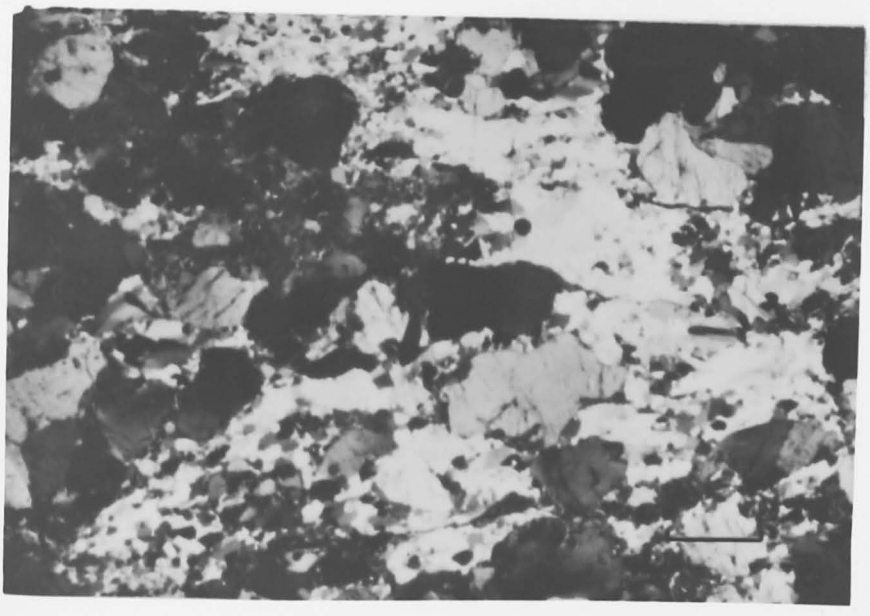

pattern although this may not be a firm basis for separating them from F2 folds. Plate 3.12c shows an open F3 fold folding the hinge of an F2 fold on the northern limb of the Eastern Hill Range.

3.4.3 Macroscopic geometry of planar and linear structures

Parts of the Atnarpa Range area have been chosen and shown as sub-areas in Fig. 3.3 for the purpose of studying the geometry in domains, homogeneous or nearly so with respect to at least one of the structures. The choice of the areas depended on three factors, (a) good exposure so that enough measurements could be obtained for a statistical study, (b) lack of clarity of the geometry of the structures shown by orientation symbols on Map 1, and (c) emphasis on a particular geometry.

Sub-areas 1, 2, 3, and 4 lie in thrust sheet no.3 and the rocks in these areas mostly form part of the upper member of the Heavitree Quartzite. The mesoscopic structures in these areas are the bedding, the L2 lineations and the F2 folds. Variations in the trend and plunge of the F2 fold axes in these areas are evident on Map 1. Fig. 3.7a is a synoptic diagram of the poles to the bedding for all the sub-areas and shows the heterogeneity of the folded bedding. Figs.3.6a to d are essentially orientation diagrams of the poles to the bedding in sub-areas 1, 2, 3, and 4 respectively but the L2 linear structures are also shown on these. These figures show that the geometry of the folding is not again homogeneous at the scale represented by the sub-areas. The poles to the bedding in Figures 3.6a and d tend to lie on a rather weakly defined girdle whereas the poles in Figures 3.6b and c are somewhat irregularly distributed. The attitude of β axis in Fig. 3.6a

FIGURE 3.6

Orientation data for bedding and L2 lineations. Diagrams a, b, c and d represent sub-areas 1, 2, 3, and 4 respectively.

. = pole to bedding; o = fold axis; x = mineral elongation lineation.

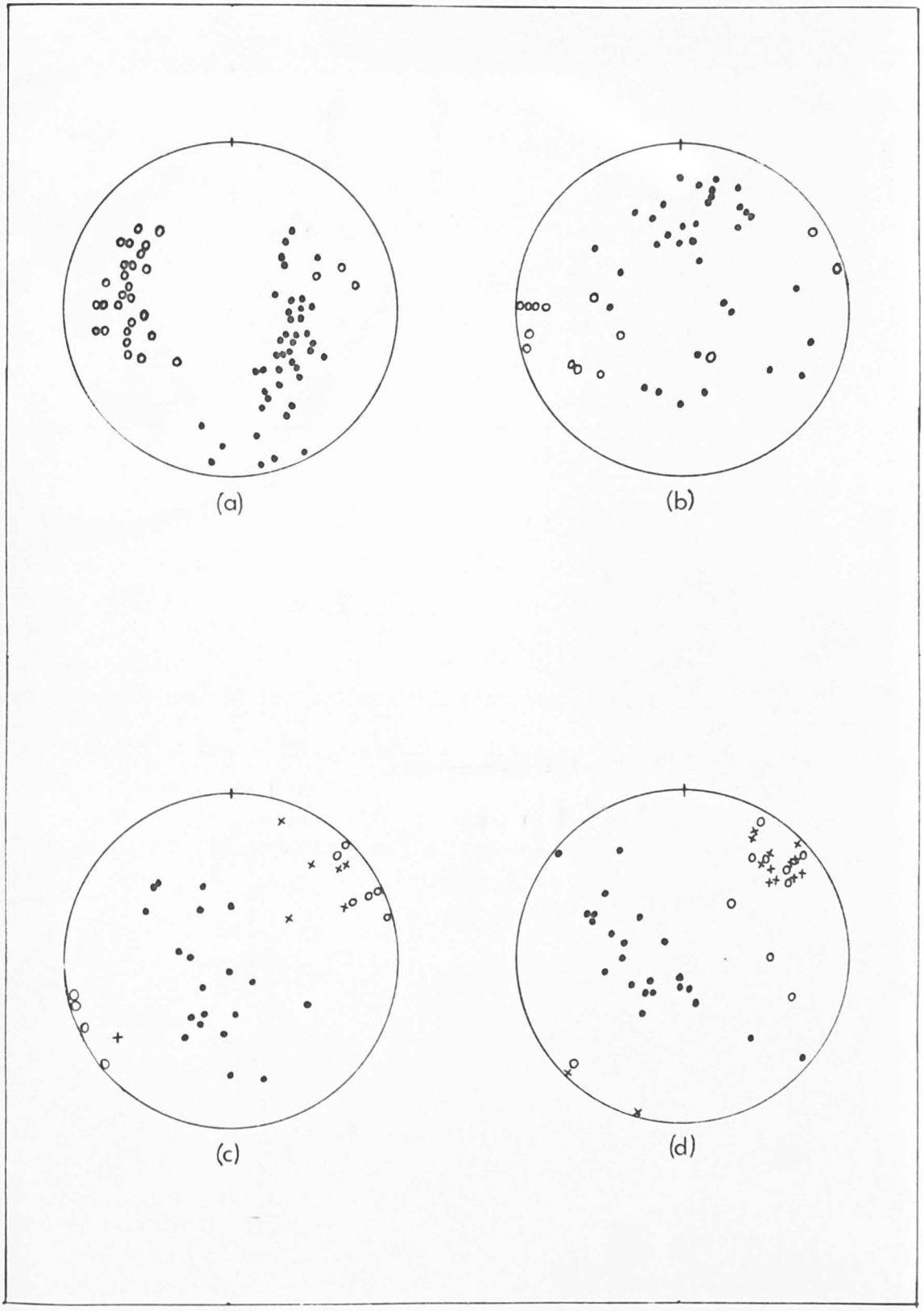
(a)
(b)
(c)
(d)

FIGURE 3.7

Orientation data for bedding, L2 lineations and axial planes.

(a) Synoptic diagram of poles to bedding for sub-areas 1, 2, 3, and 4. Contoured according to Kamb method, contour intervals are 0, 2, 4, 6, 8 and 10 σ where $\sigma = 2.8$, maxima = 11.2σ.

(b) Synoptic diagram of L2 lineations for sub-areas 1, 2, 3 and 4.

o = fold axis; x = mineral elongation lineation

(c) Synoptic diagram of poles to axial planes for sub-areas 1, 2, 3, and 4.

• = pole to axial plane

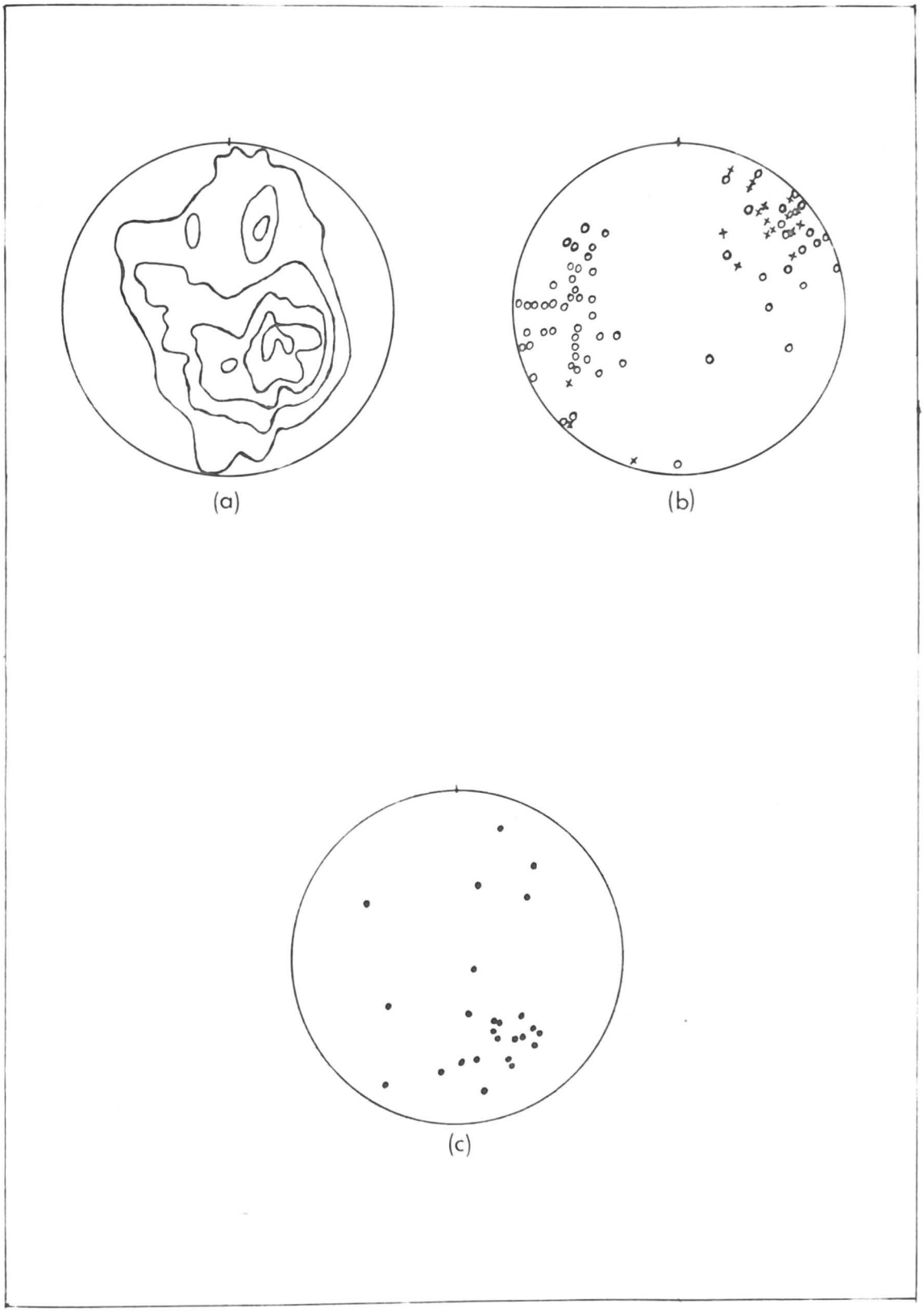
(a)
(b)
(c)

is 30° west and is about in the centre of the spread of the L2 lineations. In Figure 3.6d the β axis attitude is 16°N40E and corresponds better with the plot of the L2 lineations than in Fig.3.6a. Fig. 3.7b is a synoptic diagram of the L2 lineations from the four sub-areas. There is a variation of about 60° in the trend of these lineations in the western as well as the north-eastern sectors of the diagram and of about 45° in the amount of the plunge. The β axis has also similar variations in its trend and a variation of about 15° in the amount of its plunge. Some of the variations in the direction and amount of plunge of the L2 lineations can be attributed to conjugate folding of lower symmetry than orthorhombic in this area as described in the section on F2 folds. Fig. 3.7c is a synoptic diagram of the poles to axial planes for all the sub-areas. These poles are also irregularly distributed. The attitudes of the bedding planes, the L2 lineations, and the axial planes indicate that the folding of thrust sheet no.3 comprising the four sub-areas is of nonplane noncylindrical type (see Turner and Weiss, 1963, p. 108).

Figs. 3.8a to c represent sub-areas 5, 6, and 7 respectively. In Fig. 3.8a poles to foliation tend to lie on a girdle and the β axis is almost horizontal with a N65E-S65W trend. It seems from the diagram that the axis of the F2 folding was oriented in about the same direction in which the L1 lineations lay in the foliation plane. As a result of this coincidence the L1 lineations were not much distorted. Folding indicated by Figs. 3.8b and c is similar to that in Fig. 3.8a except that there is more dispersion of the poles to the bedding and the L2 lineations in the former than in the latter. A point that needs mentioning here is that in the area adjacent to

FIGURE 3.8

Orientation data for bedding, foliation, and lineations. Diagrams (a), (b), and (c) represent sub-areas 5, 6, and 7 respectively.

• = pole to foliation in diagram (a) and pole to bedding in diagrams (b) and (c).

o = L2 lineation; x = L1 lineation.

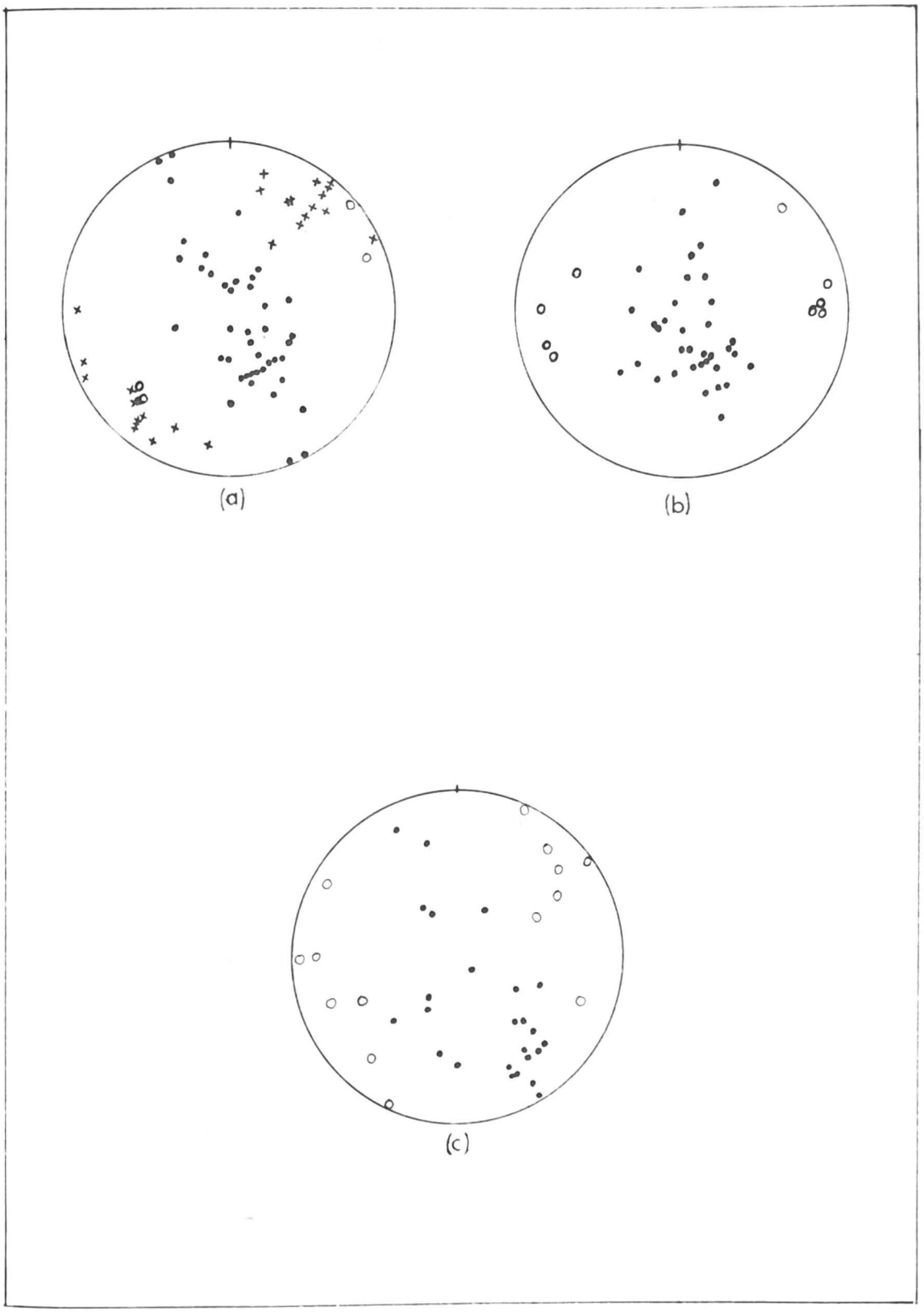
(a)
(b)
(c)

and west of sub-area 7 but within the same thrust sheet the fold axes of the mesoscopic folds consistently plunge gently eastwards (Map 1). This attitude of the fold axes is different from the attitude of the β axis in sub-area 7 which is roughly defined by a gentle plunge towards S60W and again shows variation in the trend of the F2 fold axis.

Figs. 3.9a to d represent sub-areas 8, 9, 10, and 11 in thrust sheet no.2. Each figure is different with respect to the pattern of the poles to the bedding and the orientation of the β axis as deduced from the pattern. The plot of the poles however corresponds in each figure with the map pattern in the respective sub-areas (see Map 1) as well as the β axis in each figure corresponds to the plot of the mesoscopic fold axes (L2 lineations). The L1 lineations are not abundant in the sub-areas and are scattered by the folding where present. The L1 lineations are, therefore, older than the F2 folding. From fig. 3.9a to fig.3.9d, there is a regular change in the trend of the L2 lineations amounting to about 60° and the variation in their plunge is of the order of about 15°. These variations are similar to those shown in fig.3.6a representing sub-area 1 in the Western Hill.

Sub-area 12 lies in a strongly deformed region on the northern limb of the Eastern Hill Range in thrust sheet no.5. In this area the streaky lineation, L1, is ubiquitous. The orientation diagrams of planar and linear structures in this area are shown by Figs. 3.10b and a respectively. In diagram, Fig. 3.10a, the L1 lineations are dispersed in a well defined girdle, the axis of which is within 15° to the area of maximum concentration of the fold axes of the F2 mesoscopic folds. The poles to the foliation (Fig.3.10b) are almost

FIGURE 3.9

Orientation data for bedding and lineations. Diagrams (a), (b), (c) and (d) represent sub-areas 8, 9, 10, and 11 respectively.

• = pole to bedding; o = L2 lineation; x = L1 lineation, mineral elongation.

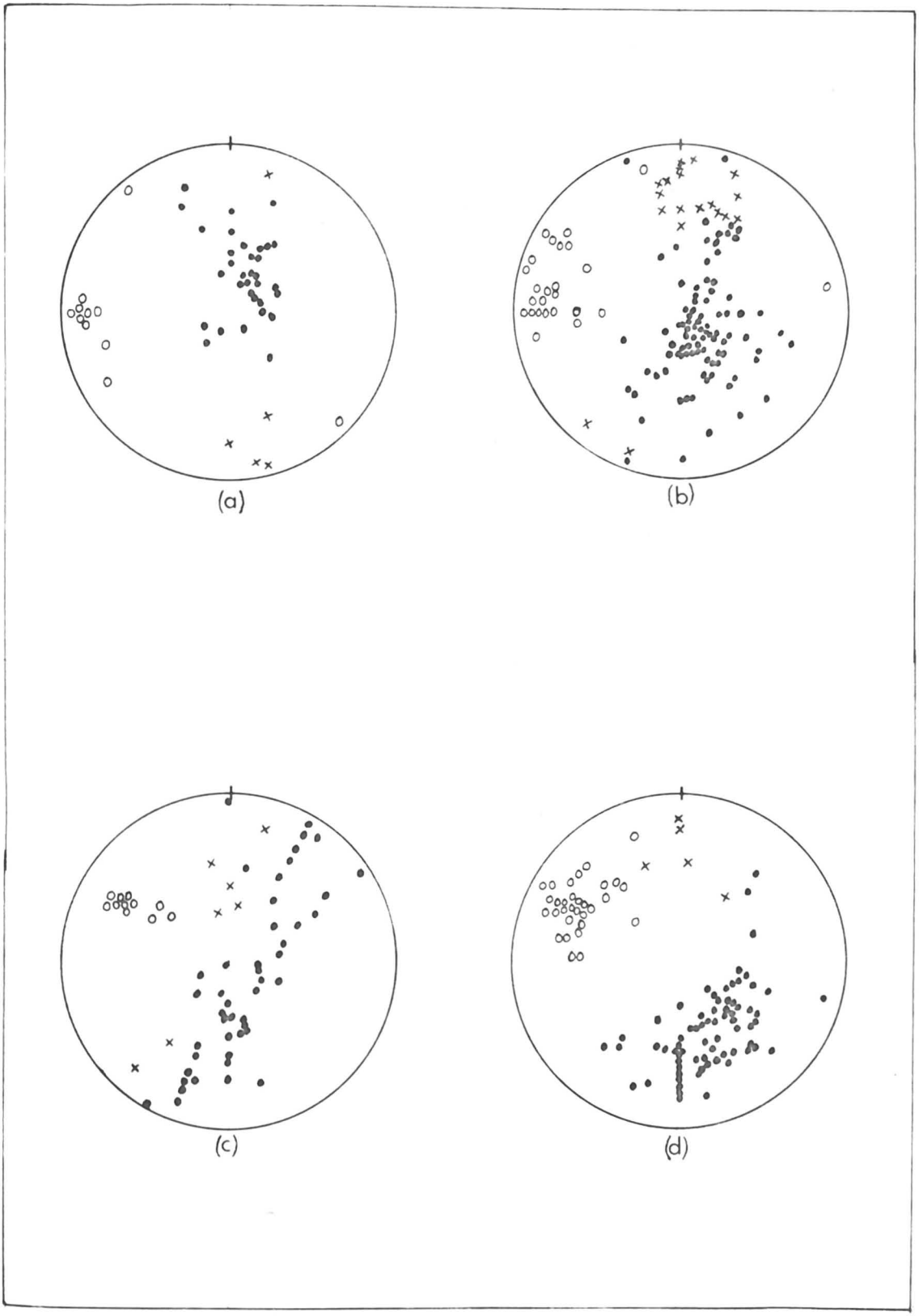
(a)
(b)
(c)
(d)

FIGURE 3.10

Orientation data for foliation and lineations. Diagrams (a) and (b) represent sub-area 12 and diagrams (c) and (d) represent the northwestern and southeastern halves of sub-area 13 respectively.

• = pole to foliation; x = L1 lineation; o = L2 lineation

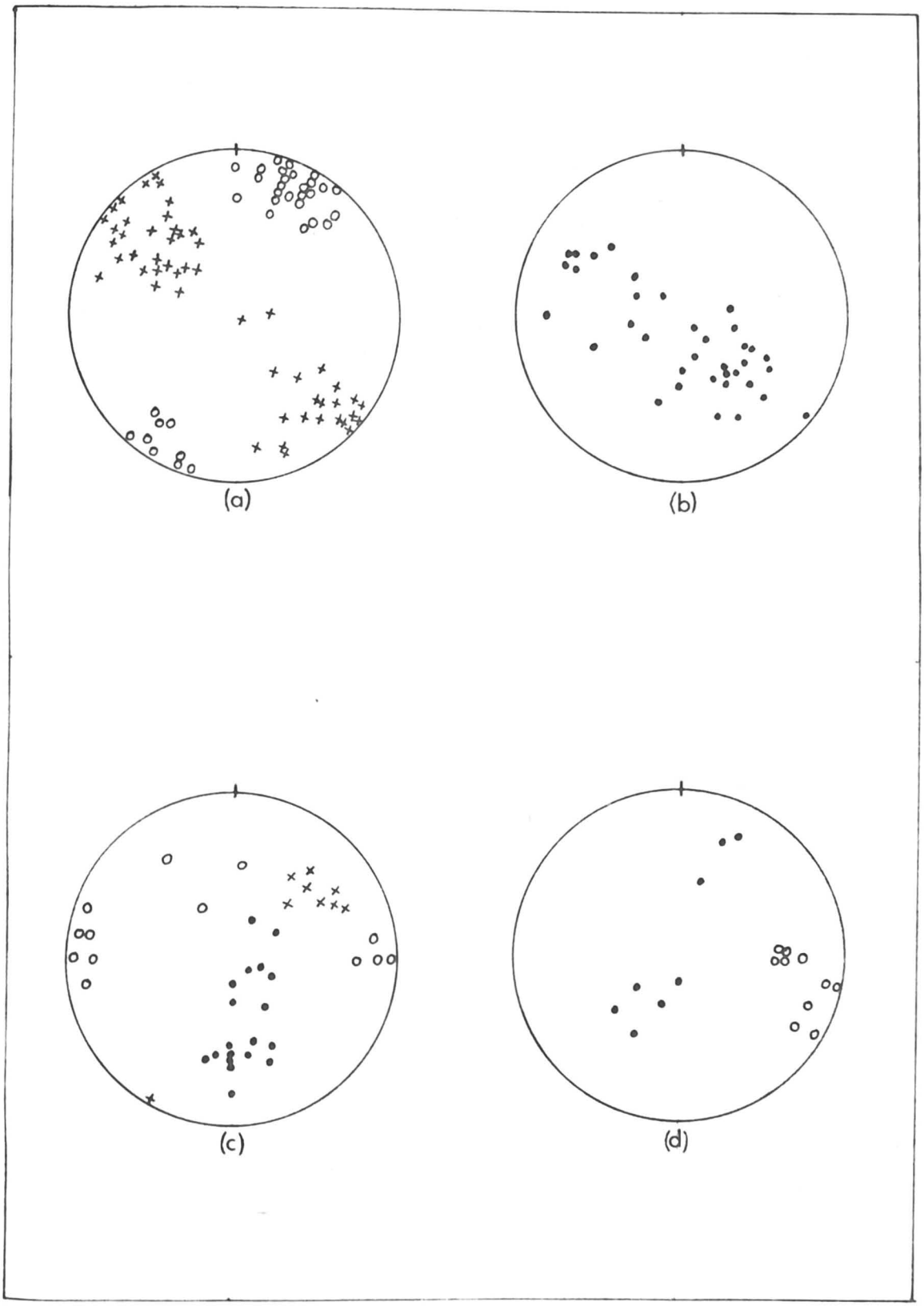
(a)
(b)
(c)
(d)

co-planar with the lineations. The mutual relationship of the lineations, L1 older than L2, is manifest. The trend of the β axis of the F2 folding in this area is N35E-S35W.

Sub-area 13 lies in thrust sheet no.2 and also on the northern limb of the Eastern Hill Range. Figs. 3.10c and d are orientation diagrams of the planar and linear structures for the two halves, the northwestern and the southeastern, of the sub-area respectively. The β axis for the first diagram plunges gently west and for the second very gently S70E. The plots of fold axes and lineations correspond to the location of the β axis. In diagram, Fig.3.10c, the lineations and the fold axes in the northeastern sector are probably early lineations, L1.

Sub-areas 14, 15, and 16 are in the cover rocks and sub-areas 17 and 18 in the basement rocks. Fig. 3.11a shows the orientation data from sub-area 14 and Fig. 3.11b shows the combined orientation data from sub-areas 15 and 16; the data was combined in one diagram because of no significant difference in the individual projections. The first diagram differs from the second in that the poles to foliation in it tend to spread out in an east-west direction rather than the north-south. The pole patterns of foliation on the diagrams accord with the map pattern of rock formations. The L1 lineations in both diagrams have a well marked northerly orientation but are dispersed in the plane of foliation as a result of the F2 folding. The diagrams however do not provide any clue to the F1 folding of which the L1 lineations are the product. The poles to foliation and lineations for sub-area 17 are shown in Fig. 3.11c and Fig. 3.11d is a combined diagram of these structures for the sub-areas 17 and 18. The lineations in diagram, Fig. 3.11c, trend almost northeast and

FIGURE 3.11

Orientation data for foliation and lineations. Diagram (a) represents sub-area 14, diagram (b) represents sub-areas 15 and 16, diagram (c) represents sub-area 17, and diagram (d) represent both the sub-areas 17 and 18.

• = pole to foliation; x = L1 lineation; o = L2 lineation; the black area in diagram (b) contains 26 L1 lineations.

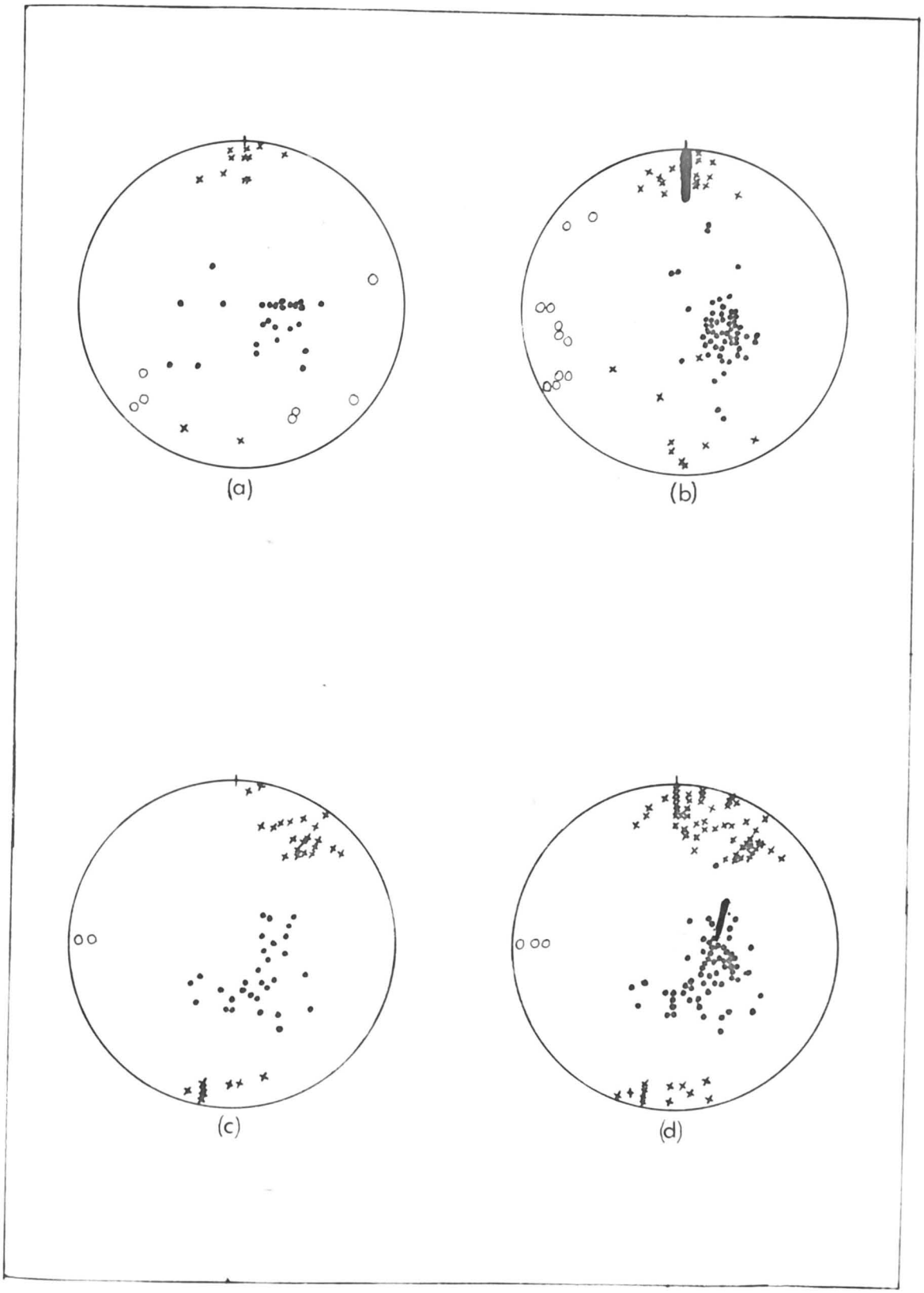

gram (a)

15 and 16,

sent both

ineation;

the pole girdle has a similar trend also. In diagram, Fig.3.11d, there is a concentration of the northerly lineations in addition to the northeasterly ones, and the concentration of poles to foliation markedly increases in the same sector of the diagram as is present in Fig.3.11b. This is due to the addition of the poles of those foliation planes in the basement rocks which lie very close to the cover rocks and in which the lineation mostly trends north, thereby showing that the basement and cover rocks have deformed in a similar fashion.

3.4.4 Conclusions

(1) The thrusts seem to originate in the basement or near the basement-cover contact and progress upwards through the cover rocks either in a more or less regular manner or like a step-bedding-plane thrust (Badgley, 1965), i.e., they remain in one glide horizon along the bedding plane for some distance and then due to an obstruction to their further more or less horizontal movement in that horizon cut upwards across the strata to find another such horizon. Evidence of the movement of the step-bedding-plane type comes from cross section DD', Map 2.

(2) Intensity of thrusting diminishes upwards and downwards in the structural sequence from thrust sheet no.2. The size of sheet no.1 is unknown in the mapped area but photogeological observations of the area east of the mapped area indicate that it is not of a larger extent than the sheet no.2. Upward in the sequence the size of the sheets gradually decreases as well as the movement on the thrust planes; the absence of the Bitter Springs Formation in thrust sheets 5, 6 and 7 on the northern side of the Western Hill is an

indication of the decrease in the intensity of the movement.

(3) Asymmetry of the folds and the west to west-north-west trend of their axes, developed in the northern part of thrust sheet no.2 beneath the thrust indicate the movement of the rocks above the thrust from north to south (Map 2, Sections CC' to EE' and Map 1).

(4) The arkosic part of the basal member of the Heavitree Quartzite, the white shales lying at the junction of the quartzite and the Bitter Springs Formation, and one or two similar horizons in the formation itself are the main horizons which because of their incompetent nature have played an important role in the development of thrusts through the cover rocks.

(5) Repetition of normal stratigraphy in almost all the sheets is a strong evidence in favour of overthrusting and formation of thrust nappes.

(6) Of the first generation structures the foliation and the lineation are only extensively developed, the folds of this generation are very much localized. The folds could be expected to have also developed extensively but it seems that strong flattening as well as recrystallization has probably effaced their profiles. The geometric relationship of the folds with the foliation is not clear but it is likely that the foliation may be due to local transposition of the bedding in the cover rocks and similar transposition of pre-existing foliation in the metamorphic rocks of the basement; this assumption is supported by the parallelism of the lineation with the axes of the folds. The foliation and the lineation are predominantly the result of the dimensional alignment of either the clastic, deformed quartz grains or the recrystallized aggregates of these grains.

The foliation is generally defined by the planes of flattening of the grains and the lineation by the direction of their maximum elongation and the combination of the foliation and the lineation in the mesoscopic sub-fabric reflects its orthorhombic symmetry. The foliation may, therefore, be equated with the XY plane of the strain ellipsoid (X being the longest axis and Y, the intermediate axis) and on the basis of the strain data is more akin to slaty cleavage and to a plane of low resolved shear stress rather than to a plane of high resolved shear stress (see Turner and Weiss, 1963, p. 458-459 and Johnson, 1967). $\sigma 1$, the maximum compressive stress, is very likely to be normal to the plane of the foliation and considering the general attitude of the foliation in the Atnarpa Range area (see Map 1) it appears that during the development of the foliation $\sigma 1$ would have been almost vertical although it is possible that the other two stresses of the stress system would have changed their directions with respect to the geographical coordinates. This change in the directions of the two stresses may be invoked to explain the directional changes of the lineation in the area during its development.

(7) The structures of the second generation are more varied particularly in orientation and to some extent in style than the first generation structures. Study of the geometry of the second generation folding at macroscopic scale has shown that the folding is markedly non-cylindrical and that it controls much of the distribution of bedding and thrust planes in the area. Dome shaped structures at or near specimen localities 104, 111 and 133 and in the Small Valley (Map 1) as well as the outcrop pattern on the northern side of the Western Hill (Map 1) also indicate the non-cylindrical nature of the

folding. In a hypothetical example in Figs. 4.4e to f the development of the kind of outcrop pattern as present on the northern side of the Western Hill has been shown. The outcrop pattern can develop as a result of superposed folding or folding in a heterogeneous strain field. The latter possibility seems more likely in the area because of the development of different styles of F2 folds (concentric, conjugate, etc.) on a mesoscopic scale.

(8) The thrusts have been folded during second generation folding and therefore their relationship with second generation structures is well established. The first generation structures seem to have developed with greater intensity at or close to the thrusts than away from them, nevertheless their relationship with the thrusts is not quite clear and will be discussed further in the last chapter of the thesis in the light of the petrofabric data.

CHAPTER 4

MICROFABRIC OF THE HEAVITREE QUARTZITE

4.1 General statement

The objects and approaches of this study have been outlined in Chapter I. Although this study is primarily concerned with the evolution of preferred orientation of the quartz lattice in progressive deformation under conditions of low grade metamorphism, other features of the microfabric such as microstructure, the strain sustained by quartz grains, and deformation lamellae were also studied. As the study progressed the mutual relationships of these elements of the microfabric became more and more obvious and a strong correspondence was found between the microstructure, the strain and the lattice preferred orientation. The quartzite preserves a good record of its microstructural development from virtually an undeformed state with sedimentary characteristics to a highly deformed state in which new, strain-free, polygonal grains completely replace the old, detrital, deformed grains. Six types of microstructure are recognisable and though the boundaries between these types are not sharp and one type tends to overlap the other, nevertheless these form a useful basis for the overall study of the microfabric. The following description of the microstructural types also includes the description of the related strain and the quartz c-axis preferred orientation. Deformation lamellae will be described in a separate section (Section 4.3.9). A discussion of the development of the preferred orientation will follow the description of the microfabric. Before proceeding with the description of the microstructural types, the methods of study of the elements of the microfabric together with the limitations involved are outlined.

4.2 Methods of study

In addition to the normal optical microscope observations of the microstructure, transmission electron micrographs were also obtained through the courtesy of Dr. Boland particularly for those features of the microstructure which could not be confidently interpreted optically.

The information regarding the strain resulting from shape changes of the quartz grains, was obtained by direct measurement of the short and the long axes of the grains in thin sections with an ocular grid and also their axial orientation as a function of the angle of the long axis from an arbitrary line. Thin sections were cut parallel to the principal planes and in quartzite samples with a foliation and a lineation, the principal planes were considered to be those which contained the observed directions of maximum shortening and elongation of the grains whereas in samples with bedding as the only planar structure, the thin sections were cut normal and parallel to it. Scatter diagrams from the values of axial ratio and axial orientation of the grains were then prepared for each two dimensional section and the two dimensional strain ratio was assessed by comparing the diagrams with the theoretically deduced curves (Dunnet, 1969). Dunnet has derived mathematical expressions which relate the final elliptical ratio and orientation of particles, subjected to homogeneous deformation, to their initial form and the magnitude and orientation of the finite rotational or irrotational strain. The three principal strain ratios can be determined from two of the principal plane sections and the third gives an independent check on the accuracy of the result. The samples used for this study were from almost pure quartzites and therefore the problems that arise

due to ductility contrast as well as due to the presence of several particle lithologies in a rock have been, to a great extent, avoided. Quartzites with evidence of recrystallization were also not used for strain determination.

For determining the orientations of the quartz c-axis in thin sections of the quartzite, a universal stage attached to a petrographic microscope was used. Thin sections from which measurements on the c-axis orientations were made were generally cut normal to the lineation, L_1, but occasionally measurements were also made from a thin section cut parallel to the lineation and normal to the foliation to check the homogeneity of the quartz sub-fabric in the domain of the sample. The measurements on an additional plane also served to check an error arising from a lack of measurements for grains whose c-axes are inclined at about 45° to the normal of the thin section. No significant difference was found in the two patterns of c-axis preferred orientation. Thin sections from samples in which L_1 was not present were cut either normal to the foliation or the bedding. Generally 300 c-axes were measured from each section but in certain cases variations were made from this practice. Traverses along which measurements were made were spaced in the thin section as suggested by Turner and Weiss (1963). The measurements were then plotted on the lower hemisphere of an equal area projection and contoured according to the method of Kamb (1959b) by an I.B.M. computer. In the explanatory text, N is the number of grains measured, E is the number of points expected to fall within a given test area A which is the area of the counting circle, and σ is the standard deviation from the expected density of a uniform population. The observed densities are therefore contoured in intervals of 2σ

at the values 0, 2σ, 4σ, etc., the expected density E for no preferred orientation being 3σ. The explanatory text for all the orientation diagrams shown in Fig. 4.1 has been provided in the appendix. In all the orientation diagrams, S denotes the sedimentary bedding, S1, the foliation, and L1, the lineation. The diagrams are arranged in Fig. 4.1 in such a way that the direction of traverses made for measurements in each thin section, representing one of the diagrams, is parallel to the north-south line in the figure. The trace of the bedding or the foliation is also parallel to this direction in all the diagrams except for three. Geographical orientation of the bedding or the foliation or the lineation for each diagram is given in the explanation of Fig. 4.1. An effort has also been made to arrange the diagrams in the figure to correspond with the general trend of the preferred orientation changes from south to north in the Atnarpa Range area although this has been hampered to some extent by the problem of space in the figure as well as local variations in the preferred orientation from the general trend. The localities of specimens of the quartzite used for the preferred orientation study as well as for the study of the other microfabric elements are also shown on Fig. 4.1 by ends of lines, the opposite ends of which point towards the specimen locality numbers. The selection of the specimen localities for this study was based on the following aims:

(a) To study the changes in preferred orientation with increase in deformation and relate the foliation and the lineation to these changes.

(b) To study the effect of the proximity of the thrusts on the preferred orientation.

(c) To study changes in the preferred orientation with respect to

FIGURE 4.1

Quartz c-axis orientation diagrams contoured according to Kamb (1959b) at the values 0, 2, 4, 6.....σ; σ = 2.9 (see also appendix). Location of specimens used for the preferred orientation study are shown on the geological map by ends of lines, at the other ends of which are given Specimen Locality numbers; these numbers also shown under the diagrams. In the diagrams S denotes the bedding, S1, the foliation, and L1, the lineation. Geographical orientation of the direction normal to each diagram and lying in the plane of the bedding or the foliation is as follows:

103	8°N65E	123	30°S20W	197	10°N50W
141	46°N30E	154	0°N35E	105	15° N15E
137	0°N30W	118	23°S40W	186	20° N30E
110	0°South	120	10°S40W	294A	20° N40E
112	0°N50E	122	8°S30W	128	38° S45W
282	0° East	101	0°N40E	159	20° N10E
212	0°N80W	237	55° North	278	28° North
144	80°S20E	195	5° N30E	161	40° N25W
147	0° West	228	26° West	164	31° N20W
150	65° South	104	41° N40E	176	34° N40W
115	0°S50W	294	22° N20E	215	25° N15W
167	0°N60E	130	40° N15W	226	74° North
146	0° East	156	65°N13W	279	10° North
				273	4° N5E

ng to
.9 (see
rred
of lines,
mbers;
rams
eation.
diagram
as follows

geographical directions in the area, particularly from south to north.

4.3 Description of the microfabric

4.3.1 Microstructural type I

The type is characterized by detrital quartz grains which in the case of pure quartzites are tightly locked together by authigenic quartz that grows in crystallographic continuity with that of the grains in the form of secondary overgrowths or enlargements on the grains (Plate 4.1a and b). The boundary between the overgrowth and the detrital grain is generally delineated by very small inclusions or impurities. The majority of the grains are rounded to sub-rounded and their degree of sphericity is usually fairly high but departures from that towards an elongate shape particularly in the small size grains are also observed. Undulatory extinction is locally present and polycrystalline grains are very rare. The type is also marked by the overall absence of dimensional orientation of the grains. The contacts between the grains are generally concavo-convex or almost straight. Quartzites with this type of microstructure are generally referred to as ortho-quartzites or pressolved quartzites (Skolnick, 1965, p.20) if they show signs of increasing compaction and initiation of grain boundary serration.

The strain in this type was determined at two specimen localities, locality 103 and locality 282 (Fig. 4.1). Plots of axial ratios from specimen locality 103 are shown on the scattar diagrams, Figs. 4.2a to c. Figs. 4.2a and b represent thin sections normal to the bedding and in these the bedding lies at ϕ = o; Fig. 4.2c represents thin section in the plane of the bedding. The plots show that planar preferred orientation of the grains is lacking in the bedding as well as in any

PLATE 4.1

Quartzite, (a) at Specimen Locality 103, (b) at Specimen Locality 282, and (c) at Specimen Locality 122. In (a) and (b) detrital quartz grains with a high degree of sphericity are shown; (c) exhibits elongate grains as well. The boundary between the overgrowth and the detrital grain is manifest in some of the grains and is generally delineated by very small inclusions or impurities. (Scale 0.5mm; crossed nicols)

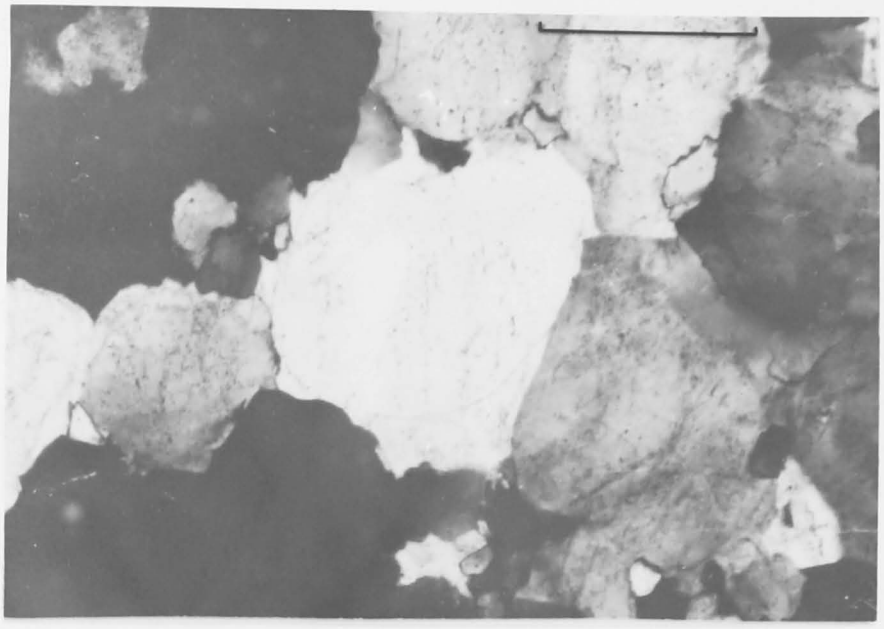

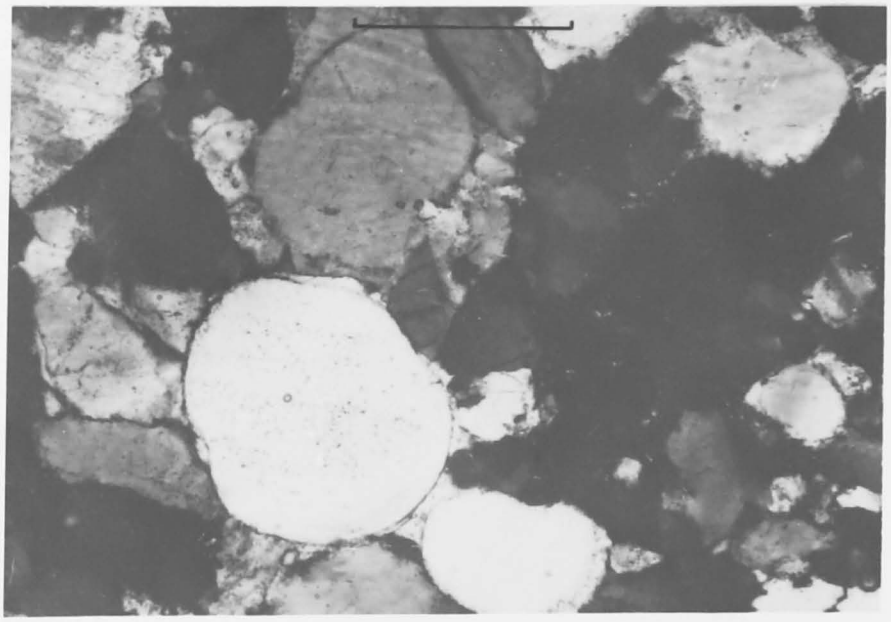

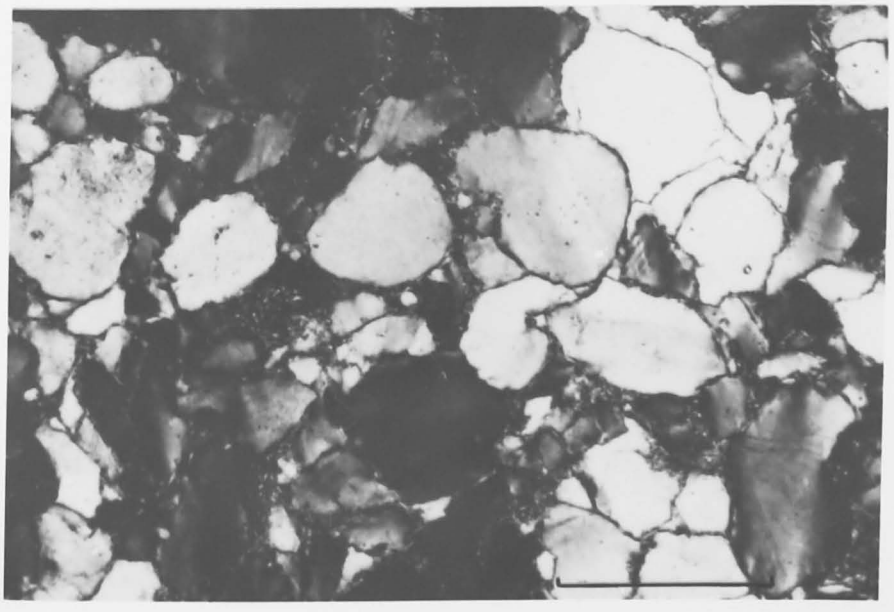

FIGURE 4.2

(a), (b), and (c). Scatter diagrams of Rf/ϕ on three mutually perpendicular planes of quartzite specimen from Specimen Locality 103. Diagrams (a) and (b) represent planes normal to the bedding and diagram (c) is in the plane of bedding.

(d), (e) and (f). Scatter diagrams of Rf/ϕ on three mutually perpendicular planes of quartzite specimen from Specimen Locality 122. Diagrams (d) and (e) represent planes normal to the foliation and diagram (f) is in the plane of foliation.

In all diagrams Rf = final deformed grain axial ratio; ϕ = angle from the Rf long axis to the maximum principal strain direction.

ly
ality
dding
y
ality
liation
ain

other direction. The finite strain ratio, Rs, is about the same in Figs. 4.2a and 4.2c but is slightly higher in Fig. 4.2b. It is not possible to derive the tectonic strain in the quartzite at the locality and the apparent strain may be due to initial variations in the shapes of the grains in the bedding. However on the assumption that Fig. 4.2b represents the XZ section of the ellipsoid and one of the rest of the figures represents the YZ section where X, Y, and Z are the longest, intermediate, and shortest axes of strain ellipsoid, the strain at the locality can be represented on the Deformation plot or Flinn diagram (Flinn, 1965, p.47) as shown in Fig. 4.5 but this is quite arbitrary. At the locality 282 it is not again clear whether the strain is tectonic or not, but it seems to be slightly higher than at the locality 103. The strain is represented by a shortening of less than 16% in the direction normal to the bedding and an elongation of less than 10% in the other two directions in the bedding in which it was measured.

The preferred orientation of the quartz c-axis within this microstructural type is shown in orientation diagrams representing specimen localities 103, 141, 110, 112, 282, 212 and 237 (see Fig. 4.1). There is no recognisable pattern of the preferred orientation in these diagrams and the randomness of the preferred orientation is obvious from the diagrams as well as from a comparison with the results obtained using random numbers to generate random poles (see Table 4.1). In the random pole diagrams the maximum concentration of the poles is at the contour value 2σ. Similar concentrations ranging from 50% to 66% are present in the c-axis orientation diagrams. The remaining area of these diagrams is divided into an area of no poles, an area defined by the 4σ contour but of about the same size as the

Table 4.1 Range of percentage areas occupied by each contour in C – axis orientation diagrams of Fig 4.1
(contours 0σ, 2σ, 4σ, etc, percentage areas 15 to 18, 68 to 72, etc)

Category of diagrams and Specimen Locality Numbers	0 σ	2 σ	4 σ	6 σ	8 σ	10 σ	12 σ	14 σ	16 σ
Random Pole Diagrams									
(a) Four, each with 200 random numbers	15 to 18	68 to 72	12 to 15						
(b) Four, each with 300 random numbers	11 to 15	67 to 70	15 to 20	0.0 to 2					
Microstructural Type I 103, 141, 110, 112, 282 212, 237	16 to 25	50 to 66	17 to 33	0.06 to 2.2					
Microstructural Type II 137, 167, 123, 154, 118, 120, 122, 101	20 to 32	40 to 60	17 to 24	1.0 to 4.5					
Microstructural Type III 144, 147, 115, 146, 104, 130 ⊐ 294 ⊐	22 to 33 41	40 to 57 27	17 to 23 26	1.3 to 4.4 5.6	0.0 to 1.5 0.4				
Microstructural Type IV 150, 156, 105, 186, 294A, 128, 159	30 to 48	18 to 46	17 to 30	2.5 to 9	0.0 to 4	0.0 to 2.4			
Microstructural Type V 195 ⊐ 228, 197, 161, 164, 176, 215, 278 ⊐ 226 ⊐	24 28 to 36 51	55 33 to 46 18	20 21 to 27 15	0.7 1.8 to 7 8	0.0 to 1.2 5	1.6	1.4		
Microstructural Type VI 279 273	51 58	18 19	15 9	9 4	6.7 3	0.3 1.6	2.2	2.2	1.0

area of no poles, and a very small area defined by the 6 σ contour, the size of which does not exceed more than 2.2% of the total area of the diagram. The major contour of the highest value is therefore 4 σ and slightly above what Kamb (1959b) considers to be random. Sedimentary bedding is the only planar structure in quartzites having this type of preferred orientation.

Quartzites with characteristics of microstructural type I generally occur in the southern part of the Atnarpa Range area and away from regions affected by thrust faults.

4.3.2 Microstructural type II

The quartz grains in this type are again detrital and the boundary between the grain and its overgrowth is manifest in a number of grains. The type differs from type I in that the grains are not generally tightly locked together by authigenic quartz, instead fine grained sericite is present along most of the grain boundaries. Other notable differences from type I are that undulose extinction is widespread, deformation lamellae are occasionally observed, the majority of the grains are elongate in shape and dimensional orientation of the grains is slight to fairly well marked (Plates 4.1c and 4.2a). The grain boundaries are straight to concavo-convex and slight serration of the boundaries is noticeable under high magnification. The grain size in these quartzites is considerably variable and ranges from about 0.1mm. to about 1mm.

The strain in this type was determined at two specimen localities nos. 122 and 118 (Fig. 4.1). The plots of axial ratios on scatter diagrams are shown in Figs. 4.2d to f for the locality 122 and in Figs. 4.3a and b for the locality 118. At both the localities a faint lineation in the quartzite is present. Figs. 4.2d to f represent the

PLATE 4.2

Quartzite, (a) at Specimen Locality — 118, (b) at Specimen Locality 128, and (c) at Specimen Locality 159.

Sections normal to the lineation. Deformed detrital quartz grains are dimensionally oriented. In some grains boundary between the detrital grain and its overgrowth is clearly seen. Grains with tapered ends are also seen. Undulose extinction is widespread and deformation bands and deformation lamellae are also evident.

(Scale 0.4mm; crossed nicols)

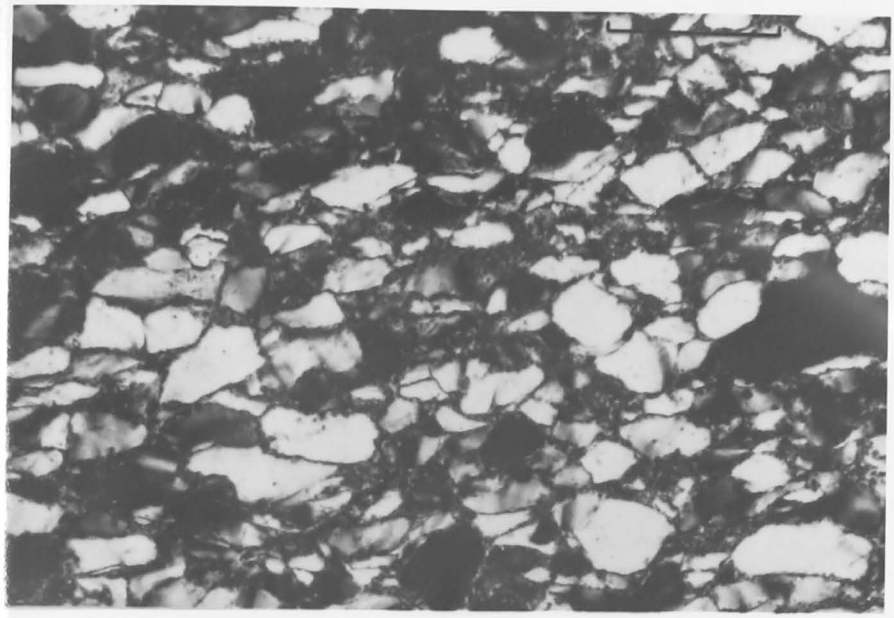

FIGURE 4.3

(a) and (b). Scatter diagrams of Rf/ϕ on two mutually perpendicular planes of quartzite specimen from Specimen Locality 118. The planes are normal to the foliation.

(c) and (d). Scatter diagrams of Rf/ϕ on two mutually perpendicular planes of quartzite specimen from Specimen Locality 156. The planes are normal to the foliation.

In all the diagrams Rf = final deformed grain axial ratio; Ri = initial undeformed grain axial ratio; Rs = finite strain axial ratio; and ϕ = angle from the Rf long axis to the maximum principal strain direction.

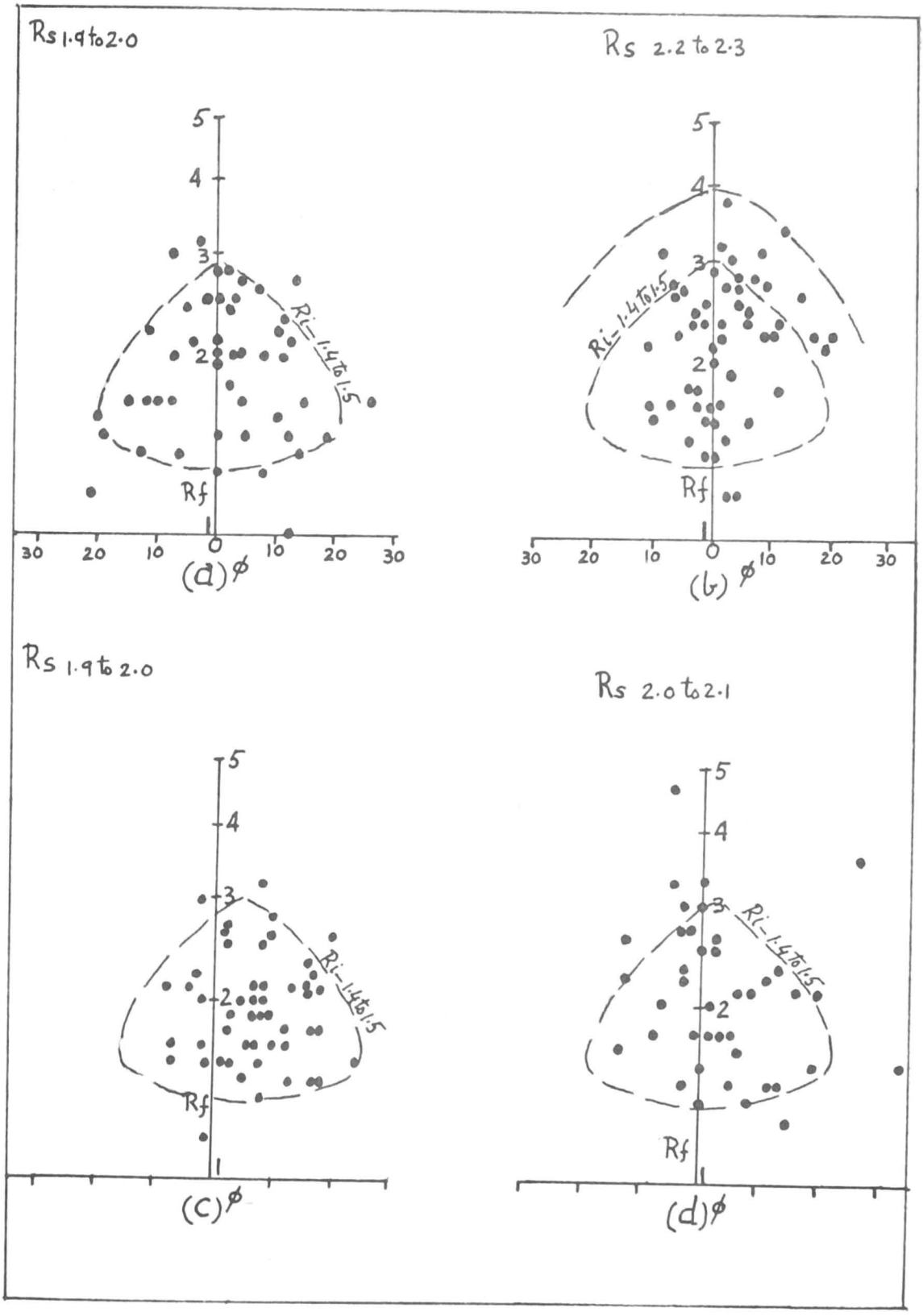
Rs 1.9 to 2.0
Rs 2.2 to 2.3
Ri = 1.4 to 1.5
Rf
(a) φ
(b) φ
Rs 1.9 to 2.0
Rs 2.0 to 2.1
(c) φ
(d) φ

YZ, XZ and XY planes of strain ellipsoid respectively and Figs. 4.3a and b represent the YZ and the XZ planes of the ellipsoid respectively. The foliation in all the diagrams except 4.2f is at ϕ = o. The deduced values of Rs, the finite strain axial ratio, are shown in the figures except in Fig. 4.2d, where the strain is not clear. The determination of strain at the locality 122 depends on what Rs value can be deduced from Fig. 4.2d, however according to an average estimate there is a shortening of between 15% and 20% normal to the foliation, an elongation of about 10% parallel to the lineation and a very slight elongation normal to the lineation in the foliation plane. The strain at the locality 118 is better defined than that at the locality 122 and shortening normal to the foliation is estimated to be between 35% and 40%, elongation normal to the lineation in the foliation plane to be between 15% and 20%, and elongation parallel to the lineation to be between 35% and 40%. The strains at both the localities have been represented on the Flinn diagram (Fig. 4.5).

The c-axis preferred orientation in this type is shown in orientation diagrams from specimen localities 137, 167, 123, 154, 118, 120, 122 and 101. The pattern and the degree of the preferred orientation slightly differs from that in type I. The patterns exhibit a tendency towards the formation of partial or complete girdles. The change in the degree of the preferred orientation is shown by some increase in the size of the pole free area in the diagrams, a decrease in the size of the area defined by 2σ contour, and an increase in the size of the areas defined by 4σ and 6σ contours. The range of percentage areas occupied by each contour are shown in Table 4.1. In orientation diagram representing specimen locality 137, a nearly complete but weak girdle lies about 60° from the bedding and in each of the two

diagrams representing specimen localities 123 and 154 weak partial girdles lie within 60° to 70° from the bedding. In the diagrams representing specimen localities 167 and 118 there is a strong suggestion of a cleft girdle about the foliation and the lineation and in the diagram representing specimen locality 122 two weak girdles one about 45° and the other 60° from the foliation intersect at about 90° from the lineation producing a weak crossed girdle pattern. The quartz sub-fabric, strictly judging, is triclinic but slight tendency towards monoclinic symmetry is noticeable. An important feature of the preferred orientation is that it is influenced by strain. The preferred orientation at specimen locality 118 is stronger than at specimen locality 122 and so is the strain greater at the former locality (see Fig. 4.5).

Quartzites with characteristics of microstructural type II generally occur in the southern and central parts of the Atnarpa range area.

4.3.3 Microstructural type III

The characteristic feature of this type of microstructure is that the quartzite is fractured and the fractures are irregular and closely spaced. Within these fractures the material appears to be very fine grained quartz or is isotropic (see Plates 4.3a and b, and 4.4a and b). Plates 4.3c and 4.4c are enlargements of small areas in Plates 4.3b and 4.4b respectively containing the very fine grained quartz. It is difficult to say from a study of these plates whether the fine grained quartz is due to brecciation or to polygonisation or nucleation and therefore transmission electron micrographs of this type of quartzite from specimen locality 146 were obtained. In the

PLATE 4.3

Quartzite, (a) at Specimen Locality 201, (b) at Specimen Locality 146, and (c) also at Specimen Locality 146. Very fine grained quartz associated with larger angular to sub-angular to sub-rounded grains. Edges of some of the grains are frayed. Fractures are easily noticeable in (b). In (c) a small area of fine grained quartz from (b) is enlarged. (Scale 0.1mm in (a), 0.4mm in (b) and 0.05mm in (c); crossed nicols)

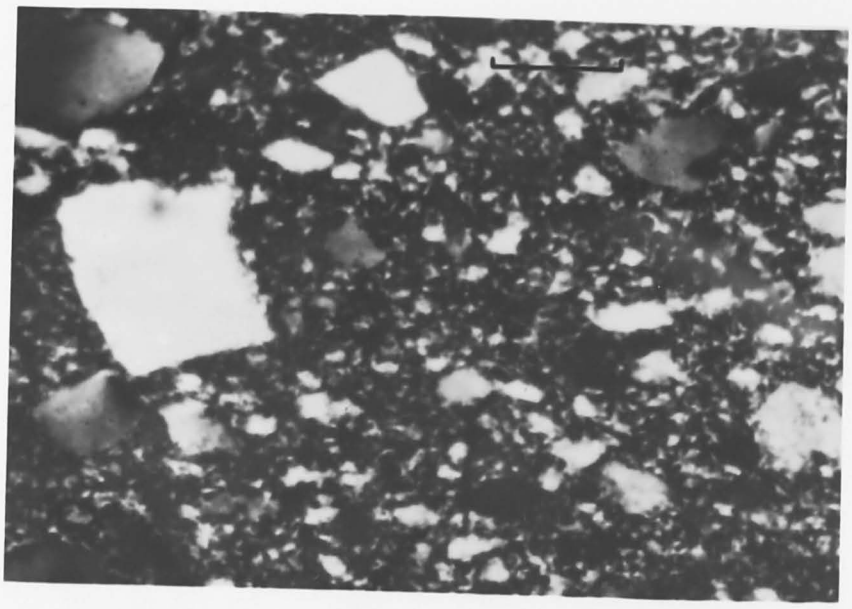

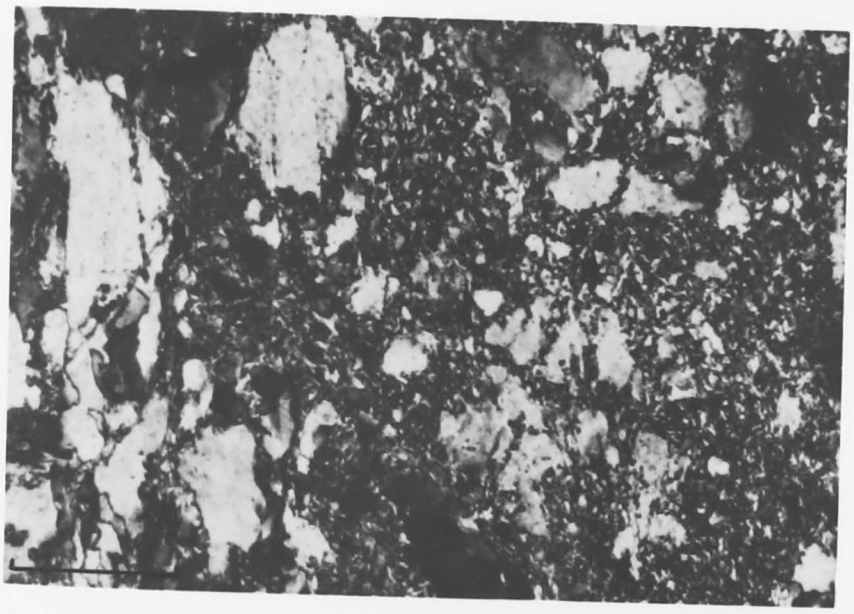

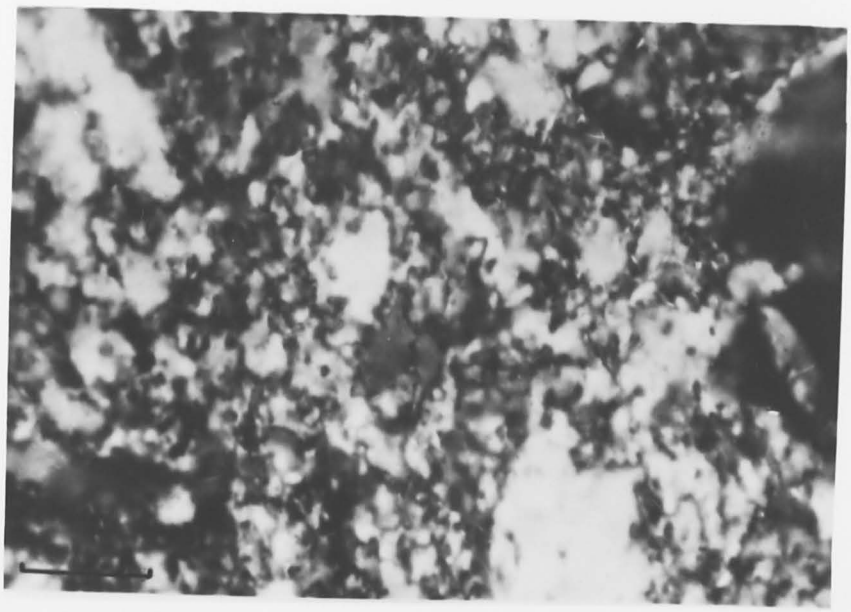

PLATE 4.4

Quartzite at Specimen Locality 294. Sections normal to the lineation. In (a) the outline of a large elongate quartz grain is shown in plane polarized light; the same grain is shown under crossed nicols in (b) and consists of very fine grained quartz associated with larger fragments. The material around this grain in the fractures is isotropic. In (c) a part of a grain within the large grain is shown under crossed nicols and new quartz grains are probably growing within the deformation bands, one set of which is more prominent than the other. (Scale 0.4mm in (a) and (b) and 0.05mm in (c).)

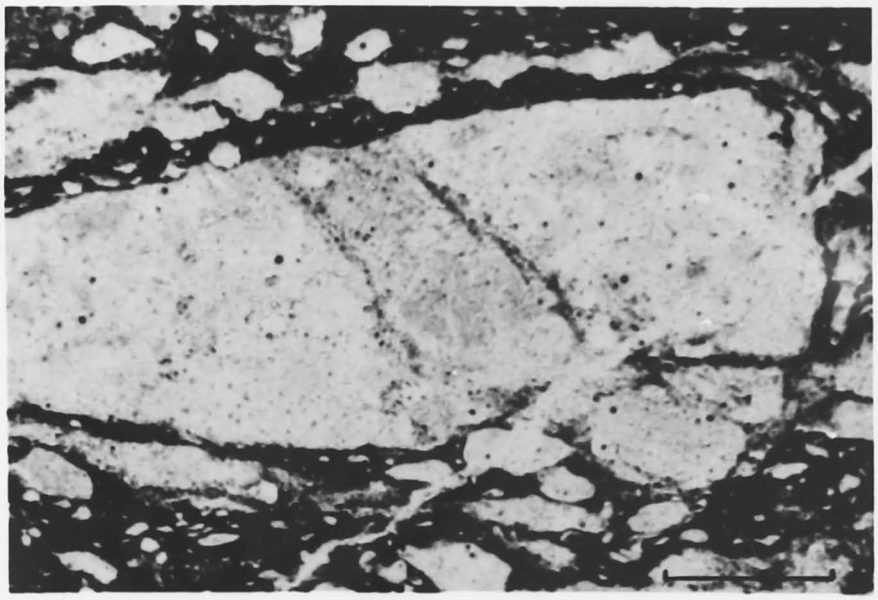

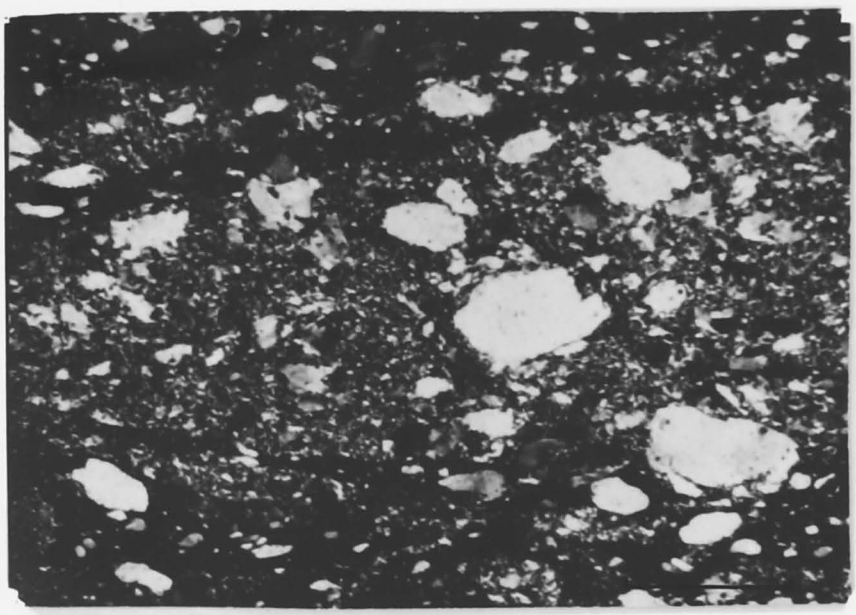

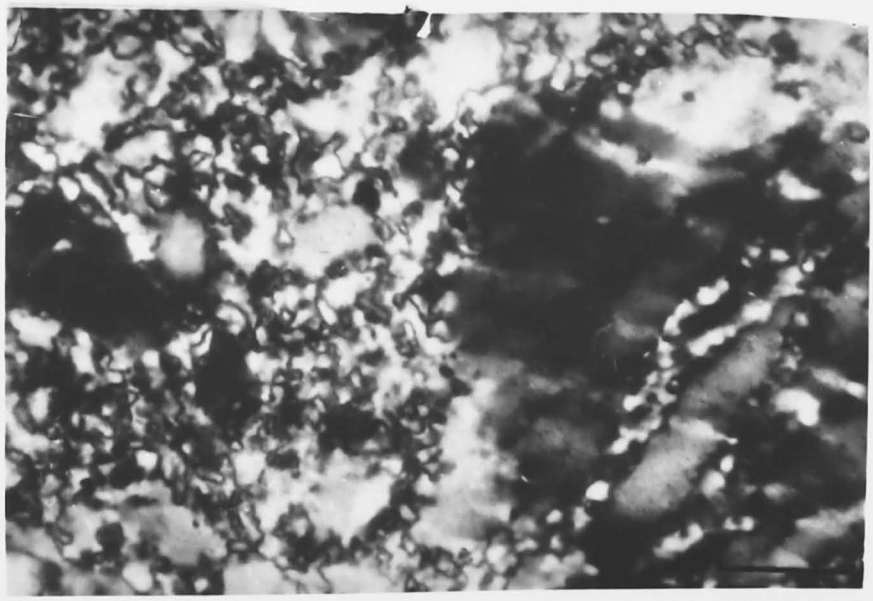

micrographs generally, the quartzite shows well defined cracks, as well as the development of polygonal structures and small strain-free sub-grains that could be interpreted as nuclei for subsequent recrystallization. Polygonal structures are evidenced by the dislocation sub-boundaries shown in Plate 4.11a. The "diamond" shaped dislocation free sub-grain having well developed polygonal outline in Plate 4.11b is a possible nucleus for recrystallization. A detailed study of the micrographs is yet in a preliminary stage but it indicates a range of dislocation substructural developments suggesting gradual changes from deformation structures to the incipient stages of recrystallization. The elongate quartz grains are rendered into angular to sub-angular and frayed grains smaller in size than the original grains as a result of slicing and granulation. Deformation lamellae in the porphyroclasts are common but the deformation bands are occasional; undulatory extinction is widespread. Plates 4.4a and b show a particular example of this type of microstructure at specimen locality 294 (see Fig. 4.1). A greater part of the quartzite around the large elongate grain is isotropic probably as a result of extreme granulation or psuedotachylization, the rest is in the form of sub-angular to sub-rounded grains of which the edges are sharp and straight or smooth and round or frayed. The outline of the elongate, large grains are clear in plane polarized light (Plate 4.4a) but are not so under crossed nicols (Plate 4.4b). The grains are internally deformed and consist of avery fine grained matrix and sub-angular to sub-rounded grains of small size. A part of one of these grains is shown in Plate 4.4c on the right hand side and this contains deformation bands within which probably new quartz is growing, also its margin appears to be granulated.

Strain measurements in this type are not possible owing to

fragmentation of the original grains.

The c-axis preferred orientation in this type is shown in orientation diagrams representing specimen localities 144, 147, 115, 146, 104, 294, and 130 (Fig. 4.1). The strength of the preferred orientation is weak to moderate and while at one end the strength is similar to that of the preferred orientation in microstructural type II, at the other it merges with that in type IV. The strongest preferred orientation in this type is at specimen locality 294 (Fig. 4.1). The range of percentage areas occupied by each contour are presented in Table 4.1 and the percentage areas for the diagram representing specimen locality 294 have been separated because they differed significantly from the rest. The symmetry of the quartz sub-fabric is triclinic in the majority of the diagrams but is monoclinic or tends to be so in the rest. The symmetric relationship of the quartz sub-fabric with the mesoscopic sub-fabric is only evident at specimen locality 294 where the two sub-fabrics have a common symmetry plane.

Quartzites having characteristics of this microstructural type generally occur along thrust faults in the western half of the Atnarpa Range area and generally lie at the footwall of the thrusts. Mesoscopically these quartzites are light gray to dark gray, highly fractured and generally are not layered or lineated, the quartzite at specimen locality 294 however, is lineated.

4.3.4 Microstructural type IV

This type represents a more advanced stage of deformation than the type II or the type III and within this type itself there is a progressive change in deformation as shown by Plates 4.2b, 4.2c, 4.5b,

4.6a, and 4.6b. In Plates 4.2b and c the clastic nature of the grains is obvious and in some grains the boundary between a grain and its overgrowth can be clearly seen. Increase in deformation is associated with increase in elongation of the grains, and in the strength of dimensional orientation. Most of the elongate grains have tapered ends probably due to inhomogeneous strain. The grain boundaries are generally undisturbed and serration where present is slight but in the most advanced stage of development of this microstructure as is shown in Plate 4.6b, the serration of the boundaries becomes more obvious. Sericite is generally present along grain boundaries and in Plate 4.6a it is extensively present. Sub-grain structure is not common but where it occurs in a grain as in Plate 4.5a the boundaries between the sub-grains are serrate. On the upper and the lower margins of the dark sub-grain shown in Plate 4.5a very small new grains have started growing and are more clearly seen under high magnification. The dark sub-grain has developed a box like or criss-cross structure which might be an early stage of polygonisation or this structure may represent two sets of deformation bands. Structures of this type have been observed to be associated with other sub-grains also. Undulatory extinction seems to be well defined in the more deformed grains and grades into deformation bands. The distinction between the undulatory extinction and deformation bands is sometimes difficult and has to be arbitrary. Carter et al. (1964) suggest that for descriptive purposes these two features of bending can be distinguished on the basis of the comparison of the radius of the bending with the width of the reoriented zone. In undulatory extinction the radius is larger whereas in deformation bands it is smaller than half of the width of the zone. In some grains two sets

PLATE 4.5

Quartzite, (a) at Specimen Locality 159, and (b) and (c) at Specimen Locality 105. Sections (a) and (b) are normal to the lineation and (c) is parallel to the lineation but normal to the foliation. (a) shows subgrains with serrate boundaries within a large, elongate grain. (b) and (c) show elongate grains with tapered ends, deformation bands, and recrystallization at a very incipient stage. (Scale 0.4mm; crossed nicols)

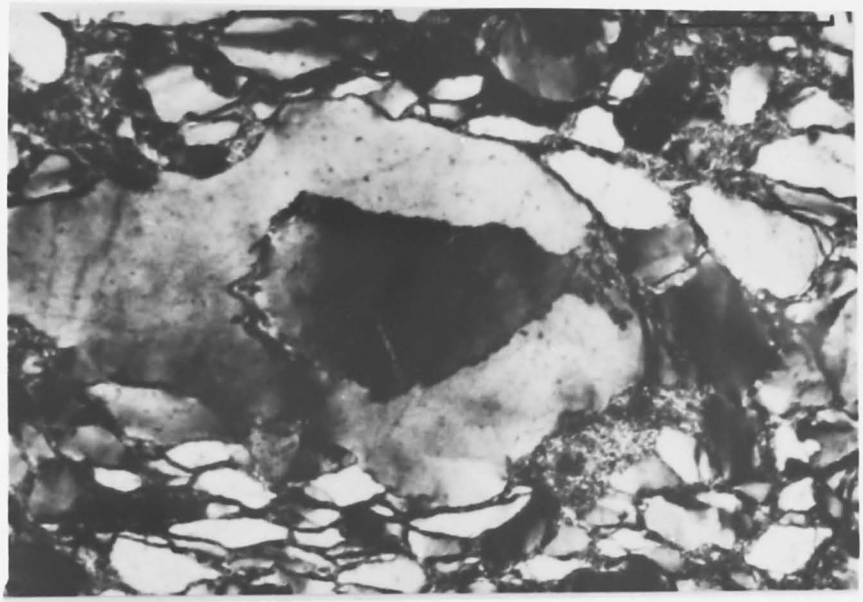

PLATE 4.6

Quartzite, (a) at Specimen Locality 184, and (b) and (c) at Specimen Locality 186. Sections normal to the lineation. In (a) and (b) deformation bands are almost parallel to the foliation. Deformation lamellae in a part of the grain close to the lower right hand corner of (a) are clearly seen. In (a) the matrix is mostly micaceous whereas in (b) it consists of very fine grained recrystallized quartz. Serration of deformation band boundaries and development of ribbon texture is evident in (b). Mode of recrystallization can be more clearly observed in (c) which is an enlargement of a small part of (b). (Scale 0.4mm in (a) and (b) and 0.05mm in (c); crossed nicols)

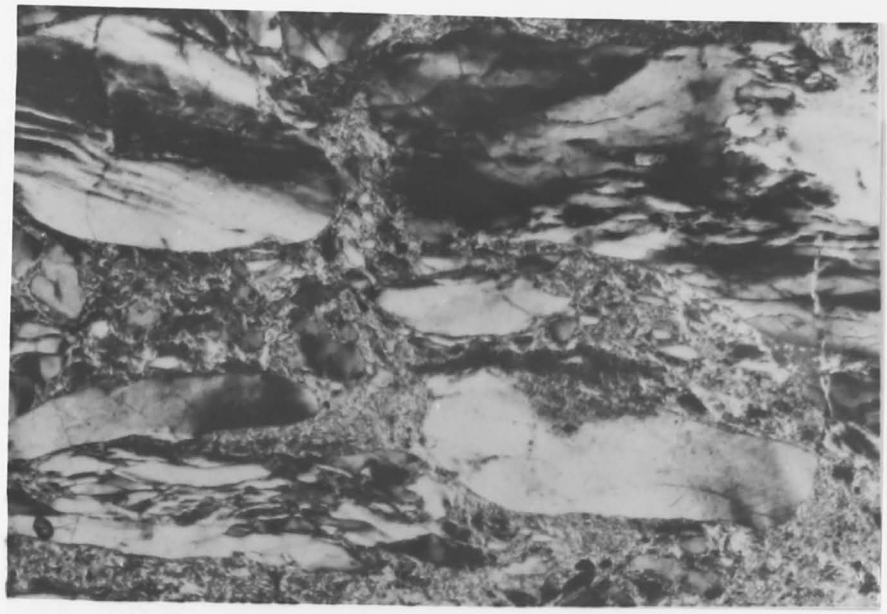

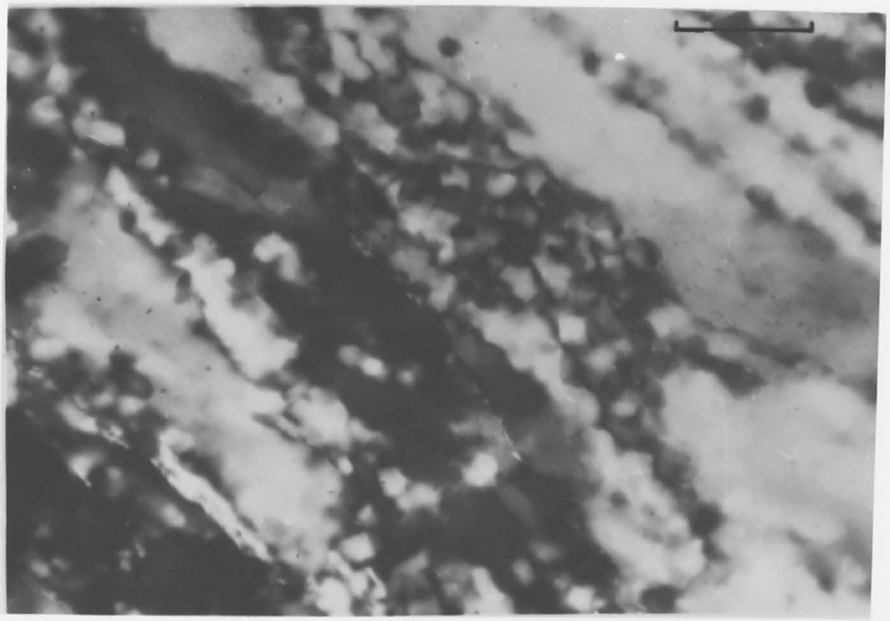

of deformation bands are observed, the more prominent one is associated with undulose extinction and the other almost perpendicular to the first is associated with deformation lamellae. A transmission electron micrograph of the early stage of development of this microstructure obtained from specimen locality 128 is shown in Plate 4.11c. A high density of dislocations and their tangled nature in the sub-grains is evident from the plate.

Plate 4.6b represents the most advanced stage of the development of this microstructural type and the microstructure in it is typically of mylonitic type. Plate 4.6a shows a slightly earlier stage in the microstructural development than Plate 4.6b and provides an insight in the development of the microstructure to a stage shown in Plate 4.6b. At this stage the elongate grains are separating into ribbons or lenticles along deformation band boundaries most of which are almost parallel to the length of the grains. All the grains are internally deformed and newly recrystallized grains can be observed within the deformation bands as well as along the band boundaries. Plate 4.6c is an enlargement of a small area in Plate 4.6b and is similar to Plate VIID of Hobbs (1968) syntectonic recrystallization experiments on quartz. The very small new grains have nearly the same orientation of the c-axis as the host grain but as they grow in size their orientation changes with the result that they stand out from the surrounding host. Deformation lamellae at this stage are very rare. Another feature of recrystallization in this microstructural type is observed at specimen locality 156 (see Plates 4.7a and b). Plate 4.7a shows a deformed, elongate grain with two sets of deformation bands, one more prominent than the other. Plate 4.7b is an enlargement of an area of the elongate grain and shows the

PLATE 4.7

Quartzite, (a) and (b) at Specimen Locality 156 and (c) at Specimen Locality 164. Sections normal to the lineation. In (a) two sets of deformation bands are seen in a large elongate grain. In (b) the growth of new grains occurring along deformation bands in a part of the large grain in (a) is shown at a larger scale. (c) shows the growth of new grains from old, deformed grains with deformation bands. (Scale 0.4mm in (a) and (c) and 0.1mm in (b); crossed nicols)

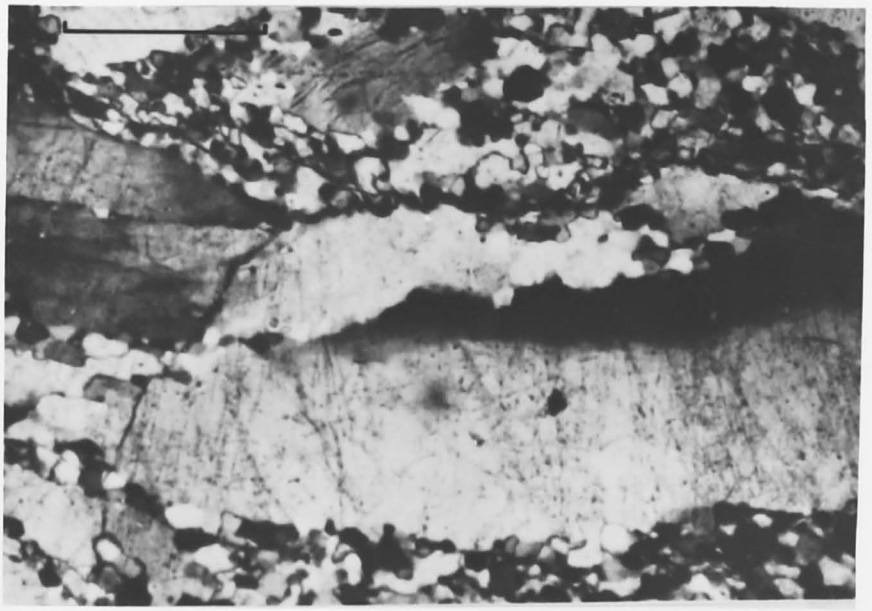

(c) at
In (a)
grain,
n bands
cale.
ns with
in (b);

growth of new grains along deformation bands. Almost all the new grains have similar orientations. Plate 4.7b is similar to Plate I D of Hobbs (1968) stress-annealed single crystals of quartz.

The strain in this type was determined at specimen localities 156, 105, 128, and 159 (Fig.4.1). The plots of axial ratios for the localities 156 and 105 are shown in Figs. 4.3c and d and Figs. 4.4a to c respectively. Figs. 4.3c and d represent the YZ and XZ sections and Figs.4.4a to c represent the YZ, XZ and XY sections of strain ellipsoid respectively. In all the figures except Fig.4.4c the foliation is at ϕ = o. The deduced Rs values are shown in the figures. An estimate of the shortening normal to the foliation and elongation parallel to the lineation in the foliation at each locality is as follows:

Specimen locality 156: Shortening between 35% and 38%; elongation between 30% and 34%; elongation normal to the lineation in the foliation between 25% and 30%.

Specimen locality 105: Shortening between 48% and 52%; elongation between 110% and 130%; shortening normal to the lineation in the foliation about 10%.

Specimen locality 128: Shortening between 36% to 40%; elongation between 80% and 84%; shortening normal to the lineation in the foliation about 12%.

Specimen locality 159: Shortening between 50% and 54%; elongation between 100% and 105%; very slight or no change in the direction normal to the lineation in the foliation.

The strains at all the localities are represented on a Flinn diagram (Fig. 4.5).

The preferred orientation of the quartz c-axis in this microstructural type is well defined and becomes stronger with the advance-

FIGURE 4.4

(a),(b), and (c). Scatter diagrams of Rf/ϕ on three mutually perpendicular planes of quartzite specimen from Specimen Locality 105. Diagrams (a) and (b) represent planes normal to the foliation and diagram (c) is in the plane of foliation.

In all the diagrams Rf = final deformed grain axial ratio; Ri = initial undeformed grain axial ratio; Rs = finite strain axial ratio; and ϕ = angle from the Rf long axis to the maximum principal strain direction.

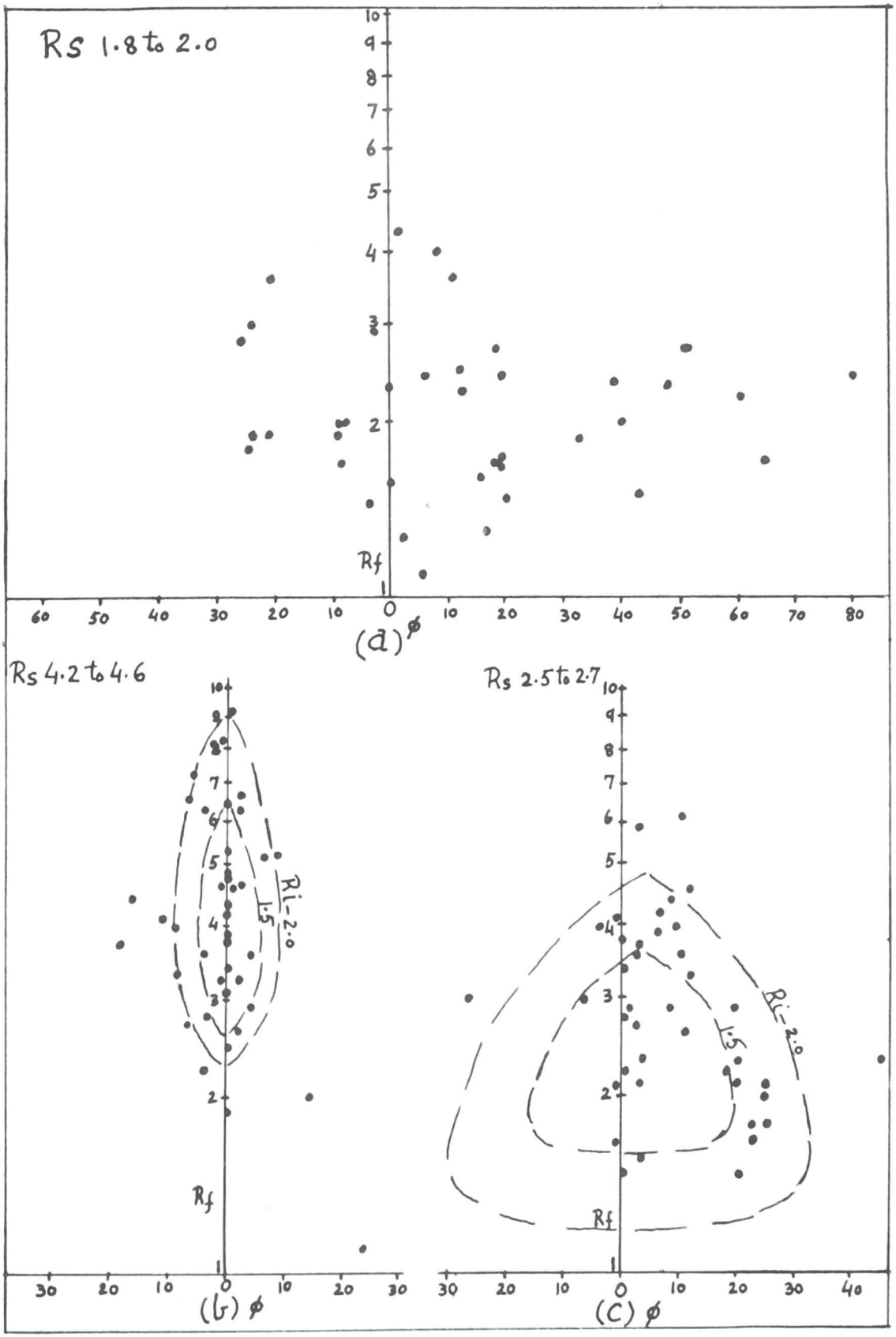
Rs 1·8 to 2·0
Rf
φ
(a)
Rs 4·2 to 4·6
Ri-2·0
1·5
Rf
(b) φ
Rs 2·5 to 2·7
Ri-2·0
1·5
Rf
(c) φ

FIGURE 4.5

Flinn diagram showing strain in the quartzite at Specimen Localities marked by crosses. X, Y and Z are the longest, intermediate and shortest axes of strain ellipsoid. Quartz c-axis orientation diagrams at five of the Specimen Localities are also shown. In these diagrams S denotes bedding; S1, foliation; and L1, lineation. The diagrams are contoured according to Kamb (1959b) at the values 0, 2, 4, 6.....σ ; σ = 2.9.

105: 300 poles, A = 0.029, E = 8.7, Max. = 11.3 σ.

128: 300 poles, A = 0.029, E = 8.7, Max. = 7.5 " .

118: 344 poles, A = 0.025, E = 8.8, Max. = 8.6 " .

122: 300 poles, A = 0.029, E = 8.7, Max. = 7.2 " .

103: 300 poles, A = 0.029, E = 8.7, Max. = 6.5 " .

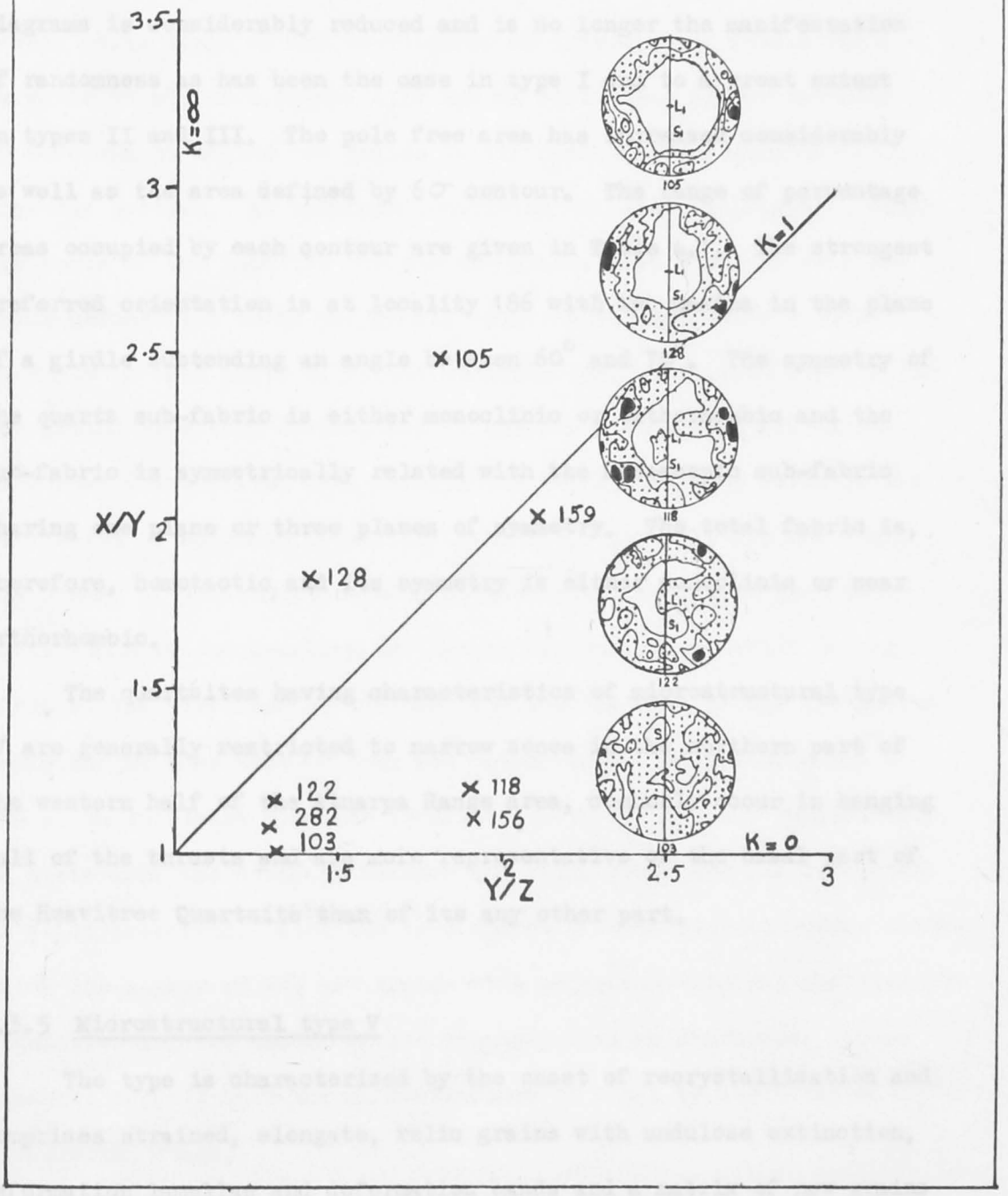
3·5
3
2·5
2
1·5
1
K=∞
X/Y
105
159
128
122
282
103
118
156
K=1
K=0
1·5
2
2·5
3
Y/Z
L1
S1
105
128
118
122
103

ment in the development of the microstructure. The strength of the preferred orientation also increases with the increase in strain. Orientation diagrams with this type of the preferred orientation represent specimen localities 150, 156, 105, 186, 294A, 128, and 159 (Fig. 4.1). The pattern in these diagrams is marked by a girdle with one or more maxima. The area defined by 2σ contour in the diagrams is considerably reduced and is no longer the manifestation of randomness as has been the case in type I and to a great extent in types II and III. The pole free area has increased considerably as well as the area defined by 6σ contour. The range of percentage areas occupied by each contour are given in Table 4.1. The strongest preferred orientation is at locality 186 with two maxima in the plane of a girdle subtending an angle between 60° and 70°. The symmetry of the quartz sub-fabric is either monoclinic or orthorhombic and the sub-fabric is symmetrically related with the mesoscopic sub-fabric sharing one plane or three planes of symmetry. The total fabric is, therefore, homotactic and its symmetry is either monoclinic or near orthorhombic.

The quartzites having characteristics of microstructural type IV are generally restricted to narrow zones in the northern part of the western half of the Atnarpa Range area, commonly occur in hanging wall of the thrusts and are more representative of the basal part of the Heavitree Quartzite than of its any other part.

4.3.5 Microstructural type V

The type is characterized by the onset of recrystallization and comprises strained, elongate, relic grains with undulose extinction, deformation lamellae and deformation bands and a matrix of new grains which are free of strain. The development of the new grains either

takes place along highly sutured sub-grain boundaries within the relic grain or on the margins of a grain or as isolated grains within the host grains apparently without any structural control (see Plates 4.7c, 4.8a, b and c). The boundaries between the new grains and their host are generally curved whereas boundaries between the new grains themselves are straight or tend to be straight. A very early stage of the development of this type of microstructure is shown in plates 4.6c and 4.7b and in both these plates the mode of development of the new grains is different as described in the previous section. At specimen localities 161 and 164 (Fig.4.1) which are north of the locality 156 the new grains have grown in size and their shapes tend to be polygonal. Plate 4.8a represents specimen locality 161 and plate 4.7c, the locality 164. The grain size of the new grains is within 0.15mm. and it appears that recrystallization is strongly associated with deformation bands. Further north in the quartzites of specimen localities 176, 215, 195, 197, 226 and 278 the number of the relic grains decreases with the result that these are minimum at the locality 226 the microstructure of which is very close to the next microstructural type and the size of the new grains increases so that most of them are 0.1mm. long. Plates 4.8b and c and 4.10a represent specimen localities 215, 197 and 278 respectively. In plate 4.8c the boundary between the relic grain and its overgrowth is still preserved. With the development of this microstructure northwards the number of the new grains with polygonal outlines and straight boundaries and the number of the triple junctions increases; these features suggest that the microstructure is close to acquiring an equilibrium stage.

The preferred orientation of the quartz c-axis in this type is

PLATE 4.8

Quartzite, (a) at Specimen Locality 161, (b) at Specimen Locality 215 and (c) at Specimen Locality 197. Sections normal to the lineation. (a),(b) and (c) show development of new, strain free quartz grains from the old, deformed grains. In (c) the boundary between the detrital grain and its overgrowth can be seen in the relic grain. (Scale 0.1mm; crossed nicols)

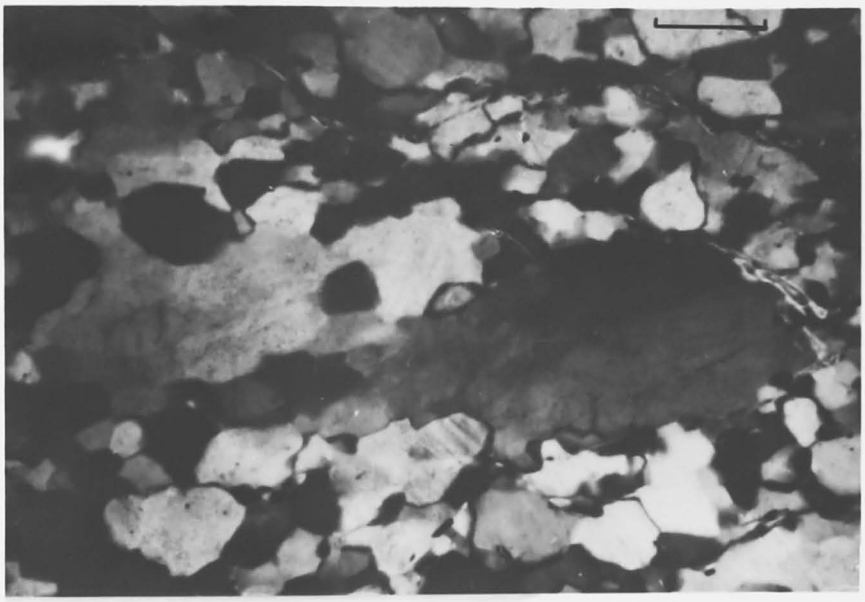

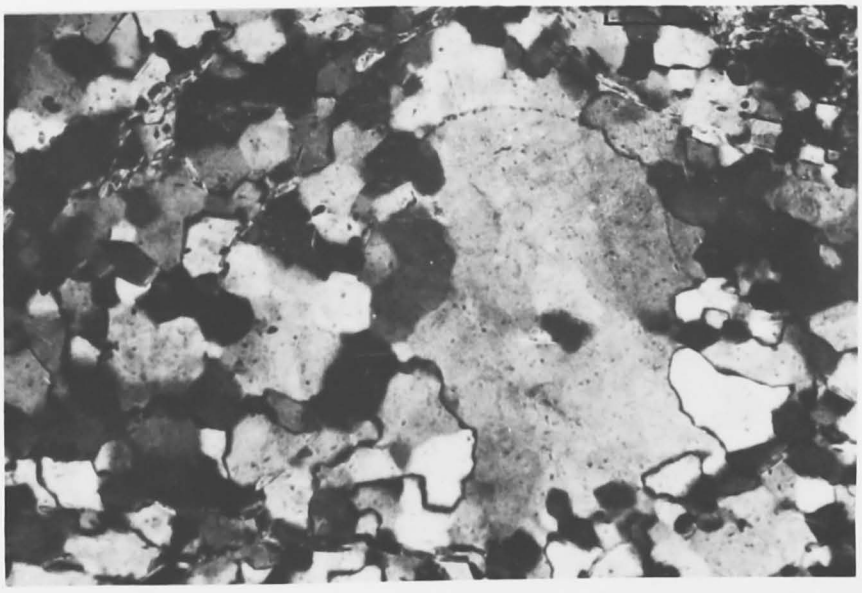

shown in orientation diagrams representing specimen localities 195, 228, 197, 161, 164, 176, 215, 226, and 278 and combines the orientation of the old and the new grains. It has been separated for the old and the new grains in some cases and presented and discussed that way in sub-section 4.3.8. Most of the diagrams show a fair to strong degree of the preferred orientation and the range of percentage areas occupied by each contour is similar to that in type IV and has been shown in Table 4.1. The strongest preferred orientation in this type is at locality 226 which is comparable in strength to the preferred orientation at locality 186 and at locality 279. In fact the microstructure at localities 226 and 279 is almost the same except that some relic grains survive at the former locality whereas none survives at the latter. The patterns of the preferred orientation of this type are marked in most cases by 20° to 30° shift of the girdle from the periphery. In some diagrams there is a tendency for the development of a crossed girdle pattern and this tendency is well marked at the locality 215. Another feature of the preferred orientation is the development of a second pole free area at or in the vicinity of the pole to the foliation. This area merges with the main pole free area at the locality 226. The new girdle which in most cases lies at 60° to the foliation either strikes parallel to it or across it as at specimen locality 161. The symmetry of the preferred orientation varies from near orthorhombic to near monoclinic but at specimen locality 228 it is triclinic. The symmetry of the quartz sub-fabric does not accord with that of the mesoscopic sub-fabric and the total fabric, therefore, is heterotactic.

The microstructural type is only developed on the northern limb of the Eastern Hill Range.

4.3.6 Microstructural type VI

This is the most advanced stage of microstructural development in the Atnarpa Range area and is characterized by complete recrystallization with the result that no relic grains are present and the microstructure comprises a net work of new, mostly polygonal, inequant, strain free grains with a tendency in the larger grains to be dimensionally oriented. The size of the new grains has increased and varies from about 1mm. to about 2mm. Triple point junctions are common and the microstructure seems to have reached a stage of equilibrium. Plates 4.9a and b exhibit this type of microstructure and are from specimen localities 273 and 279.

The c-axis preferred orientation in this type is marked by a high degree of preferred orientation and is shown in orientation diagrams representing specimen localities 279 and 273 (Fig. 4.1). The diagrams are marked by a large pole free area; the percentage areas occupied by each contour are given in Table 4.1. The pattern at the locality 279 is marked by a small circle girdle with three symmetrically situated maxima which appears to have evolved from a peripheral girdle with two maxima. The pattern at the other locality is that of an elongated maximum in the plane of a partial to complete girdle. The symmetry of the quartz sub-fabric in both cases is orthorhombic but does not correspond with that of the mesoscopic sub-fabric.

The quartzites with the characteristics of this microstructural type occur all along the thrust marked by specimen locality 279 on the northern limb of the Eastern Hill Range and northeast of the road and Atnarpa Range junction. These are ubiquitous in the outcrop of the quartzite north of the thrust in the same area and also occur at a few localities along the northernmost thrust between specimen locality 226 and the yard.

PLATE 4.9

Quartzite, (a) at Specimen Locality 273 and (b) at Specimen Locality 279. Sections normal to the lineation. Polygonal shaped, inequant, strain free, recrystallized grains with many triple point junctions. (Scale 0.1mm; crossed nicols)

Specimen

al shaped,

iple point

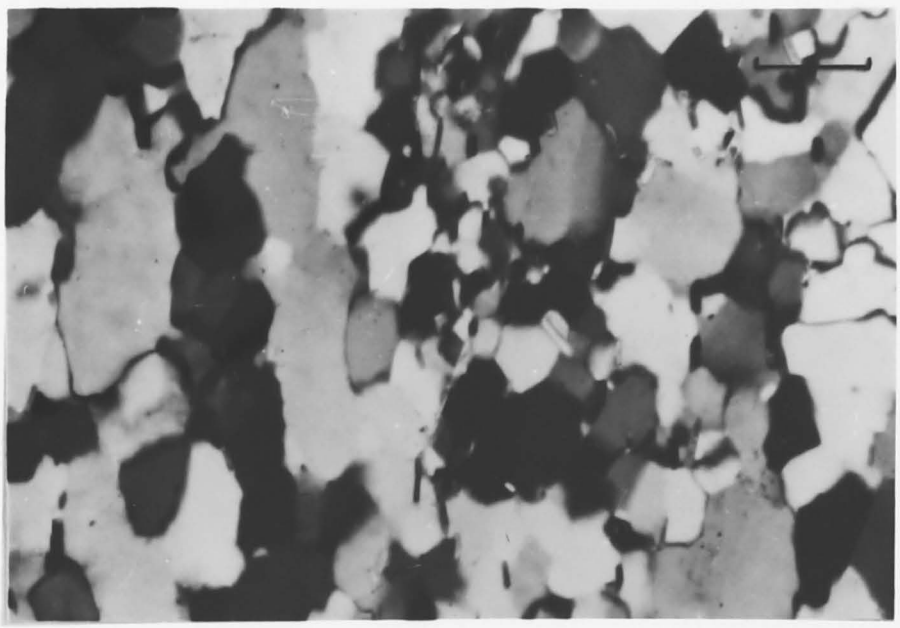

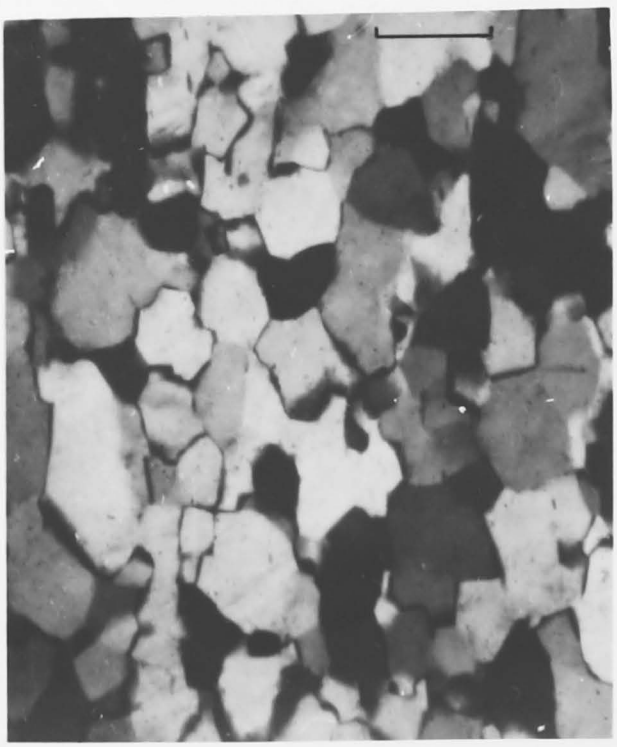

4.3.7 Relationship of the preferred orientation with the thrust

The microstructure and the preferred orientation at specimen locality 278 are of type V and at specimen locality 279 are of type VI, the preferred orientation at the latter locality is much stronger than at the former and the quartzite of the locality 278 lies vertically below that of the locality 279 and, therefore, also below the thrust (see Fig. 4.1 and Map 1). These features suggest that the strength of the preferred orientation and its development in this area are related to the distance from the thrust. To test further the validity of this relationship two specimens of the quartzite were collected across the strike and in the up dip direction from the locality 279 and at stratigraphic intervals of 5 and 10 metres from it. The locality of the first specimen is referred as 279A and that of the second as 279B. The preferred orientation was determined in the two specimens and is shown in Fig. 4.6 together with the preferred orientation at the localities 278 and 279. The change in the strength of the preferred orientation from the locality 279B to the locality 279 is evident and substantiates the above observation. The microstructure also changes from the locality 279B to the locality 279 and this change is shown in Plates 4.10b and c; in Plate 4.10a the microstructure at the locality 278 is shown for comparison. Dimensional orientation is lacking in recrystallized grains at the locality 279B, it appears at the locality 279A and is well marked at the locality 279. Recrystallization consumes all relic grains at the locality 279 whereas these are present at the other two localities.

4.3.8 Preferred orientation and host control

The microstructural type V offers the opportunity of studying the c-axis orientation relationship between the new and the old grains. A

FIGURE 4.6

Quartz c-axis orientation diagrams showing changes in the strength and pattern of preferred orientation with proximity of a thrust. In the diagrams S1 denotes foliation and L1, lineation.

The diagrams are contoured according to Kamb (1959, b) at the values 0, 2, 4, 6,..... σ ; σ = 2.9.

278 :	300 poles,	A = 0.029,	E = 8.7,	Max. =8.2 σ
279B:	200 poles,	A = 0.043,	E = 8.6,	Max. =8.7 σ
279A:	224 poles,	A = 0.039,	E = 8.7,	Max. =13.5 σ
279:	200 poles,	A = 0.043,	E = 8.6,	Max. =10.5 σ

278

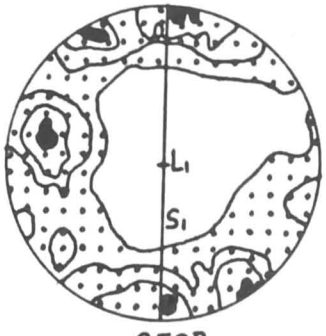

279B

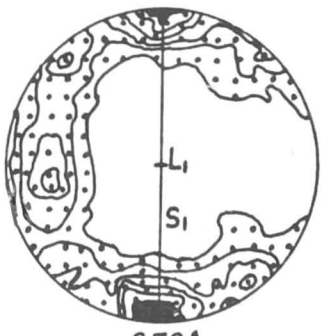

279A

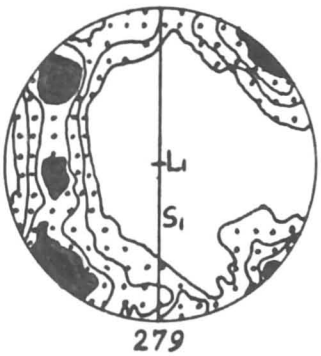

279

PLATE 4.10

Quartzite, (a) at Specimen Locality 278, (b) at Specimen Locality 279B and (c) at Specimen Locality 279. Sections normal to the lineation. (a), (b) and (c) show changes in microstructure with proximity of the thrust. Specimen Locality 279 is at the thrust. (Scale 0.4mm; crossed nicols).

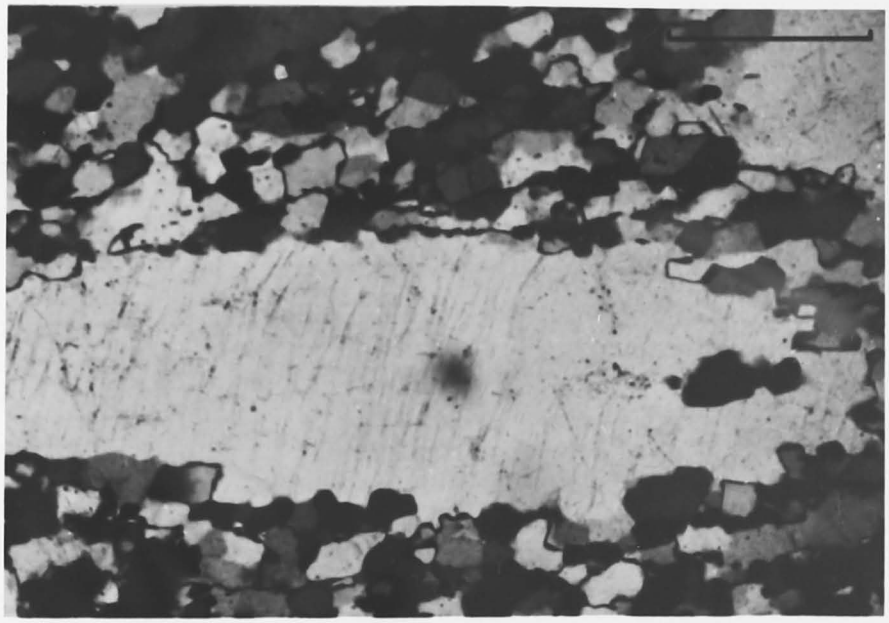

PLATE 4.11

(Transmission Electron Micrographs by courtesy of Dr. J. N. Boland.)

Quartzite, (a) and (b) at Specimen Locality 146, and (c) at Specimen Locality 128. Sub-grains with dislocation sub-boundaries are shown in (a). In (b) a "diamond" shaped dislocation free sub-grain (possible nucleus for recrystallization) is shown within a matrix of deformed sub-grains. Both (a) and (b) represent a part of a region of very fine grained quartz as shown in Plate 4.3b. In (c) sub-grains with high density of tangled dislocations are seen. (Scale is one micron)

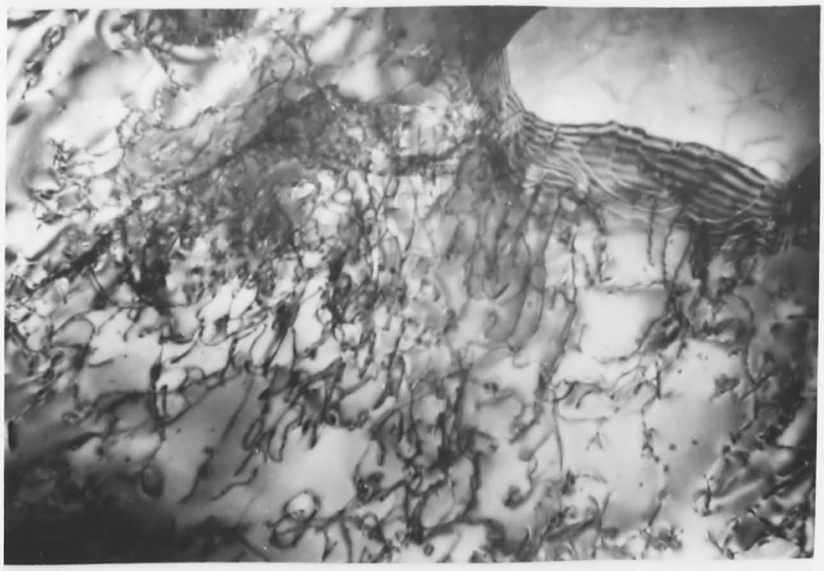

knowledge of this relationship is important, for preferred orientation in recrystallized material may be dependent on host control rather than on any other factor. The old grains can be distinguished from the new grains on the basis of their larger grain size, the presence of deformation features within the grain and the misorientation across new and old interfaces. The c-axis orientations of the old and the new grains have been shown separately in Fig.4.7 and also compared with their combined orientations. The orientation diagrams show that the c-axes of the old grains tend to lie at or very close to the periphery and the c-axes of the new grains tend to concentrate in a partial or complete girdle 20° to 30° from the periphery. The angular relationships between the old and the new c-axes at five specimen localities are plotted on frequency diagrams and shown in Fig.4.8 separately for each locality. A comparison has been illustrated in all diagrams with a line which depicts the distribution of a random population expressed as a frequency per cent. This line was derived from the probability theory for a random point on a sphere (see, for example, Plummer, 1940, p.83). If lines emanating from an origin intersect a concentric sphere, the random directions of the lines are represented by random points on the surface of the sphere. If θ is the distance from a fixed pole on the sphere it can be shown that the chance of a point falling within the zone θ and $(\theta + \delta\theta)$ of a hemisphere is $\cos\theta - \cos(\theta + \delta\theta)$. The peaks in the diagrams represent the angles favoured for growth by most of the new grains and these angles differ so that the prominent peak is between 60° and 70° at

FIGURE 4.7

Quartz c-axis orientation diagrams showing relationship between the preferred orientation of the c-axes of old, host grains and the preferred orientation of the c-axes of new grains at Specimen Localities 215 and 218. Diagrams with combination of the preferred orientation of old and new grains are also shown.

In the diagrams S1 denotes foliation and L1, lineation.

The diagrams are contoured according to Kamb (1959b) at the values 0, 2, 4, 6,..... σ ; σ =2.9.

215 combined :	300 poles,	A = 0.029,	E = 8.7,	Max. = 7.9σ
215 old :	200 poles,	A = 0.043,	E = 8.6,	Max. = 9.1 "
215 new :	200 poles,	A = 0.043,	E = 8.6,	Max. = 7.3 "
278 combined :	300 poles,	A = 0.029,	E = 8.7,	Max. = 8.2 "
278 old :	110 poles,	A = 0.074,	E = 8.3,	Max. = 7.6 "
278 New :	130 poles,	A = 0.064,	E = 8.4,	Max. = 8.5 "

FIGURE 4.8

Histograms showing frequency, F, of angles, Θ, between quartz c-axes of new grains and the c-axes of adjacent old grains at Specimen Localities 164, 215, 197, 278 and 226. Superimposed on the histogram is a curve showing the theoretical distribution between 2 lines, one of fixed and one of random orientation.

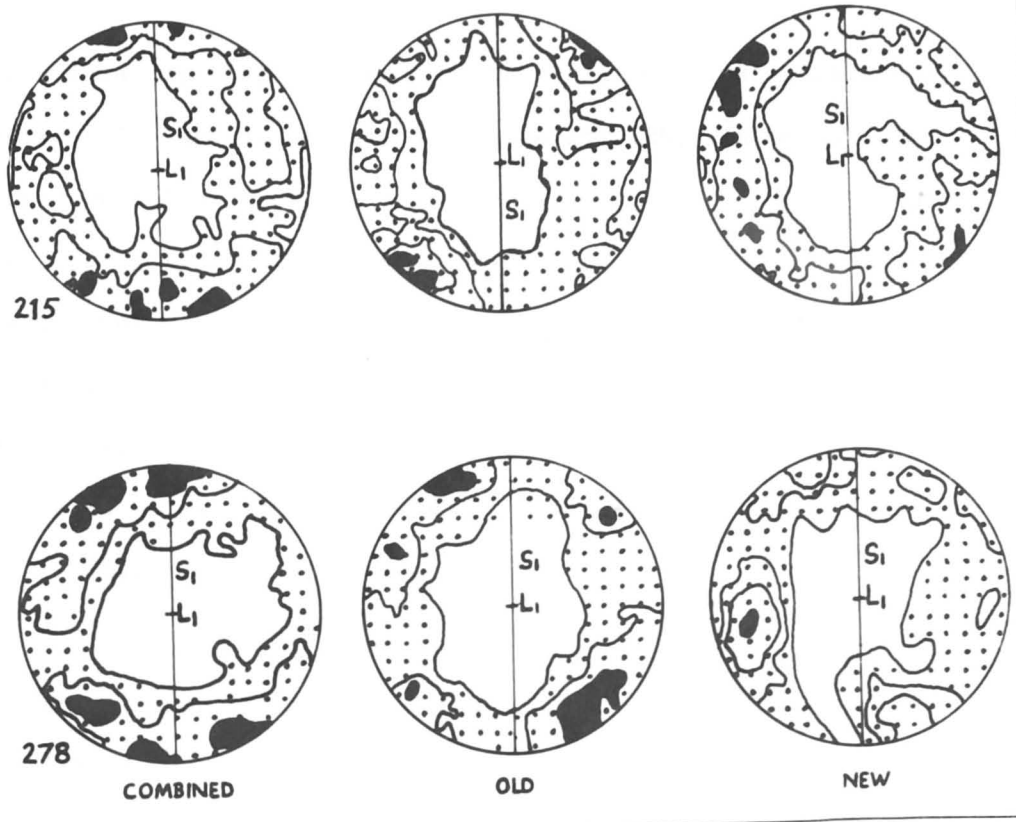
S1
L1
215
L1
S1
S1
L1
S1
L1
278
S1
L1
S1
L1
S1
L1
COMBINED
OLD
NEW

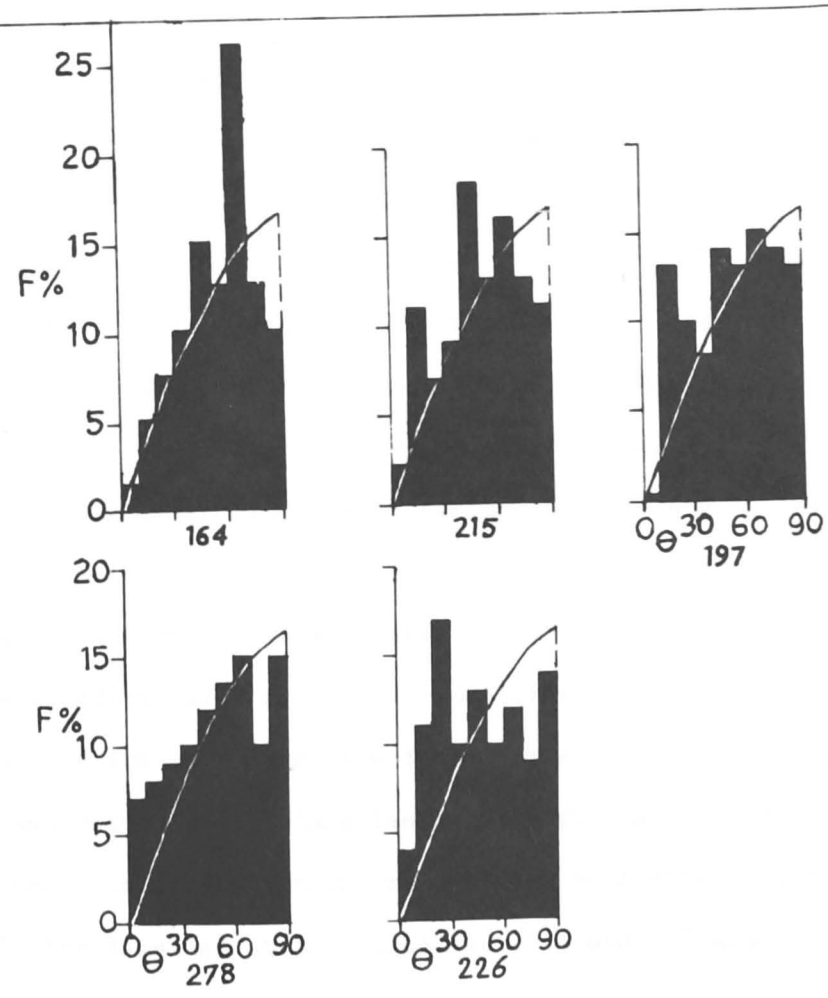
25
20
15
F%
10
5
0
164
215
0 θ 30 60 90
197
20
15
F%
10
5
0
0 θ 30 60 90
278
0 θ 30 60 90
226

specimen locality 164, between 40° and 50° at specimen locality 215, and between 10° and 30° at specimen locality 226. It needs to be mentioned here that there is a progressive change in the development of the microstructure from specimen locality 164 to specimen locality 226, which may be related with the variations in angles favoured for the growth. However, it is apparent from the diagrams that any tendency towards a preferred relationship between old and new c-axes is not as marked as those reported by Hobbs (1968), Ransom (1971) or Wilson (1970).

4.3.9 Deformation lamellae

Data on the orientation of deformation lamellae was obtained from seven specimen localities; four of these localities representing microstructural type III are 130, 144, 294, and 147; the other three are 122, 156 and 197 and represent microstructural types II, IV and V respectively. Figure 4.9 shows the orientation of the lamellae with respect to the quartz c-axis at each of the above mentioned localities. At specimen localities 144 and 122 there is a wide range of the lamellae orientation and about 70% of the lamellae lie at 10°-50° to the base. This range narrows down at the localities 130, 294 and 147 and the small peak between 20° and 30° at the two former localities increases in height at the localities 130 and 294. A peak of same height as at locality 294 develops between 10° and 20° at the locality 147. At the two localities 156 and 197 peaks between 20° and 30° are more significant than at any other locality and the sub-basal nature of the lamellae is strongly marked. According to the recent classification of the lamellae by Ave'Lallemant and Carter (1971), the lamellae at the localities 156 and 197 and also to a great

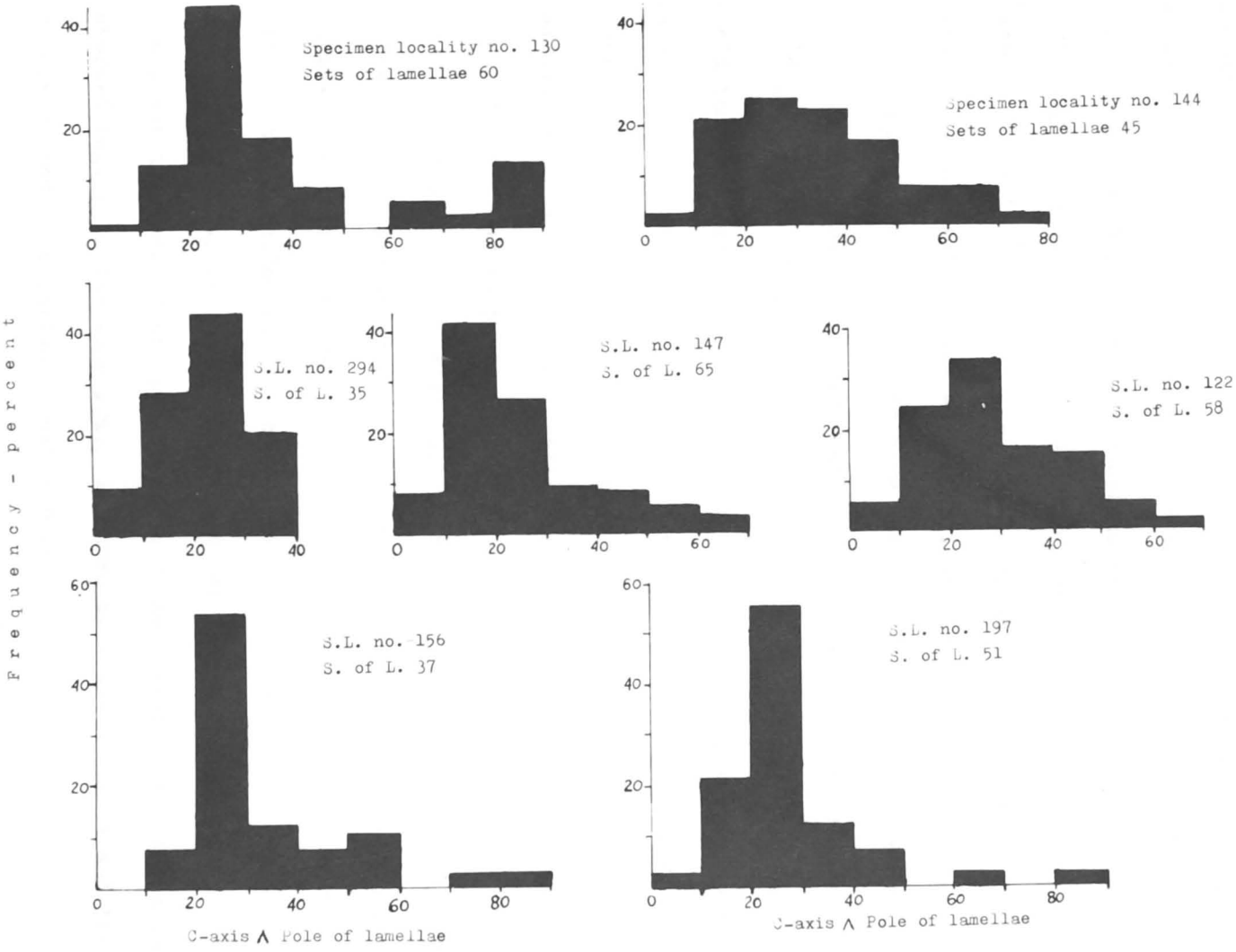

Fig. 4.9. Histogram showing the orientation of quartz deformation lamellae with respect to the c-axis in seven quartzite specimens.

extent at the localities 130, 294 and 147 are of sub-basal I type (average 16° to 30° from the base) and such lamellae are most common in nature but the origin of these non-rational sub-basal lamellae is still unknown. In the experiments of Ave'Lallemant and Carter (1971) these were produced at temperatures above 600°C and in the confining pressure range of 5 to 20 Kb and at a constant strain rate of 7.8×10^{-6}/sec. In the Atnarpa Range area their development would have taken place at a much lower temperature and the lower temperature is likely to have been compensated by decrease in strain rate (natural strain rates are estimated to be between 10^{-12}/sec. to 10^{-14}/sec.). It has been shown in the experimental field that increasing the temperature by 100°C has approximately the same effect as decreasing the strain rate by one order of magnitude (Heard and Carter, 1968). The changes in the orientation of the lamellae with respect to the c-axis appear to be related with the microstructural development.

In the diagrams of Figs. 4.10a, b, c, d, e, f, and g the poles to the lamellae are shown by the points of arrows and the c-axes are shown by the ends of arrows. Each arrow drawn along a great circle connects the lamellae pole to the c-axis of the host grain. In the diagram of Fig. 4.10h the c-axis within the less deformed region of a grain is shown by an open circle and the c-axis within the more deformed region of the same grain is shown by a solid circle and the two are joined by a partial great circle.

In experimentally deformed specimens of quartz the lamellae form at angles near but most commonly less than 45° to $\sigma 1$ (Carter, 1971). The c-axes in the more highly deformed parts of individual grains lie closer to $\sigma 1$, the maximum principal compressive stress, than those in

FIGURE 4.10

Orientation diagrams except 197(b) showing poles to deformation lamellae in quartz (points of arrows) and quartz c-axes (ends of arrows). Each arrow connects the lamellae pole to the c-axis of the host grain. In the last diagram, 197(b), the c-axis in the less deformed region of a grain (open circle) is connected to the c-axis in the more deformed region of a grain (solid circle). In the diagrams, S denotes bedding; S1, the foliation, and L1, the lineation. Orientation data is from Specimen Localities 130, 144, 294, 147, 122, 156, and 197.

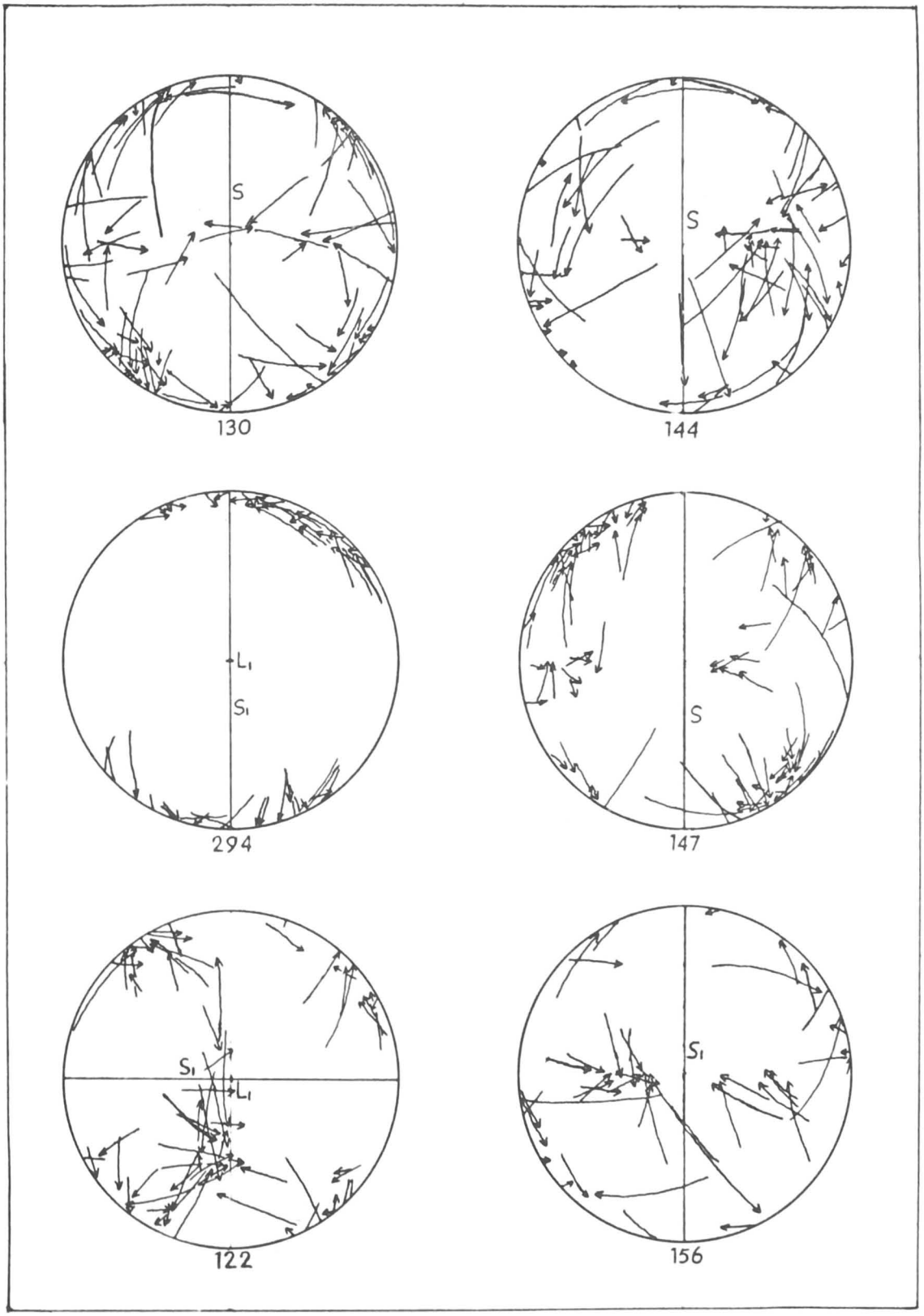
S
130
S
144
L1
S1
294
S
147
S1
L1
122
S1
156

FIGURE 4.10

FIGURE 4.11

Histogram showing frequency, F, of angles, θ, between quartz c-axes of adjacent deformation bands in grains; number of angles measured is 50. Data from Specimen Locality 186.

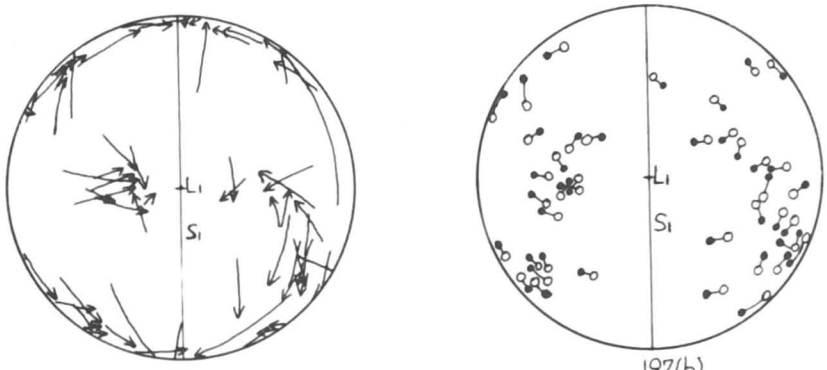

197(a)

197(b)

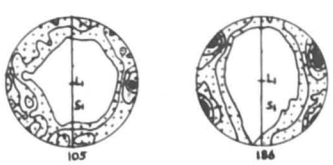

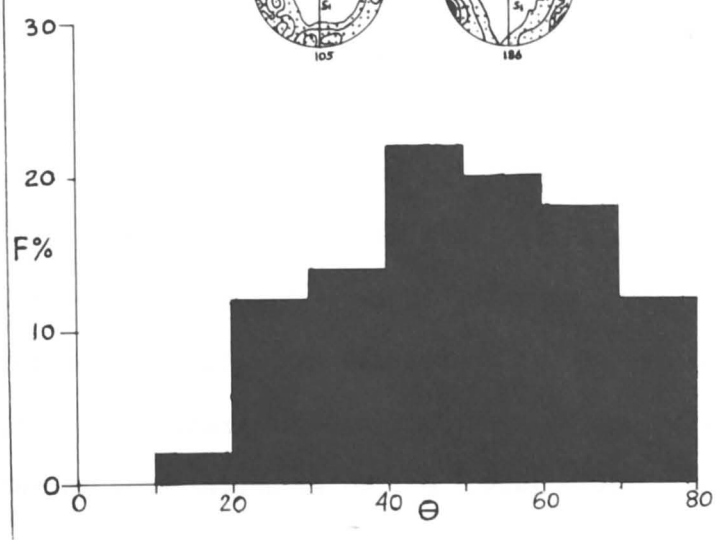

the less deformed parts, and poles to lamellae lie nearer $\sigma 3$ than do the c-axes. Similar relative orientations of the sub-fabric elements are evident in nature (Carter and Friedman, 1965) and can be used for determination of the orientations of principal stresses.

The inferred orientations of the principal stresses in each diagram of Fig. 4.10 is given below:

Figs. 4.10a, 4.10d, 4.10f, 4.10g and 4.10h - $\sigma 1$ at or near the pole of the bedding or the foliation $\sigma 2$ and $\sigma 3$ in the plane of the bedding;

Fig. 4.10c - $\sigma 1$ and $\sigma 2$ in the plane normal to the foliation and containing lineation, $\sigma 3$ in the foliation normal to the lineation;

Figs. 4.10b and e - Orientations not clear, appear to be unrelated to the foliation, the lineation or the bedding.

4.3.10 Summary of c-axis preferred orientation changes

Six types of preferred orientation have been described in sub-sections 4.3.1 to 4.3.6 corresponding to the microstructural types. These are briefly reviewed here. The first type is characterized by random preferred orientation and is associated with a microstructure in which detrital quartz grains rarely exhibit signs of deformation. The tectonic strain is either not present or is of very low magnitude in this type. The second and the third types are nearly the same except that these are associated with different types of microstructure. The preferred orientation is characterized by weak partial to complete girdles and crossed girdles with weak maxima. The symmetry of the preferred orientation is of the lowest order i.e., triclinic, but in some cases tends to be monoclinic or orthorhombic. The girdles lie at high angles to the bedding or the foliation, this angle ranging from 60° to 90°, and the geometric relationship of the preferred orientation with the mesoscopic elements of the fabric is generally not symmetric.

In the microstructure associated with the second type of preferred orientation, the detrital quartz grains are deformed to strains as represented in Fig. 4.5. The microstructure associated with the third type of the preferred orientation combines the effects of plastic deformation and cataclasis. The fourth type of preferred orientation is strong and is generally marked by a girdle normal to the foliation and the lineation with one or two maxima in the plane of the girdle. Its symmetry is generally very close to orthorhombic and its relationship with the foliation and the lineation strongly tends to be symmetric. In the associated microstructure the detrital quartz grains have undergone a fair to high amount of strain and the deformation changes from flattening type to constrictional type (Fig. 4.5). Fig. 4.5 also shows the increase in the strength of the preferred orientation with the amount of the strain. Recrystallization has locally started in this type but is at a very incipient stage.

The significant features of the fifth and the sixth types of the preferred orientation are a 20° to 30° shift of the girdle from the periphery, a tendency to develop crossed girdles, and the development of a second pole free area at or in the vicinity of the pole to the foliation. The development of the first and the third features enhances with the change from the fifth type to the sixth type and the symmetry of the preferred orientation strongly tends to become orthorhombic from triclinic or monoclinic. The relationship between the quartz sub-fabric and the mesoscopic sub-fabric is unsymmetric in the fifth type and remains so in the sixth type. The microstructure associated with these types of preferred orientation exhibits the formation of new strain free grains at the expense of the old

deformed grains to a stage where the microstructure completely comprises the new grains.

4.4 Development of preferred orientation

4.4.1 Introduction

On the basis of the microstructural evidence the development of quartz c-axis preferred orientation in the Atnarpa Range area can be attributed to two processes, namely intracrystalline slip and recovery and or recrystallization.

In metallurgy deformation textures are patterns of preferred orientation developed in metals by intracrystalline slip. Deformation of metals by intracrystalline slip at temperatures low enough to permit appreciable strain hardening is termed cold-working (plastic deformation without recrystallization) as contrasted with hot-working at temperatures too high for strain hardening to occur. Barret and Masalski (1966) have summarized the patterns of preferred orientation observed in many cold-worked metals. Chin (1969) has reviewed the actual means of achieving such preferred orientations by homogeneous deformation where lattice rotations and preferred orientation patterns may be predicted for different mechanisms such as pure slip and rotation, cross slip, latent hardening, deformation faulting and mechanical twinning. All these models for predicting patterns of preferred orientation are based on the von Mises (1928) - Taylor (1938) theory of five independent slip systems, required to satisfy the imposed strain. Taylor's approach and its subsequent refinement by Bishop and Hill (1951) have been discussed to some extent in Chapter I.

Preferred orientation of quartz c-axis by intracrystalline slip

processes has also been produced in experimentally deformed quartz. In this respect the recent study by Tullis (1971) of the preferred orientation in the original grains of a coarse grained quartz aggregate deformed in the laboratory under a variety of physical conditions is important to this study as far as the development of the preferred orientation in the Atnarpa Range area can be attributed to intra-crystalline slip. Blacic and Griggs (1965) were the first to produce preferred orientations in the plastically deformed original grains of quartzites and this they could achieve at a very slow strain rate (10^{-7}/sec.). Tullis performed her experiments on samples of randomly oriented ortho-quartzites by subjecting them to axial compression at 15 Kb confining pressure, over a large range of temperatures (400° to 1100°C), strain rates (10^{-5}, 10^{-6} and 10^{-7}/sec.), and strains (1 to 75% shortening). The main results of her study are:

(1) The strength of the quartzites gradually decreases with increasing temperature and water content and with decreasing strain rate. It seems to decrease abruptly at a temperature roughly 100°C below that for the onset of grain boundary recrystallization, although this should be tested by more carefully controlled experiments.

(2) At lower temperatures and faster strain rates, deformation of the grains is very inhomogeneous; sharp deformation bands are common at lower strains while a ribbon texture is developed at higher strains. At higher temperatures or slower strain rates, the original grains show smooth undulatory extinction and tend to be continuously flattened with increasing strain.

(3) At lower temperatures and faster strain rates, deformation lamellae are primarily sub-basal at low strains, but all orientations are found at higher strains. Lamellae of different orientations are commonly seen

in different parts of the same grain. At higher temperatures and slower strain rates only sub-basal and sub-prismatic lamellae are seen, with the former predominating.

(4) At lower temperatures or faster strain rates, the original grains develop a maximum of c-axes parallel to $\sigma 1$. At higher temperatures or slower strain rates, the c-axes in the original grains form small circle girdles about $\sigma 1$. The opening angle of this girdle increases with increasing temperature and decreasing strain rate, varying from approximately 15° to 45°.

(5) At any given temperature and strain rate the strength of the preferred orientation increases with increasing strain. At equivalent strains, c maximum fabrics are not as strong as small circle girdle fabrics.

Tullis believes that a combination of intragranular slip and mechanical Dauphiné twinning, acting independently, is responsible for all of the preferred orientations produced in the original grains of the quartzite during the experimental deformation. According to her, slip at higher temperatures or slower strain rates only takes place on basal and prism planes whereas at lower temperatures or faster strain rates, slip systems of all orientations are operative, although realistic models of exactly how these slip processes operate are still lacking. About Dauphiné twinning she says that it requires such low stresses at relatively low temperatures to develop that it should be extensive in natural quartz rocks.

The difference between the processes of recovery and recrystallization is that in recovery the strain hardened grain divides into several sharply bounded homogeneous strain-free sectors differing slightly in orientation; this process is also referred to as polygonisation, whereas in recrystallization the unstrained grains growing

from new nuclei completely replace the strained crystals of the cold-worked aggregate. This type of recrystallization is termed annealing recrystallization and occurs at temperatures higher than required for recovery. Another type of recrystallization is termed syntectonic recrystallization in geology or hot-working in metallurgical literature and occurs during deformation at high temperatures. Strain hardening does not take place in syntectonic recrystallization or the rate of strain hardening is low because of high temperatures. In the experimental deformation of calcite and marble strain hardening ceases to be appreciable at 500°C and the deformation above this temperature is categorised as hot-working (Turner and Weiss, 1963, p.328). There are no petrographic criteria for distinguishing the microstructure produced under annealing or syntectonic recrystallization conditions.

Comparison between experimental and natural deformations should be made cautiously because most of the experiments are performed under axial stress whereas the states of stress in nature are general or of lower symmetry, the rate of strain is much lower (about 10^{-12} to 10^{-14} per sec.) in natural than experimental deformations, and the conditions in which natural deformations take place are much more varied than the controlled conditions of experiments. In spite of the above, the information obtained on physical conditions of deformation from experiments is valuable and provides for certain limitations to be placed on the interpretation of natural deformation.

Before returning to the discussion of the development of the preferred orientation in the Atnarpa Range area, it is useful to take into account the general physical conditions expected to be prevalent during the process of deformation in the area on the basis of the knowledge of the general geology of the Arltunga Nappe Complex. The

lithostatic pressure at the base of the Amadeus Basin sequence, between 7000 metres to 8000 metres thick, could be expected to be about 2 Kb and the temperature to be between 200°C to 300°C. These are the conditions favourable for the start of the greenschist facies grade of metamorphism (Turner, 1968, p.366) and are relevant to the southern parts of the Atnarpa Range area where the quartzite away from the thrust zones does not exhibit signs of being plastically deformed and is randomly oriented crystallographically as well as dimensionally in general. In the thrust zones also, it has undergone predominantly brittle deformation and plastic deformation is slight and local. The intensity of the deformation increases northwards in the Atnarpa Range area with plastic deformation becoming more and more widespread so that in the northernmost parts of the area this is the only deformation which the quartzite has undergone during the development of the first generation structures. Similar observations with regard to the increase in deformation and also in metamorphism northwards in the area of the Arltunga Nappe Complex have been made by Stewart (1971) and Forman (1971). Stewart on the basis of mineral assemblages in the basement rocks concludes that metamorphism in the southern part of the nappe is in the lowest part of the greenschist facies and in the northern part, in the middle part of the greenschist facies. According to Forman, metamorphism is slight in the south and is of greenschist facies grade in the north. The increase in the metamorphism towards the north in the nappe complex can be attributed to increase in temperature or both, the temperature and the pressure. The temperature could rise as a result of the extra heat generated by exothermic reactions probably initiated in the basement leading to its mobilisation or as Forman (1971) thinks due to the incoming of the mantle near the surface of

the earth in the area north of the nappe complex or locally to a small extent due to friction along surfaces of movement during thrusting (Reitan, 1969). The pressure could build up as tectonic overpressure. Turner (1968, p.380) says that it is not unlikely that relatively cold rocks under high confining pressure might be able to maintain stresses of 2 or 3 Kb induced by tectonic forces.

4.4.2 Development of the preferred orientation in microstructural types I to IV.

Returning to the discussion of the development of preferred orientation it appears reasonable to infer from what has been said above that microstructural type I with random preferred orientation reflects the conditions prevailing in the very basal part of the Amadeus Basin sequence before the nappe formation or the initiation of deformation. Microstructural types II, III, and IV primarily comprise old or detrital quartz grains which are deformed so as to become flat and elongate as well as showing a number of microscopic strain effects such as undulatory extinction and deformation lamellae. In microstructural type III evidence of brecciation such as angular grains and microscopic fractures associated with a ground mass of very fine grained quartz is present and in microstructural type IV effects of recovery and or recrystallization in the form of tiny quartz grains are locally observed. The deformation of the old grains is also associated with their dimensional orientation. It is also observed that the deformation, vis-a-vis the strain, increases from microstructural type I to microstructural type IV and this also means increase in deformation and strain northwards because of the general locations of the microstructural types in the area. The increase in

deformation is also related to the thrusts but as earlier stated thrust zones in the southern part exhibit more brittle than plastic deformation. The advanced stages of microstructural type IV along the northern front of the western part of the Atnarpa Range area particularly at or near specimen localities 105 and 186 (Fig.4.1 and Map 1) are akin to mylonitic texture or ribbon texture as described by many workers in the natural field and also by Tullis (1971). In fact a number of stages of the microstructural development observed by Tullis are similar to the microstructural development stages in the types II and IV of this study and her observation that the ribbon texture develops at higher strains is also consistent with this study.

The development of quartz c-axis preferred orientation in microstructural types I, II, III, and IV is related to the development of the microstructure and therefore to the two other factors viz., location in the area with respect to the northern part and the proximity of the thrusts. The strength of the preferred orientation increases with the amount of strain and again this is consistent with the results of Tullis (1971). Although the results of this study and those of Tullis' are similar in many aspects of the development of microstructure and preferred orientation, these are different with regard to the patterns of preferred orientation. In this study the pattern in microstructural type IV is either marked by a maximum in the plane of a girdle or two symmetrically situated maxima in the same plane. The girdle is normal to the foliation and the lineation, the maximum in the former case lies at or very close to the pole of the foliation, and in the latter case the pole to the foliation is about midway with respect to the two maxima. The symmetry of the pattern

tends to be orthorhombic. The patterns of preferred orientation in Tullis' study are either marked by a maximum parallel to $\sigma 1$ and normal to the foliation or by a small circle girdle about $\sigma 1$. The difference in the patterns as observed in the two studies can be attributed to the different types of strain; strains associated with the patterns of preferred orientations observed in this study are shown in Fig. 4.5, strains are axial in the study of Tullis.

The high degree of the preferred orientation, its strong tendency towards an orthorhombic symmetry at specimen localities 105, 186, 294, 294A and 159 along thrust faults and its association with a mylonitic type of texture very closely compares with that of the mylonite zones in other parts of the world (for example: Christie, 1963; Eisbacher, 1970).

The preferred orientation in these microstructural types is only representative of the c-axis orientations in the old or detrital deformed grains. It is, therefore, reasonable to attribute the development of the preferred orientation to the process of intra-crystalline slip which would have led to a shape change with bodily rotation in each grain finally giving rise to a state of the preferred orientation in an aggregate. The development of such a preferred orientation takes place under the broad framework of von Mises - Taylor criteria of five independent slip systems required to effect shape changes homogeneously within an aggregate. The preferred orientation acquired in metals during cold work and the results of Tullis (1971) in this regard substantiate the conclusion reached above. The development of the microstructure in so far as the formation of flat and elongate quartz grains from the detrital, more or less spherical, grains is concerned would have also taken place by the

processes of intracrystalline slip. It has been shown that the strength of the preferred orientation is dependent on the amount of strain and thus the preferred orientation would have also depended on the ability of the quartzite to sustain strain, in other words its ductility.

The ductile behaviour of a rock as of any other material is dependent on confining pressure, temperature, rate of strain, pressence of pore fluids and grain size. It is generally agreed that ductility increases with increase in confining pressure and temperature, presence of pore fluids and slower strain rate. During deformation of the quartzite in the Atnarpa Range area it is unlikely that the rate of strain would have varied appreciably to alter the course of deformational events. In a general way increase in temperature and perhaps also in confining pressure northwards in the area would have stimulated the activity of the slip processes thus providing means for a progressive development of the microstructure and the preferred orientation northwards. The decrease in the scatter of the angle between the quartz c-axis and the pole to the deformation lamellae from specimen locality 144 to specimen locality 156, the latter locality is situated about 4Km north of the former, (see Figs. 4.9 and 4.1) probably also reflects the change in the activity of the slip processes as stated above.

High density of dislocation tangles has been observed in the old deformed grains in quartzites of microstructural types III and IV by transmission electron microscopy (see McLaren and Hobbs, 1972; and Plate 4.11c) and is evidence of strain hardening in these rocks. This indicates that the deformation of the quartzites in these microstructural types, at least up to the development of the early stages

of microstructural type IV, is much closer to cold-work than to creep or hot-work and accords with the inferences made about temperature conditions during the development of these types.

Some of the local and more specific variations in the microstructure and the preferred orientation in the microstructural types will now be described and an attempt is made to explain these with regard to the physical factors enunciated above.

(1) Specimen locality 103 represents microstructural type I and specimen localities 147 and 150 represent microstructural types III and IV respectively but the localities 147 and 150 are southwest and south of the locality 103 (see Fig. 4.1). The higher stages of the development of the microstructure and the preferred orientation at the localities 147 and 150 can be attributed to their location at or very close to the thrust. Again the stage of development of the microstructure and the preferred orientation is different at these localities also, and this may be related to the differences in the lithology of the quartzite at the two localities. It has been observed in sub-section 3.4.2.3 of this thesis that the foliation also preferentially developed in certain lithologies particularly the one associated with the basal part of the quartzite.

(2) Specimen localities 294 and 294A belong to different microstructural types, the former represents type III and the latter type IV, but the preferred orientation at these localities is similar (see Fig. 4.1). The two localities are situated close to each other but lie in different thrust sheets. The original nature of the quartzite with regard to its lithology at locality 294A can be ascertained by the mesoscopic and microscopic observations of its present state as well as from its position in the Heavitree sequence but the same

observations do not provide information with regard to the original nature of the quartzite at locality 294. It is, therefore, difficult to even guess what physical factors are responsible for the differential development of microstructure at these localities, nevertheless it is possible that greater permeability and confining pressure would have resulted in greater ductility at locality 294A than at 294. On the other hand locality 294 represents a transition between brittle and ductile behaviour of the quartzite.

(3) Specimen locality 156 is about $\frac{1}{2}$ kilometre north of specimen locality 159 and both have been placed in microstructural type IV but the preferred orientation at locality 159 is stronger than at locality 156. Moreover the strain is also greater at locality 159 than at locality 156. The two localities also lie within the same thrust sheet. The microstructure at locality 156 exhibits the growth of tiny new quartz grains within the old deformed grains (see Plates 4.7a and b) and it seems that the process of growth is at its very early stage whereas this process is not obvious at locality 159. It seems that the differences in temperature and the nature of the quartzite at the two localities may be responsible for the differences in the microstructure. The nature of the quartzite at locality 159 is evident from its location at the base of the Heavitree sequence. Some increase in temperature at locality 156 with respect to locality 159 is expected as it is situated north of locality 159, and this may have induced recrystallization even at comparatively less strain.

(4) A notable feature of the microstructural type IV is the development of ribbon texture at specimen locality 186. The ribbons are deformation bands developed generally parallel to the elongation direction of the grains. With increase in deformation, the bands tend

to separate along their boundaries giving rise to elongate slices or ribbons. Tullis (1971) observed that at lower temperatures and faster strain rates ribbon texture is developed at higher strains. At higher temperatures or slower strain rates, the original grains tend to be continuously flattened with increasing strain. Wonsiewicz and Chin (1970) noted that single crystals of copper divided into four differently oriented regions by a process involving surface friction during plastic deformation. It seems more likely that in the example of the microstructure at the locality 186 cited above the inherent weakness of kinked zones within the quartz lattice facilitates separation of the misoriented regions rather than the friction. The pattern of quartz c-axis preferred orientation at specimen locality 186 is marked by a peripheral girdle with two maxima subtending an angle between 60° and 70° whereas at specimen locality 105 only one maximum lies in the girdle at a position which is about midway with respect to the two maxima at the former locality. The ribbon texture is not developed at the latter locality. In order to explore the possibility that the two maxima at specimen locality 186 represent the two new orientations of the original orientation of the c-axes represented by a maximum at specimen locality 105, the angle between the c-axes in deformation bands, which were considered to be originally part of one grain but were in the process of separating as well as possessed differing undulatory extinction, was measured. A majority of 50 such angles lies between 40°-70° in Fig. 4.11 and this shows that the change in the pattern of preferred orientation from the locality 105 to the locality 186 is associated with the formation of deformation bands.

4.4.3 Development of the preferred orientation in microstructural types V and VI

The growth of new, strain free, grains from the old, deformed, grains in microstructural type V strongly suggests that the processes of intracrystalline slip and primary recrystallization[3] would have, both, contributed to its development and finally would have led to the development of microstructural type VI with complete recrystallization. The occurrence of these two microstructural types only on the northeastern limb of the Eastern Hill Range is significant and indicates a change in physical conditions in this part of the Atnarpa Range area with respect to its other parts. This change in physical conditions would have, itself, been progressive and again seems to depend on two factors, viz., the location in the north and the proximity of a thrust. Microstructural type V is widespread on the northern limb of the Eastern Hill Range but microstructural type VI with associated strong c-axis preferred orientation is limited to the northern fringe of this limb. Plate 4.10 and Fig. 4.6 show progressive change in microstructure and the preferred orientation with proximity to the thrust at specimen locality 279. It has not been possible to determine the amount of strain in microstructural type V because the shapes of the deformed, old, grains are modified by recrystallization. However, the relationship of the strain to the preferred orientation is established in microstructural types II and IV. As the strength of the preferred orientation is not stronger in microstructural type V than in type IV particularly in orientation diagrams shown in Fig. 4.7 in which only the orientation of the c-axes

---

3. Recrystallization at this stage of microstructural development is equivalent to primary recrystallization in metallurgy.

of the old grains has been measured, it would be reasonable to assume that the strain in microstructural type V has not increased as compared to the type IV. While specifically discussing the development of microstructural type IV it was pointed out that incipient recrystallization commenced at specimen locality 156 and not at the locality 159 in spite of the fact that at the latter locality the strain was more and the degree and symmetry of the preferred orientation higher than at the former locality. It is tempting to conclude, therefore, that increase in temperature would have favoured primary recrystallization, for recrystallization is a process which is controlled by diffusion and all processes involving nucleation and diffusion such as recrystallization must be accelerated by rising temperature (Turner and Weiss, 1963, p. 354). In the experimental field the influence of temperature on recrystallization has been observed by many workers for example in case of marble by Griggs, et al (1960), and in case of quartz by Tullis (1971).

The development of the preferred orientation in the microstructural types is related to recrystallization. With the change in microstructure from microstructural type IV to the type V as a result of the onset of recrystallization, the pattern of preferred orientation has changed also. The pattern again changes with complete recrystallization in microstructural type VI, this change being more significant than that in type V, and the strength of preferred orientation also increases. It is possible that the type of strain in microstructural type VI was different from that in microstructural type V.

Development of preferred orientation during recrystallization has been attributed by many workers to the host control phenomenon,

described in Chapter I. Hobbs (1968) in his hydrostatic annealing and stress annealing experiments noted that growth of new quartz grains appears to be anisotropic so that grains in which c-axis is within 10° of the host c-axis remain small; grains in which c-axis lies at 20°-40° to the host c-axis grow fastest. In his syntectonic experiments Hobbs (1968) found that the c-axes of new grains tend to lie at 30°-50° to the c-axis of the adjacent host but this pattern may also be stress controlled in that new c-axes tend to lie at 50° to $\sigma 1$. Since then, two studies on recrystallization of quartz in nature, one by Wilson (1970) and the other by Ransom (1971), have shown the orientation dependence of the newly recrystallized grains on the orientation of host grains from or in which they grew. In this study it has been found that a weak tendency for the host control on the growth of new grains exists at four of the five specimen localities investigated (Fig. 4.8) and this does not seem to be able to explain all the features of the preferred orientation. It seems that the following characteristics of the patterns of preferred orientation may have been influenced during their development by host control but the possibility also exists that some other factor or factors have influenced their development. In order to fully establish or rule out the host control idea it would be necessary to establish the complete crystallography of each grain rather than just the c-axis. This requires either micro-Laue techniques or electron diffraction and was beyond the scope of this thesis. The characteristics of the patterns are as follows:

(1) The peripheral girdle which is a characteristic of the pattern of preferred orientation of the host c-axis in microstructural type

IV has been replaced by one or two girdles lying at 20° to 30° from it with a new pole free area developing at or near the pole to the foliation at the cost of pole concentrations in the new girdle or girdles. (see Fig. 4.1).

(2) In orientation diagrams where the host and the new c-axes have been separated (Fig. 4.7), the host c-axes tend to lie at the periphery whereas the c-axes of the new grains at 20° to 30° from the periphery and without any significant change in the strength of the preferred orientation.

(3) The preferred orientation at specimen locality 279 (Fig. 4.1) still shows the features of the pre-existing preferred orientation from which the new small circle girdle has evolved and the pole of this girdle lies within the new pole free area developed at the periphery. The pre-existing pattern seems to have been a peripheral girdle with two maxima very much like the pattern at specimen locality 186. The new preferred orientation is strong and so was the pre-existing one. This, then, is consistent with the prediction of Hobbs (1968) and others that if the orientation of the host has a significant influence on the orientation of the newly recrystallized grains it follows that in order for a preferred orientation to develop during recrystallization of a polycrystalline aggregate, the host grains must develop a preferred orientation during deformation and prior to or during the formation of the new grains.

4.5 Kinematic and dynamic aspects of the preferred orientation

Turner and Weiss (1963) have stressed the importance of symmetry in the kinematic interpretation of the mineral orientation. In ascertaining the kinematic and dynamic implications of the

preferred orientation the well developed orientation patterns will be used because in this type of structural analysis of tectonites only these can be interpreted with confidence. Most of the orientation diagrams from microstructural types IV, V and VI and a few from the types II and III are considered to be satisfactory in this respect. The first case to be considered is from microstructural types II, III and IV and in this the mesoscopic sub-fabric with a foliation and a lineation has orthorhombic symmetry; the quartz sub-fabric marked by a girdle with maxima has approximately monoclinic or orthorhombic symmetry (see for example, orientation diagrams at specimen localities 118, 294, and 294A). The lineation lies at or very close to the girdle axis and the only symmetry plane common to the two sub-fabrics is the ac plane. The lineation defined by the maximum elongation direction of the quartz grains can be equated with the X axis of the strain ellipsoid and the symmetry of the fabric suggests that $\sigma 3$ has this orientation also. It can also be inferred that the plane of the quartz c-axes girdle at specimen localities 294 and 294A contains $\sigma 1$ and $\sigma 2$.

The second case is represented by the preferred orientation at specimen localities 105 and 186 where the symmetry of both the sub-fabrics is approximately orthorhombic and the three symmetry planes commonly shared so that the total fabric is homotactic. The three mutually perpendicular directions of intersections of the planes of symmetry can be equated with the axes of principal strains and stresses. Here again the strains in mesoscopic fabric are X>Y>Z and are very well defined. $\sigma 1$ and $\sigma 2$ lie in the plane of c-axes girdle, normal to the foliation, and in the plane of the foliation normal to the lineation respectively and $\sigma 3$ is concordant with the girdle axis.

In microstructural types V and VI the total fabric becomes heterotactic because the symmetric relationship of the two sub-fabrics is destroyed by recrystallization or indirect componental movements which influence the development of the preferred orientation with the result that the overall movement picture becomes more complex than what could be inferred from mesoscopic sub-fabric alone. However, the stress system does not seem to change its orientation with respect to the preferred orientation and this is reflected in the quartz sub-fabric in three ways:

(1) Sylvester and Christie (1968) suggested that the intersection of crossed girdles in c-axis diagrams of lineated quartz tectonites constitutes the intermediate principal axis of stress. In some of the orientation diagrams of microstructural type V a tendency towards the formation of crossed girdles exists and the girdle intersection tends to lie in the plane of foliation normal to the lineation. If the positions of $\sigma 2$ and $\sigma 3$ are thus established, $\sigma 1$ should lie normal to the foliation in the diagrams.

(2) Fig. 4.6g shows partial great circles connecting poles to deformation lamellae (points of arrows) with the host c-axes (ends of arrows) and fig. 4.6h shows partial great circles connecting c-axes in the less deformed or host regions (open circles) to c-axes in more deformed regions (solid circles) in individual grains. It has been established from experimental and natural studies of deformed quartz that the arrows point away from $\sigma 1$ and the c-axis in the more deformed region of a grain rotates towards $\sigma 1$ (Carter and Friedman, 1965). $\sigma 1$ can be expected to lie in the vicinity of the pole to the foliation in both the figures.

(3) Carter *et al.* (1964) have shown that the c-axis in the more

deformed part of a quartz grain tends to rotate towards σ_1. This means that the c-axes of all those grains which are more deformed than the others would lie close to σ_1. The more deformed grains will provide more sites for nucleation to take place and, therefore, are liable to be replaced by new grains as a result of recrystallization much sooner than the less deformed grains. The development of the new pole free area at and in the vicinity of the pole to the foliation in many of the diagrams substantiates the arguments with regard to the location of σ_1 stated above.

It may be inferred from what has been said above that in areas of low strain the movement picture is less likely to correspond in the sub-fabrics in spite of the fact that the sub-fabrics would have formed as a result of direct componental movements. On the other hand the discordance in the symmetry elements of the sub-fabrics in regions of high strains points out the complex nature of the movement picture as a result of indirect componental movements.

CHAPTER 5

CONCLUSIONS AND INTERPRETATION OF THE HISTORY OF DEFORMATION

5.1 General statement

In this chapter the important results of this study will be presented first in summary form and then a synthesis of these results will be used in an attempt to interpret the structural evolution of the Atnarpa Range area. Finally an interpretation of the structure of the area will be considered in the context of the existing interpretation of the structure of the entire nappe complex.

5.2 Summary of the results

The effects of both, low grade dynamic and regional metamorphism, have been observed in the Atnarpa Range area. These effects are progressive in the cover rocks and retrogressive in the basement rocks and increase in intensity with the proximity of the thrust faults as well as from south to north in the area.

Imbricate thrusting in which both, the basement and the cover rocks, are involved has divided the Atnarpa Range area into many thrust sheets. Seven of these sheets have been mapped and normal stratigraphy was found to repeat in almost all these sheets. The boundary of the cover rocks on both flanks of the Atnarpa Range is marked by a thrust (Map 1) and this implies that the basement rocks in the area have travelled at least for a distance of 5Km over the cover rocks in the form of thrust nappes. The asymmetry of the folds that developed in the cover rocks beneath the thrust and the west to

west-north-west trends of their axes (Map 2, sections CC', DD' and EE' and Map 1) indicate a general north to south movement of the rocks above the thrust. Similar trend of movement has been reported from other parts of the nappe complex (Forman, 1971).

The planar and the linear structures have been separated into three generations on the basis of overprinting relationships. The structures formed either as a result of the deformation of the sedimentary bedding or a pre-existing foliation in the metamorphic rocks of the basement or of the igneous rocks of the basement. Sedimentary bedding is the dominant planar structure in cover rocks in the western, southern and central parts of the Atnarpa Range area. Structures of the first generation are locally developed on the northern flank of the western half of the Atnarpa Range area but are extensive in development on the northern limb of the Eastern Hill Range; the folds of this generation nevertheless, are rarely observed in the area as a whole. The first generation foliation and lineation are generally defined by the planes of flattening of quartz grains and the direction of their maximum elongation respectively. The folds of this generation are tight to isoclinal and very close to similar in style. The quartz elongation lineation is genetically related with the folds and is parallel to their axes but the geometric relationship of the foliation with the folds is not clear although the two seem to be genetically related because the lineation lies in the foliation plane . As compared to F1 folds, the folds of the second generation attain large size; the whole of Atnarpa Range is an anticlinal structure belonging to this generation. The second generation folding is markedly noncylindrical at macroscopic scale and controls much of the distribution of the foliation,

the bedding and the thrust planes. On a mesoscopic scale the second generation folds are either nearly concentric or disharmonic or conjugate in style. Flattening of the bedding or the foliation or their internal reconstitution as a result of this folding has not been observed. The third generation structures are very rare in occurrence and have only been observed in the form of open folds of small size.

In the southern parts of the Atnarpa Range area the microstructure of the Heavitree Quartzite is characterized by detrital quartz grains which rarely exhibit signs of deformation (Microstructural type I). In the central parts of the area the grains are deformed into a shape resembling that of an oblate spheroid and the strain within the grains is manifest by widespread undulose extinction and other deformational features (Microstructural type II). In these areas at or in the proximity of the thrusts the microstructure exhibits the effects of both, cataclasis and plastic deformation (Microstructural type III). In some parts of the northern flank of the western half of the Atnarpa Range area the detrital grains are strongly flattened and elongated into shapes resembling that of a triaxial ellipsoid and finally transformed into ribbons (Microstructural type IV). Incipient recrystallization is associated with this type of microstructure. This type of microstructure has also been observed to develop preferentially in certain lithologies particularly in the basal conglomeratic and arkosic part of the quartzite. Up to this stage of microstructural development, there is not much evidence of grain boundary migration and the deformation of the grains is mostly accomplished by intragranular slip. The microstructure is associated with the first generation foliation

and lineation. In these stages of microstructural development measurements of strain have shown that shortening increases with the microstructural development and corresponds to about 50% in microstructural type IV. In the early stages of microstructural development and in the southern and central parts of the Atnarpa Range area the deformation is of flattening type, in the advanced stages of microstructural development and in the northern parts of the area it is of constrictional type (Fig.4.5). On the northern limb of the Eastern Hill Range the microstructure exhibits the formation of new, small size, strain free grains at the expense of the old, deformed, grains and in the northernmost parts of this area, particularly along the basement-cover thrust contact, the old grains are completely consumed and the microstructure comprises new, strain free, mostly polygonal grains (Microstructural types V and VI).

The quartz c-axis preferred orientation is related with the development of the microstructure and the strain. With increasing strain the strength and degree of symmetry of the preferred orientation increases and the advanced stages of microstructural type IV may correspond to a steady state orientation. At this stage the combined symmetry of both the sub-fabrics, the quartz sub-fabric and the mesoscopic sub-fabric, is almost orthorhombic and it is considered that the incremental strains here involved only a pure shear with no rotation. Recrystallization alters the patterns of preferred orientation in microstructural types V and VI and on the basis of the available evidence it is believed that the preferred orientation of the new grains is controlled to some extent by that of the host. Recrystallization also destroys the homotactic relationship

of the two sub-fabrics. The patterns of preferred orientation are marked by a weak partial or complete girdle in microstructural types II and III, by a strong great circle girdle with one or more maxima in microstructural type IV, by weak, acutely inclined crossed girdles in microstructural type V, and by a strong small circle girdle or by an elongated maximum in the plane of a partial to complete great circle girdle in microstructural type VI. The L1 lineation defines the girdle axis in microstructural type IV and also in some cases in microstructural types II and III. The crossed girdles in microstructural type V tend to intersect in the foliation normal to the lineation and the axis of the small circle girdle tends to lie very close to the pole to foliation without any symmetric relationship with the mesoscopic fabric. In microstructural type IV the pattern of preferred orientation changes with the formation of deformation bands and in microstructural type V and VI the strength of the preferred orientation increases with the proximity of a thrust. The development of the preferred orientation in the Atnarpa Range area is attributed to processes of intracrystalline slip and recovery or recrystallization.

The movement picture changes from direct componental movements of irregular nature in areas of low strains in the south to componental movements of largely regular nature in areas of high strains in the north and further to indirect componental movements in areas marked by the onset of recrystallization.

In the first generation structures it is possible to equate the XY plane of the ellipsoid with the foliation plane and the X axis with the lineation, L1. During the generation of these structures the strain field would have changed its orientation with

respect to geographical coordinates as there is a variation of about 45° in the orientation of the lineation in the area. In areas where the quartz sub-fabric is well developed the lineation lies at or very close to the axis of the c-axis girdle and the two sub-fabrics share a common plane of symmetry. In some areas where the two sub-fabrics have near orthorhombic symmetry and share three symmetry planes the principal strain axes can be equated with the stress system. On the basis of symmetric relationships of the two sub-fabrics, the quartz sub-fabric and the mesoscopic sub-fabric, and from the interpretation of some of the features of the quartz sub-fabric σ_1 is considered to have lain at or close to the pole of the foliation in the northern parts of the area.

5.3 Synthesis

The development of the microfabric is associated with the first generation structures in the Atnarpa Range area and both the microscopic and the mesoscopic fabric generally progressively develop from south to north in the area. In addition their development is also associated with the thrusts. The first generation structures overprint structures of the second generation and whereas the second generation structures occur throughout the area, the first generation structures are only extensively developed on the north side of the area. The problem is to establish the position of the thrusts in the sequence of structural development. The possibility that the thrusts developed before the development of the first generation structures is ruled out by the fact that structures and microfabric of the first generation

progressively develop with the proximity of the thrusts and are more intensively developed within the thrust zones than away from them. The thrusts did not develop after the second generation structures because they do not cut across them. Therefore three possibilities can only be considered:

(1) The development of the thrusts and the first generation structures was concomitant.

(2) The thrusts developed after the first generation structures but before the second generation structures.

(3) The thrusts and the second generation structures developed at the same time.

Another aspect of this problem is that the general direction of transport of the thrust nappes in the area, that is from north to south, is commonly parallel to the quartz elongation lineation which forms the axis of quartz c-axis girdles. This situation is similar to that observed in other parts of the world such as in the thrust belt of the Caledonides of Scandinavia and Scotland (Kvale 1953, Phillips 1937, Jhonson, 1957) and in the Taconic region of the northern Appalachians (Balk, 1952) and its interpretation in terms of symmetry arguments has led to a considerable controversy. Some geologists believed that the lineation developed as a result of the thrusting, others attributed its development to differential movements generated at right angles to the direction of transport during thrusting. On the other hand while evaluating the symmetry of the quartz sub-fabric the effects of factors such as recrystallization, which is capable of modifying the patterns of preferred orientation, were not considered.

5.4 Interpretation of the history of deformation

On the basis of the results of this study it seems more likely that in the northern parts of the Atnarpa Range area the development of the first generation structures started before the initiation of the thrusting in response to a stress system in which σ_1 was vertical and in such physical conditions in which the rocks were ductile enough to sustain the kind of strain exhibited by them. Amongst the physical factors responsible for the ductile behaviour of the rocks increase in temperature is more likely to have played an important role as suggested in the preceding chapter. The ductility seems to have gradually decreased towards the south and this is the reason why first generation structures did not develop in that part of the area. Vertical flattening or thinning of the rocks without volume reduction necessarily means their horizontal expansion and if this is restricted in one direction in the horizontal plane then it is most likely to be accomplished in a direction normal to the former and this will then be the lineation direction or the direction of the axes of the flattened folds in the Atnarpa Range area. This is also the direction in which the rocks ought to be displaced if the vertical flattening is on a regional scale. Strain measurements at specimen localities 128 and 105 have shown the constrictional nature of the deformation (Fig.4.5) implying restriction in the strain field as enunciated above. Johnson (1967) says, "The mylonite zones are intensively flattened ($0 \leq K < 1$ modified to $1 < K \leq \infty$ in certain domains) and are not necessarily related to any large scale translative movements. It must be realized, however, that unless mylonitization is accompanied by volume reduction the development of mylonite zones

results in translative movements, that is, the flattened mylonitized zone must be displaced relative to the undeformed surrounding rocks". The displacement of the rocks along suitable fractures which could have developed during the deformation possibly as a result of competency difference in the rocks is capable of producing the thrust nappe structure present in the area. It follows, therefore, that thrusting would have started when the deformation related to the first generation structures would have arrived at a stage favourable for displacement to occur in the direction of minimum resistance. During thrusting shearing in the thrust zones augmented the development of the first generation structures in these zones as it was taking place in the direction of the lineation. Further south depending on the competency of the rocks this shearing produced the asymmetric folds with axial planes dipping towards the north and axes oriented west to west-north-west in the overridden rocks or produced the effects of brecciation in them. As the thrust sheets piled and the push from the north continued the thrusts were also folded.

In the earlier interpretation of the structural evolution of the Arltunga Nappe Complex (Forman and Milligan, 1967, p.24), the western half of the Atnarpa Range area was considered a part of the White Range Nappe and this would have meant the overturning of the normal stratigraphy in the Atnarpa area. The present study establishes that the rocks maintained their normal stratigraphic order in that part. In the most recent interpretation of the evolution of the entire nappe complex (Forman, 1971 Fig.2), the western half of the Atnarpa Range area is shown as a thrust sheet lying in between the White Range Nappe and the Ruby Gap Nappe

(see Fig.2.2 of this thesis). Map 3 shows the whole of Atnarpa Range area as the top of the Ruby Gap Nappe except for a small part of it within the Small Valley which has been shown as the base of the White Range Nappe. The position of this small part corresponds to the position of the thrust sheet no.4 in the Small Valley (Fig.3.2) and thrust sheet no.4 in this area on the basis of the present study comprises normal stratigraphic order. The surface which recurs at various structural levels in Map 3 has been described as an unconformable or thrust contact between the rocks of the basement and the cover (Forman, 1971) and therefore the interpretation of the structure of the Atnarpa Range area shown on Map 3 is not inconsistent with the interpretation based on this study if this surface is considered a thrust in case of the base of Ruby Gap Nappe. However, the interpretation of the small part shown as base of Ruby Gap Nappe is not in accord with this study.

It will be hazardous to comment on the structural evolution of the whole of the nappe complex on the basis of the study of a part of it of about 3 to 4% of its size. However, if vertical flattening is found to be the main component of the strain field throughout the northern part of the nappe complex then the movement picture deduced for the Atnarpa Range area may be relevant for the entire nappe complex and in that case the emplacement of the nappe complex would have taken place mainly by thrusting.

REFERENCES

AVE LALLEMANT, H.G. and CARTER, N.L., 1971 Pressure dependence of quartz deformation lamellae orientations. Amer. J. Sci., 270, pp. 218-235

BADGLEY, P.C., 1965 Structural and tectonic principles: Harper and Row

BALK, R., 1952 Fabrics of quartzites near thrust faults. J. Geol., 60, pp. 415-435

BARRETT, G.S. and LEVERSON, L.H., 1939 Structure of iron after drawing, swaging, and elongation in tension. Trans AIME. 135, pp. 327-343.

BARRETT, C.S. and MASSAISKI, T.B., 1966 Structure of metals: McGraw-Hill 654pp.

BECK, P.A. and Hu, H., 1966 The origin of recrystallization textures: In: Recrystallization Grain Growth and Textures, edited by H. Margolin, Amer. Soc. Metals, pp. 393-433.

BISHOP, J.F.W. and HILL, R., 1951 A theory of the plastic distortion of a polycrystalline aggregate under combined stresses. Phil. Mag. 42, pp. 414-427

BLACIC, J.D. and GRIGGS, D.T., 1965 New phenomena in experimental deformation of quartz at low strain rate (abstract), Eos Trans. AGU 46, p. 541

BRACE, W.F., 1960 Orientation of anisotropic minerals in a stress field. Geol. Soc. Amer. Mem. 79, pp. 9-20.

BROWN, H.Y.L., 1902 Report on the White Range gold mines, Arltunga Goldfield. S. Aust. parl. Pap. 76.

_____ 1903 Report on gold discoveries near Winnecke's Depot, etc. Ibid., 59.

CARTER, N.L., CHRISTIE, J.M., and GRIGGS, D.T., 1964 Experimental deformation and recrystallization of quartz. Jour. Geol., vol. 72, pp. 687-733.

CARTER, N.L. and FRIEDMAN, M., 1965 Dynamic analysis of deformed quartz and calcite from the Dry Creek ridge anticline, Montana, Amer. J. Sci. 263, pp. 747-785.

CARTER, N.L., 1971 Static deformation of silica and silicates. Jour. Geophys. Res. 76, pp. 5514-5540.

CHEWINGS, C., 1894 Notes on the sedimentary rocks in the MacDonnell and James Ranges. Trans. Roy. Soc. S. Aust. 18, pp.197-199.

_____ 1914 Notes on the stratigraphy of central Australia. Trans. Roy. Soc. S. Aust. 38, pp. 41-52.

_____ 1928 Further notes on the stratigraphy of central Australia. Ibid. 52, pp. 62-81

_____ 1935 The Pertatataka Series in central Australia, with notes on the Amadeus Sunkland. Ibid., 59, pp. 141-163.

CHIN, G.Y., 1969 Deformation textures: In: Textures in Research and Practice, edited by Grewen, J. and Wasserman, G. Springer-Verlag, Berlin, pp. 51-80.

CHRISTIE, J.M., 1960 Mylonitic rocks of the Moine Thrust Zone in the Assynt region, northwest Scotland. Trans. Edin. Geol. Soc. 18, pp. 79-93

_____ 1963 The Moine Thrust Zone in the Assynt region northwest Scotland. Univ. Calif. Pubs. Bull. Dep. Geol. 40, pp. 345-440.

CHRISTIE, J.M., GRIGGS, D.T. and CARTER, N.L., 1964 Experimental evidence of basal slip in quartz. Jour. Geol. 72, pp. 734-756.

DUNNET, D., 1969 A technique of finite strain analysis using elliptical particles. Tectonophysics 7, pp.117-136

EISBACHER, G.H., 1970 Deformation mechanics of mylonitic rocks and fractured granites in Cobequid Mountains, Nova Scotia, Canada. Geol. Soc. Amer. Bull. 81, pp. 2009-2020.

ELLIS, H.A., 1937 Report on some observations made on a journey from Alice Springs, N.T., to the country north of the Rawlinson Ranges in West Australia, etc. Ann. Rep. Geol. Surv. W. Australia.

ETHERIDGE, M.A., 1971 Experimental investigations of mica preferred orientation. Ph.D. Thesis Aust. Nat. Univ. (Unpublished)

FERREIRA, M.P. and TURNER, F.J., 1964 Microscopic structure and fabric of Yule Marble experimentally deformed at different strain rates. Jour. Geol. 72, pp. 861-875.

FLEUTY, M.J., 1964A The description of folds. Proc. Geol. Ass. 75, pp. 461-492

FLINN, D., 1965 Deformation in metamorphism: In: Controls of metamorphism edited by Pitcher, S.W. and Flinn, G.W., Oliver and Boyd, London, pp. 46-72.

FORMAN, D.J., 1965 The geology of the southwestern margin of the Amadeus Basin, central Australia. Bur. Min. Resour. Aust. Rep. 87.

_____ 1971 The Arltunga Nappe Complex, MacDonnell Ranges, N.T., Australia. Journ. Geol. Soc. Aust. 18, pp.173-182.

FORMAN, D.J., MILLIGAN, E.N., and McCARTHY, W.R. 1967 Regional geology and structure of the northeastern margin of the Amadeus Basin, Northern Territory. Rep. Bur. Miner. Resour. Geol. Geophys. 103.

GREEN, H.W., 1967 Extreme preferred orientation produced by annealing. Science 157, pp. 1444-1447.

GREEN, H.W., GRIGGS, D.T., CHRISTIE, J.M., 1971 Syntectonic and annealing recrystallization of fine-grained quartz aggregates: In: Experimental and Natural Rock Deformation edited by Paulitsch, P., Springer-Verlag, Berlin, pp.272-335.

GRIGGS, D.T. and BELL, J.F., 1938 Experiments bearing on the orientation of quartz in deformed rocks. Bull. Geol. Soc. Amer. 49, pp. 1723-1746.

GRIGGS, D.T. and BLACIC, J.D., 1965 Quartz: Anomalous weakness of synthetic crystals. Science 147, pp. 292-295

GRIGGS, D.T. and HANDIN (Editors), 1960a Rock deformation. Geol. Soc. Amer. Mem. 79.

GRIGGS, D.T., TURNER, F.J., and HEARD, H.C., 1960b Deformation of rocks at 500°C to 800°C. Geol. Soc. Amer. Mem. 79, pp. 39-104.

GRIGGS, D.T., 1967 Hydrolytic weakening of quartz and other silicates. Geophys. J. Roy. Astra. Soc. 14, pp. 19-31.

HARKER, A., 1939 Metamorphism: Methuen, London.

HEARD, H.C. and CARTER, N.L., 1968 Experimentally induced 'natural' intergranular flow in quartz and quartzite. Amer. J. Sci. 266, pp. 1-42.

HILLS, E.S., 1953 Elements of structural geology: Methuen, London

HOBBS, B.E., 1965 Structural analysis of the rocks between the Wyangala Batholith and the Copper Hannia Thrust, New South Wales. Journ. Geol. Soc. Aust. 12, pp. 1-24.

_____ 1968 Recrystallization of single crystals of quartz. Tectonophysics 6, pp. 353-401.

HOSSFIELD, P.S., 1954 Stratigraphy and structure of the Northern Territory of Australia. Trans. Roy. Soc. S. Aust., pp. 103-161

JOHNSON, M.R.W., 1956 Conjugate fold systems in the Moine Thrust Zone in the Lochcarron and Coulin Forrest areas of Western Ross. Geol. Mag. 93, pp. 345-350.

_____ 1957 The structural geology of the Moine Thrust Zone in Coulin Forrest, Western Ross. Q. Jl. Geol. Soc. Lond. 113, pp. 241-270

_____ 1967 Mylonite zones and mylonite banding. Nature 213, pp. 246-247.

JOKLIK, G.F., 1955 The geology and mica-fields of the Harts Range, central Australia. Bur. Min. Resour. Aust. Bull. 26.

KAMB, W.B., 1959a Theory of preferred crystal orientation developed by crystallization under stress. J. Geol. 67, pp. 153-170.

_____ 1959b Ice petrofabric observations from Blue Glacier Washington, in relation to theory and experiment. J. Geophys. Res. 64, pp. 1891-1909

KVALE, A., 1953 Linear structures and their relation to movement in the Caledonides of Scandinavia and Scotland. Geol. Soc. London Quart. Jour. 109, pp. 51-73.

LANGRON, W.J., 1962 Amadeus Basin reconnaisance gravity survey using helicopters. Bur. Miner. Res. Aust. Rec. 24 (unpub.)

LONSDALE, G.F. and FLAVELLE, A.J., 1963 Amadeus and South Canning Basins reconnaisance gravity survey, N.T. and W.A. Bur. Miner. Res. Aust. Rec. 152 (unpub.)

MCLAREN, A.C. and HOBBS, B.E., 1972 Transmission electron microscope investigations of some naturally deformed quartzites. (In press).

MADIGAN, C.T., 1932 The geology of the eastern MacDonnell Ranges, central Australia. Trans. Roy. Soc. S. Aust. 56, pp.71-117.

MARSHALL, C.E. and NARAIN, H., 1954 Regional gravity investigations in the eastern and central Commonwealth. Dep. Geol. Geophys. Univ. Sydney Mem. 2.

MARTIN, H. 1935 'Ueber Striemung, Transport und Gefuge', Geol. Rundsch 26, pp. 103-108.

MAWSON, D. and MADIGAN, C.T., 1930 The pre-ordovician rocks of the MacDonnell Ranges. Quart. J. Geol. Soc. Lond. 86, pp.415-429.

MEANS, W.D., 1963 Mesoscopic structures and multiple deformation in the Otago Schist. N.Z. Joun. Geol. Geophys. 6, pp. 801-806

_____ 1966 A macroscopic recumbent fold in schist near Alexendra, Central Otago. N.Z. Journ. Geol. Geophys. 9 pp. 173-190.

MEANS, W.D. and PATERSON, M.S., 1967 Experiments on the preferred orientation of slaty minerals. Contr. Mineral. Petrol. 13 pp. 108-133.

PATERSON, M.S. and WEISS, L.E., 1961 Symmetry concepts in the structural analysis of the deformed rocks. Geol. Soc. Am. Bull. 72, pp. 841-882.

PHILLIPS, F.C., 1937 A fabric study of some Moine schists and associated rocks. Geol. Soc. Lond. Quart. Jour. 93, pp. 581-616.

PLUMMER, H.C., 1940 Probability and frequency: MacMillan London.

PRICHARD, C.E. and QUINLAN, T., 1962 The geology of the southern half of the Hermannsburg 1:250,000 sheet. Bur. Min. Resour. Aust. Rep. 61

RALEIGH, C.B., 1965 Crystallization and recrystallization of quartz

in a simple piston-cylinder device. J. Geol. 73, pp.369-377.

RAMSAY, J.G., 1962 The geometry of conjugate fold systems. Geol. Mag. 99, pp. 516-526.

_____ 1967 Folding and fracturing of rocks. McGraw Hill.

RANFORD, L.C., COOK, P.J., and WELIS, A.T., 1965 Geology of the central part of the Amadeus Basin, N.T. Bur. Min. Resour. Aust. Rep. 86

RANSOM, D.M., 1971 Host control of recrystallized quartz grains. Mineral. Mag. 38, pp. 83-88.

REITAN, P.H., 1969 Temperatures with depth resulting from frictionally generated heat during metamorphism. Geol. Soc. Am. Mem. 115, pp. 495-512.

SANDER, B., 1930 Gefugekunde der Gestine. Springer Verlag, Vienna.

SHARPE, D., 1849 On slaty cleavage. Geol. Soc. London Quart. Jour. 5, pp. 111-129

SKOLNICK, H., 1965 The quartzite problem. Journ. Sed. Petr. 35, p. 12.

SORBY, H.C., 1856 On slaty cleavage as exhibited in the Devonian limestones of Devonshire. Phil Mag. 11, pp. 20-37.

STEWART, A.J., 1971 Structural evolution of the White Range Nappe, Central Australia. Ph.D. thesis Yale Univ. (unpub.)

SYLVESTER, A.G. and CHRISTIE, J.M., 1968 The origin of crossed-girdle orientations of optic axes in deformed quartzites. J. Geol. 76, pp. 571-580.

TAYLOR, G.I., 1938 Plastic strain in metals. J. Inst. Metals 62, pp. 307-324.

TULLIS, J., 1971 Preferred orientations of experimentally deformed quartzites. Ph.D. thesis, Univ. of Calif.

TULLIS, T.E., 1971 Experimental development of preferred orientation of mica during recrystallization. Ph.D. thesis Univ. of Calif.

TURNER, F.J. 1968 Metamorphic petrology: McGraw-Hill New York

TURNER, F.J., GRIGGS, D.T., and HEARD, H., 1954 Experimental deformation of calcite crystals. Geol. Soc. Am. Bull. 65, pp. 883-934.

TURNER, F.J. and VERHOOGEN, J., 1960 Igneous and metamorphic petrology, 2nd. Ed. McGraw-Hill New York

TURNER, F.J. and WEISS, L.E., 1963 Structural analysis of metamorphic tectonites. McGraw-Hill New York

VOISEY, A.H., 1939 A contribution to the geology of the eastern MacDonnell Ranges, central Australia. J. Roy. Soc. N.S.W. 72, pp. 160-174.

VONMISES, R.Z., 1928, angew. Math. Mech. 8, p.161.

WEISS, L.E., and McINTYRE, D.B. 1957 Structural geometry of Dalradian rocks at Loch Leven, Scottish Highlands. Journ. Geol. 65, pp. 575-601.

WELLS, A.T., FORMAN, D.J., RANFORD, L.C. and COOK, P.J., 1970 Geology of the Amadeus Basin, Central Australia. B.M.R. Bull. 100.

WILLIAMS, P.F., 1968 Tectonic studies of rocks exposed along the south coast of N.S.W. Ph.D. thesis Univ. of Sydney (unpublished)

WILSON, C.J.L., 1970 The microfabric of a deformed quartzite sequence, Mt. Isa, Queensland. Ph. D. thesis Aust. Nat. Univ. (unpublished).

WONSIEWICZ, B.C. and CHIN, G.Y., 1970 Inhomogeneity of plastic flow in constrained deformation. Metall. Trans. 1, pp. 57-61

APPENDIX

Additional data on quartz c-axis orientation diagrams of Fig.4.1

Specimen Loc.No.	Number of Poles	A	E	Maxima
161	320	0.027	8.8	7.9 σ
164	350	0.025	8.8	10.6"
176	300	0.029	8.7	10.6"
215	300	0.029	8.7	7.9"
226	300	0.029	8.7	14.8"
279	200	0.043	8.6	10.5"
273	300	0.029	8.7	17.8"
278	300	0.029	8.7	8.2 "
105	300	0.029	8.7	11.3"
186	240	0.036	8.7	12.8"
294A	200	0.043	8.6	10.1"
128	300	0.029	8.7	7.5 "
159	300	0.029	8.7	9.3 "
197	340	0.025	8.8	7.9 "
104	340	0.025	8.8	7.9 "
294	240	0.036	8.7	9.10"
130	340	0.025	8.8	7.2 "
156	300	0.029	8.7	8.2 "
101	350	0.025	8.8	10.3"
237	300	0.029	8.7	7.9 "
195	250	0.034	8.7	6.9 "
228	300	0.029	8.7	7.2 "
118	340	0.025	8.8	8.6 "

Specimen Loc. No.	Number of Poles	A	E	Maxima
120	340	0.025	8.8	8.9 σ
122	300	0.029	8.7	7.2 "
147	300	0.029	8.7	8.9 "
150	350	0.025	8.8	13.3"
115	300	0.029	8.7	12.4"
167	300	0.029	8.7	7.6 "
146	360	0.024	8.8	7.5 "
123	300	0.029	8.7	7.2 "
154	320	0.027	8.8	8.2 "
103	300	0.029	8.7	6.5 "
141	300	0.029	8.7	7.6 "
137	260	0.033	8.7	7.6 "
110	340	0.025	8.8	7.9 "
112	340	0.025	8.8	6.8 "
282	300	0.029	8.7	7.6 "
212	300	0.029	8.7	6.6 "
144	380	0.023	8.8	7.8 "

GEOLOGY OF THE ATNARPA RANGE AREA
NORTHERN TERRITORY

0 km 1 MI
0
1:15 000

MAP AREA IN RELATION TO 1:250 000

NAPPERBY	ALCOOTA	HUCKITTA
HERMANNSBURG	ALICE SPRINGS	HARDING SPRING
HENBURY	RODINGA	HALE RIVER

LOCALITY MAP

N.T.

CAINOZOIC
QUATERNARY
Qa Alluvium, river gravel

PRECAMBRIAN
UPPER PROTEROZOIC
Bitter Springs Formation — Bub Siltstone, shale, phyllite, quartzite and dolomite
Heavitree Quartzite — Euh Quartzite, sandstone, pebbly sandstone
Euh1 Platy quartzite
Euh2 Quartzite, sandstone
Euh3 Conglomerate, siltstone, pebbly sandstone, arkose
Arunta Complex — Basement igneous and metamorphic rocks
pEg Granite
Quartzo-feldspathic rocks
Mafic rocks

Geological boundary, position accurate
Position approximate
Concealed
Anticline, showing plunge
Position approximate
Syncline, showing plunge
Position approximate
Plunge of fold showing 'S' vergence, cremulation parallel to fold axis
Plunge of fold showing 'Z' vergence, cremulation parallel to fold axis
Plung of fold showing 'M' vergence, crenulation parallel to fold axis
Plunge of fold showing strike & dip of its axial plane
Plunge of minor antiform
Plunge of minor synform
Locality of superposed folds
Fault, position accurate
Position approximate
Inferred
Inclined (measured)
Fault containing mylonite or breccia
Fault with slickensides
Strike and dip of strata, measured
Strike and dip of overturned strata
Strike and dip of vertical strata
Strike and dip of upright strata
Strike and dip of strata with plunge of lineation
Strike and dip of strata parallel to foliation with plunge of lineation
Strike and dip of strata parallel to foliation with horizontal lineation
proved direction of younging based on sedimentary structures, indicated by dot. For arrowheads applicable to other types of lineation see under Lineation below
Trend line
Strike and dip of foliation, measured
Vertical foliation
Foliation with plunge of lineation (both measured)
Foliation with horizontal lineation
Trend and plunge of lineation (undifferentiated, measured)
Trend and plunge of lineation (mineral elongation)
Trend and plunge of lineation (slickensides)
Trend and plunge of lineation (crenulation)
Horizontal lineation
X 206 Specimen locality
Dyke or vein, q-quartz
Water bore with windpump
Road
Vehicle track
Atnarpa homestead
Yard
Photo centre: wing point
Line of cross section

Pig Hole Creek
ATNARPA
WESTERN HILL RANGE
EASTERN HILL RANGE
SMALL VALLEY
LARGE VALLEY
"Atnarpa"
HALE RIVER
5160
5227

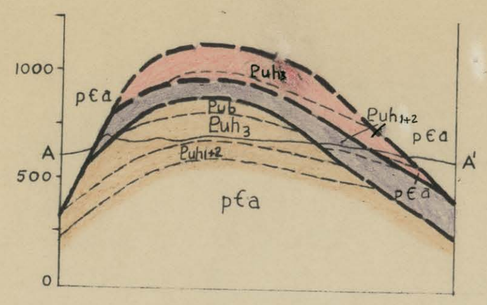

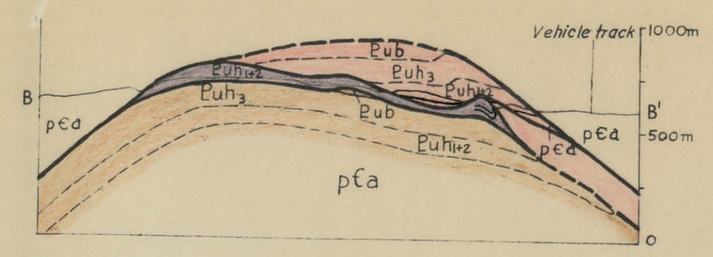

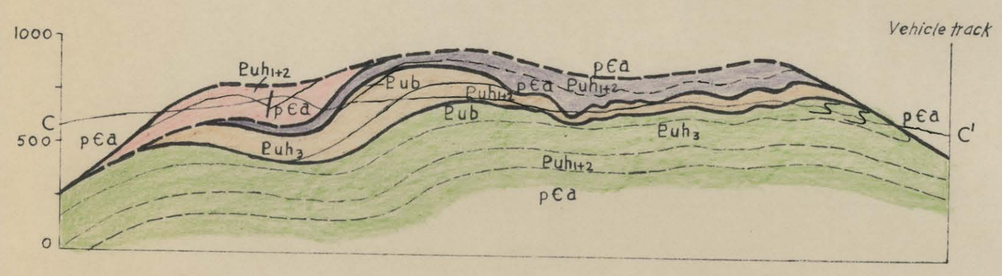

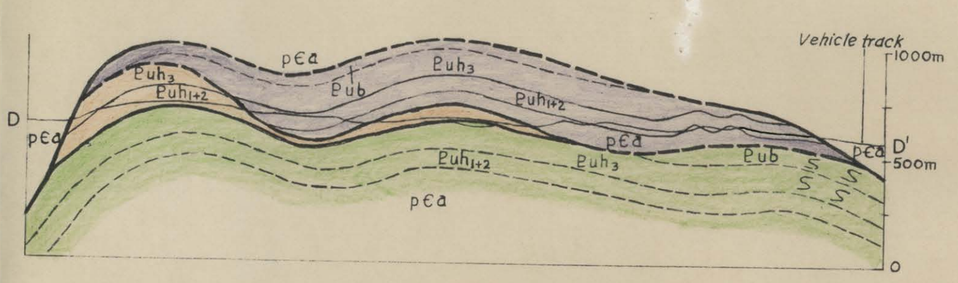

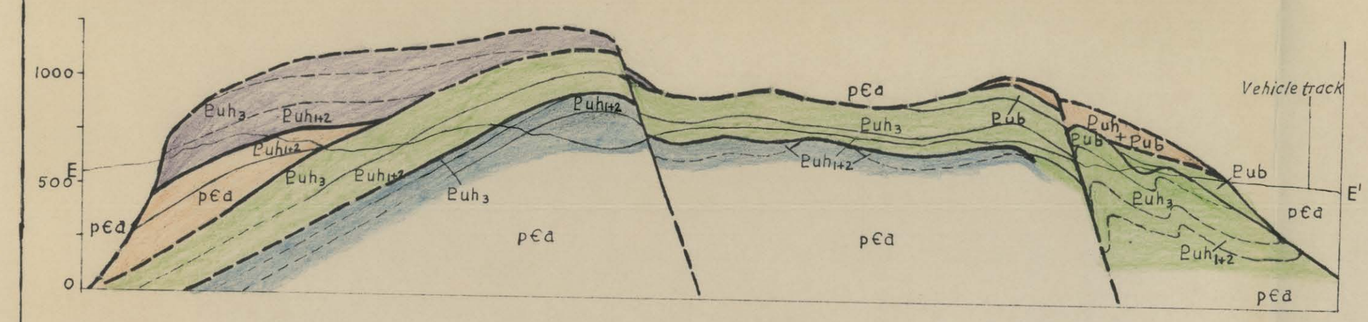

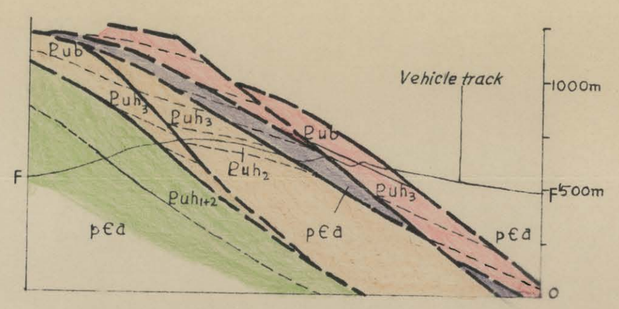

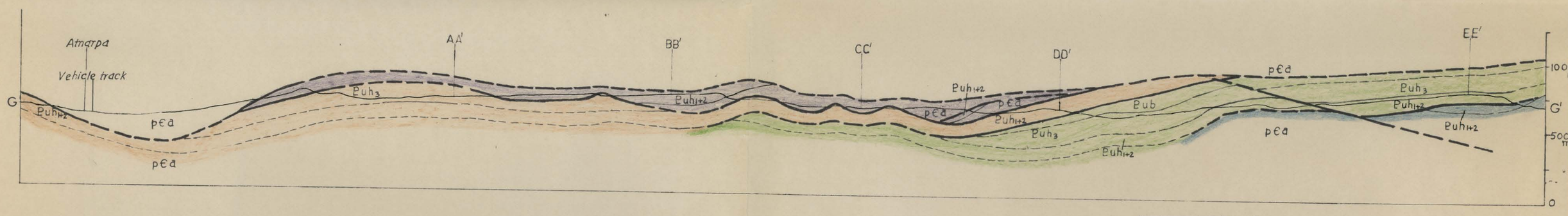

0 1 2km

CROSS SECTIONS (Line of section shown on Map 1)

Thrust sheet, in order of superposition

Fig 3.2

MAP SHOWING THE THRUST SHEETS, ATNARPA RANGE AREA